
Identification of Erbin interlinking MuSK and ErbB2 and its impact on acetylcholine receptor aggregation at the neuromuscular junction

Luca Simeone

Dottorato in Scienze Biotecnologiche – XXII ciclo

Indirizzo Biotecnologie Mediche

Università di Napoli Federico II



Dottorato in Scienze Biotecnologiche – XXII ciclo
Indirizzo Biotecnologie Mediche
Università di Napoli Federico II



Identification of Erbin interlinking MuSK and ErbB2 and its impact on acetylcholine receptor aggregation at the neuromuscular junction

Luca Simeone

Dottorando: Luca Simeone

Relatore: Prof.ssa Gabriella Esposito

Coordinatore: Prof. Ettore Benedetti

Alla mia famiglia

INDICE

RIASSUNTO	pag.9
1. Introduction	
1.1.Synapse	pag.13
1.2. Neuromuscular junction	pag.13
1.2.1. Development of neuromuscular junction	pag.15
1.3. Clustering of AChRs	pag.15
1.3.1. Agrin	pag.15
1.3.2. Muscle specific kinase (MuSK)	pag.18
1.4. Signaling downstream of MuSK	pag.21
1.4.1. Src kinases	pag.21
1.4.2. Rho-family GTPases	pag.22
1.5. MuSK interacting proteins	pag.23
1.5.1. MAGI-1c	pag.23
1.5.2. Synaptic nuclear envelope-1 (Syne-1)	pag.23
1.5.3. Dishevelled	pag.23
1.5.4. CollagenQ (ColQ)/Acetylcholinesterase (AChE)	pag.23
1.5.5. Src homology 2-domain-containing tyrosine phosphatase 2 (Shp2)	pag.24
1.5.6. 14-3-3 γ	pag.24
1.5.7. Abelson tyrosine kinases (Abl)	pag.24
1.5.8. Geranylgeranyltransferase 1 (GGT-1)	pag.25
1.5.9. Protein interacting with C kinase (PICK1)	pag.25
1.5.10. Docking Protein -7 (Dok-7)	pag.25
1.5.11. Protein kinase CK2	pag.25
1.5.12. Src-class kinases (SFKs)	pag.26
1.5.13. Putative ariadne-like E3 ubiquitin ligase (PAUL)	pag.26
2. Aim of the Study	pag.26
3. Material and methods	pag.27
3.1. Materials	pag.27
3.1.1. Reagents	pag.27
3.1.2. Devices	pag.28
3.1.3. Oligonucleotides	pag.29
3.1.4. siRNAs	pag.35
3.1.5. Enzymes	pag.36
3.1.6. Kits and Columns	pag.37
3.1.7. Antibodies	pag.38
3.1.8. Frequently used solutions	pag.38
3.1.9. Cell culture	pag.39
3.2.1. Molecular Biology Methods	pag.40
3.2.1.1. Isolation of plasmid DNA	pag.40
3.2.1.2. Determination of DNA/RNA concentration	pag.40
3.2.1.3. Electrophoretic separation of DNA fragments in agarose gel	pag.40
3.2.1.4. PCR amplification of DNA	pag.40

3.2.1.5. Cloning techniques	pag.41
3.2.1.6. Plasmid constructs	pag.42
3.2.1.7. Transformation of <i>E. coli</i> competent cells	pag.44
3.2.1.8. Site directed mutagenesis	pag.45
3.2.1.9. Total RNA isolation	pag.46
3.2.1.10. ComplementaryDNA-synthesis (Reverse Transcription)	pag.47
3.2.1.11. Lightcycler PCR	pag.47
3.2.1.12. Yeast-two-hybrid techniques	pag.48
3.2.2. Protein Biochemistry methods	pag.51
3.2.2.1. Preparation of protein extract from cells and tissues	pag.51
3.2.2.2. Immunoprecipitation	pag.51
3.2.2.3. Protein expression and extraction from bacteria	pag.52
3.2.2.4. GST-pulldown	pag.53
3.2.2.5. Electrophoresis of proteins	pag.53
3.2.2.6. Staining of protein gels	pag.54
3.2.2.7. Western blot	pag.54
3.2.3. Cell culture methods	pag.54
3.2.3.1. Cultivation of HEK293, Cos7, C2C12, and MuSK-deficient myoblasts	pag.54
3.2.3.2. Transient transfection of cells	pag.55
3.2.3.3. Luciferase reporter test	pag.56
3.2.3.4. Agrin treatment	pag.56
3.2.3.5. Immunocytochemistry	pag.57
3.2.3.6. Quantification analysis of AChR clusters	pag.57
3.2.3.7. Immunohistochemistry	pag.57
4. Results	pag.58
4.1. Yeast-two-hybrid screens	pag.58
4.1.1. Generation of MuSK baits	pag.58
4.1.2. Outcome of the yeast-two-hybrid screens	pag.59
4.3. Detailed investigation of MuSK - Erbin interaction	pag.60
4.3.1. Quantitative determination of Erbin transcript level in different tissues	pag.60
4.3.2. Localization of Erbin at the NMJ	pag.61
4.3.3. Verification of the interaction between Erbin and MuSK in HEK293 cells, myotubes and muscle extracts	pag.63
4.3.4. Mapping of epitopes of MuSK interacting with Erbin	pag.64
4.3.5. Mapping of epitopes of Erbin interacting with MuSK	pag.66
4.3.6. The Smad interacting domain of Erbin mediates the interaction with the kinase domain of MuSK	pag.68
4.3.7 Erbin enhances aggregation of AChRs <i>in vivo</i>	pag.71
4.3.8 Erbin associates ErbB2 with MuSK and TGF- β signalling at the NMJ	pag.74
4.3.9 LAP family members like Lano and Scribble but not Densin-180 are expressed at the NMJ	pag.76
5. Discussion	pag.77

6. References

pag.79

7. Appendice

pag.84

7.1.1 Laboratori frequentati

pag.84

RIASSUNTO

Il progetto di ricerca su cui ho svolto i miei studi è iniziato con lo scopo di individuare nuovi interattori di MuSK ed è proseguito con la caratterizzazione dei meccanismi in cui sono coinvolti. MuSK è un recettore tirosina chinasi, espresso nelle fibre muscolari, nelle quali regola lo sviluppo della giunzione neuromuscolare. Studi pubblicati negli ultimi anni, hanno dimostrato che MuSK non è coinvolto solo nella formazione iniziale della giunzione neuromuscolare, ma anche nel mantenimento dell'apparato postsinaptico e nel controllo della crescita assonale.

La giunzione neuromuscolare trasmette segnali dai motoneuroni alle fibre muscolari multinucleate. Un fenomeno che caratterizza l'apparato postsinaptico, è l'aggregazione dei recettori dell'acetilcolina (AChR) (Sanes and Lichtman, 1999). Solo i nuclei muscolari a diretto contatto con la sinapsi, trascrivono i geni codificanti per le subunità del AChR (Merlie and Sanes, 1985). Normalmente, l'aggregazione degli AChRs, è indotta dalla proteina agrina, secreta dai motoneuroni, e dalle neoreguline. Studi dimostrano che queste ultime stimolano la trascrizione dei geni dell'AChR (Falls et al., 1993). Esperimenti recenti indicano, comunque, che le neureguline non sono essenziali per la trascrizione sinapsi-specifica dei geni delle subunità del recettore, perché, in topi mancanti di ErbB2 ed ErbB4, selettivamente nel muscolo scheletrico, ed in quelli mancanti della neuregulina nei motoneuroni e nelle fibre muscolari, sono stati riscontrati fenotipi modesti o del tutto normali (Escher et al., 2005; Jaworski e Burden, 2006). Altri dati suggeriscono che il ruolo primario delle neureguline, nell'apparato postsinaptico, consiste nella regolazione dell'aggregazione e nella migrazione degli AChRs sulla superficie cellulare (Ponomareva et al., 2006).

Le neureguline attivano i recettori tirosina chinasi della famiglia del recettore EGF (ErbBs). L'eterodimero ErbB2/4 è il recettore con maggiore funzionalità nell'apparato postsinaptico (Trinidad et al., 2000). Le proteine ErbB sono concentrate al sito postsinaptico della giunzione neuromuscolare (Altiok et al., 1995; Moscoso et al., 1995; Zhu et al., 1995; Trinidad et al., 2000) o nel sistema nervoso centrale (Garcia et al., 2000; Huang et al., 2000). La localizzazione sinaptica di ErbB4 nel sistema nervoso centrale, è mediata da un'interazione del suo dominio carbossi-terminale con il dominio PDZ della proteina PSD-95 (Postsynaptic Density Protein) (Garcia et al., 2000; Huang et al., 2000). Al contrario, PSD-95, interagisce debolmente o per niente, con ErbB2 ed ErbB3.

Un'altra proteina contenente un dominio PDZ, Erbin, interagisce specificatamente con ErbB2 (Borg et al., 2000; Huang et al., 2001). Erbin è la capostipite di una famiglia di proteine denominata LAP (Leucine-rich-repeats and PDZ domain), caratterizzate da 16 ripetizioni "leucine-rich" (LRR) nella porzione amino-terminale e da 1 a 4 domini PDZ in quella carbossi-terminale (Borg et al., 2000). Tutte le proteine della famiglia LAP sono coinvolte nella determinazione della polarità cellulare (Bryant e Huwe, 2000; Kolch, 2003). Di recente è stato dimostrato che, il dominio tra la LRR e il PDZ di Erbin, interagisce con EBP50 (Rangwala et al., 2005) e Smad3 (Dai et al., 2007).

Il ruolo e le interazioni molecolari di Erbin nella giunzione neuromuscolare, non sono stati ancora studiati. In questo studio noi dimostriamo (1) che Erbin è localizzata alla giunzione neuromuscolare, (2) interazioni di Erbin con il recettore tirosina chinasi MuSK, che media l'azione dell' agrina, come principale regolatore della formazione

dell'apparato postsinaptico, e con ErbB2, (3) che il dominio di Erbin interagente con MuSK, si sovrappone al dominio interagente con Smad3, (4) che Erbin o MuSK, attenuano la trascrizione mediata da Smad3.

Tre diverse isoforme (splice variants) di Erbin sono state identificate in cellule muscolari, tutte contenenti il dominio di interazione con MuSK. Esperimenti di knockdown in cellule muscolari, attribuiscono ad Erbin un ruolo nel controllo della densità di aggregati di recettori dell'acetilcolina. In aggiunta ad Erbin, altre proteine della famiglia LAP sono state individuate nella giunzione neuromuscolare: Lano e Scribble. Il rate di trascrizione dei geni codificanti per queste 2 proteine, aumenta quando i mioblasti differenziano in miotubi.

Il nostro scopo era di identificare, tramite yeast-two-hybrid screening, nuove proteine interagenti con il dominio intracellulare di MuSK. Per questo, abbiamo fuso 2 parti del dominio intracellulare del recettore (MuSK2xWT), creando così un dimero che somigliasse il più possibile al dimero di MuSK, conformazione attiva in vivo (Cheusova et al., 2006). Un secondo costrutto è stato generato allo stesso modo, ma per una variante di MuSK priva di attività chinasi, per capire se il legame con altre proteine fosse dipendente dalla fosforilazione del dominio intracellulare. L'espressione di questi costrutti, la loro funzionalità e la loro applicabilità allo screening, sono stati descritti precedentemente (Cheusova et al., 2006).

Tra i cloni identificati, 2 consistevano della porzione carbossi-terminale dal residuo aminoacidico 1007 fino al codone di stop della isoforma umana di Erbin (hErbin-ND-1007), proteina della famiglia LAP. Nell'uomo, sono state descritte diverse varianti di Erbin. Quella da noi identificata corrisponde alla porzione carbossi-terminale della variante 2 (hErbin-V2). La stessa interazione si è osservata anche con la variante di MuSK priva di attività chinasi.

Per confermare l'interazione con altri approcci sperimentali, abbiamo effettuato una transfezione transiente di cellule HEK293 dei vettori di espressione per Erbin, MuSK2xWT e la variante con inattivazione del dominio chinasi, gli ultimi 2 contenenti una T7-tag. Immunoprecipitati degli estratti proteici hanno confermato i dati precedentemente ottenuti.

Per determinare se l'interazione fosse facilitata dall'over-espressione delle proteine, abbiamo effettuato immunoprecipitati da estratti proteici di una linea di cellule muscolari (C2C12) e da muscolo scheletrico (Gastrocnemius) murino. In queste condizioni, dove sia Erbin che MuSK sono endogenamente espressi allo stesso livello, è stato ancora possibile co-precipitare entrambe con i rispettivi partners.

Poiché Erbin e MuSK interagiscono fisicamente, abbiamo voluto determinare il profilo di espressione di Erbin nelle regioni sinaptiche e post-sinaptiche. Attraverso RT-PCR abbiamo misurato la quantità di trascritto di Erbin e l'abbiamo paragonato a quello di proteine concentrate normalmente alla giunzione neuromuscolare (MuSK, AChR). L'RNA totale è stato estratto dalla regione sinaptica e quella extra-sinaptica del diaframma di topo. Come previsto, sia MuSK che AChR erano altamente espressi a livello della regione sinaptica, così come Erbin. L'espressione del trascritto di Erbin a livello sinaptico, è stata confermata anche da ibridazione in situ su diaframmi di topi.

Il nostro obiettivo successivo era quello di dimostrare la localizzazione di Erbin nell'apparato postsinaptico. Attraverso tecniche di immunoistochimica su sezioni

trasversali dei muscoli gastrocnemius e soleus (zampe posteriori) di topo, abbiamo osservato un'accumulo significativo di Erbin alla giunzione neuromuscolare, dove co-localizzava con i recettori dell'acetilcolina.

Per identificare gli epitopi di MuSK ed Erbin che interagiscono tra loro, abbiamo usato una serie di mutanti di MuSK con delezioni nella porzione carbossi-terminale. Dapprima, nello screening yeast-two-hybrid, abbiamo osservato che i lieviti crescevano solo quando hErbin-N Δ -1007 era usata come "esca" con i vettori "preda" contenenti i costrutti MuSK-515-868 e MuSK-515-857, che comprendono il dominio intracellulare di MuSK e il dominio chinasi, rispettivamente. Tramite esperimenti di GST pull down, l'interazione osservata con i lieviti, ha avuto un'ulteriore conferma.

Il passo seguente è stato quello di procedere all'identificazione del dominio di hErbin-N Δ -1007, interagente con MuSK. Anche in questo caso sono stati generati diversi mutanti, tramite delezioni, sia nella porzione amino-terminale, che in quella carbossi-terminale. Solo i lieviti contenenti il frammento con delezione fino al residuo aminoacidico 1200 (hErbin-N Δ -1200), come hErbin-PDZ (hErbin-N Δ -1261), crescevano su terreno selettivo. In caso di delezioni nella parte carbossi-terminale, riuscivano a crescere solo i lieviti contenenti Erbin dal residuo aminoacidico 1007 fino al 1266 (hErbin- Δ PDZ) o 1204 (hErbin-1007-1204). Gli epitopi identificati sono stati verificati anche in esperimenti di GST pull down.

Avendo dimostrato che Erbin interagisce con MuSK, collegando quindi MuSK con ErbB2, abbiamo voluto investigare il significato biologico di questa interazione. L'approccio usato, è consistito nello studiare se l'ablazione o l'over-espressione di Erbin avesse una conseguenza sull'aggregazione dei recettori dell'acetilcolina. Per questo abbiamo clonato diversi vettori codificanti per shRNA, e testato la loro efficienza nel diminuire l'espressione dei trascritti di Erbin. Ciò è stato fatto sia mediante saggi di luciferasi, sia mediante western blot su lisati proteici di HEK293, transfettate con gli shRNAs. Allo scopo di analizzare l'effetto del knockdown di Erbin sugli aggregati, abbiamo transfettato cellule C2C12 con Erbin shRNA. Dopo aver stimolato l'aggregazione dei recettori, tramite aggiunta di agrina nel mezzo di coltura, abbiamo incubato le cellule con la bungarotossina coniugata alla rodamina. Grazie all'alta affinità di legame della tossina verso la subunità alfa dei recettori, è possibile osservarli tramite fluorescenza. Livelli minori del trascritto di Erbin riducono significativamente la densità dei recettori. L'analisi della densità è stata effettuata tramite microscopia confocale.

Di recente è stato dimostrato che Erbin inibisce la cascata di segnali di TGF- β attraverso un dominio interagente con Smad (Dai et al., 2007). Era di nostro interesse sapere se le cellule C2C12 esprimessero TGF- β e Smad, e se questo accadesse in dipendenza o meno dall'agrina. Tramite RT-PCR abbiamo dimostrato l'espressione dei recettori TGF- β RI e TGF- β RII e Smad3 nelle cellule muscolari. Per identificare il ruolo di Erbin e MuSK nel signaling di TGF- β abbiamo transfettato C2C12 con un vettore di espressione codificante per Smad3. Abbiamo osservato, come riportato in letteratura (Liu et al., 2001) che questa proteina inibiva la differenziazione dei mioblasti in miotubi. Noi dimostriamo che, la co-transfezione di Smad3 con hErbin-v2, blocca l'inibizione e i mioblasti riescono a differenziarsi nuovamente.

Per identificare la presenza di altre proteine della famiglia LAP in cellule muscolari, abbiamo eseguito esperimenti di RT-PCR su mioblasti e miotubi C2C12. Abbiamo così

individuato la presenza di Scribble e Lano. Un altro dato interessante è che l'espressione di Scribble è di gran lunga maggiore di quella di Lano e si osserva un suo ulteriore aumento dopo stimolazione dell'aggregazione dei recettori, tramite agrina.

Al momento è in corso lo studio dell'effetto che il knockdown di Scribble e Lano, anche in combinazione con quello di Erbin, ha sulla densità degli aggregati dei recettori. Stiamo valutando gli stessi effetti anche su colture primarie di muscolo scheletrico, a seguito del knockdown delle suddette proteine.

I nostri dati dimostrano per la prima volta un'interazione tra Erbin e MuSK a livello della giunzione neuromuscolare e presentano un inizio per un approfondimento del ruolo delle proteine LAP nell'apparato postsinaptico.

L'identificazione di interazione tra proteine è un prerequisito per lo studio di meccanismi di signaling. Lo stato dell'arte riguardante la trasduzione del segnale della giunzione neuromuscolare è molto limitato. L'identificazione di interazioni alla giunzione, può dare la possibilità di conoscere meglio lo sviluppo e le patologie della sinapsi. Per esempio, dati recenti riguardo l'interazione tra MuSK e la porzione C-terminale di Co1Q, una "coda" collagenica che trasporta l'Acetilcolinesterasi alla giunzione neuromuscolare, hanno dimostrato che MuSK è responsabile della localizzazione sinaptica dell'esterasi, ed hanno dato spiegazioni per certe forme di sindromi di miastenia congenita, associate con mutazioni nella parte C-terminale di Co1Q (Engel et al., 2003).

1. Introduction

1.1. Synapse

The word synapse first appeared in 1897, in the seventh edition of Michael Foster's *Textbook of Physiology* and describes the point of contact between two cells. Synapses are specialized structural units for cellular communication in the nervous system. The formation of synapses requires a series of steps. First, the parts of the two cells have to migrate to the place where the synapse will form. Second, these subcellular structures of the cells have to differentiate to specialized presynaptic terminals and postsynaptic membranes (Bowe and Fallon, 1995). Much of the knowledge about synapses came from the study of neuromuscular junctions.

1.2. Neuromuscular junction

The neuromuscular junction (NMJ) is a synapse composed by a specialized part of a motoneuron and a muscle fiber (Hall and Sanes, 1993). The NMJ consists of the presynaptic nerve terminal, the postsynaptic muscle fiber and the presynaptic Schwann cells (PSCs, also known as "terminal" Schwann cells). Additionally between the nerve terminal and the muscle membrane, a synaptic basal lamina develops, which is composed of extracellular matrix and factors produced and secreted by both nerve and muscle (Bloch and Pumplin, 1988; Sanes and Lichtman, 1999).

Neuromuscular junctions have been widely used for analyses of synaptic structure, function and development because of several advantages over the synapses from the central nervous system (Burden, 1998; Sanes and Lichtman, 1999; Wyatt and Balice-Gordon, 2003), namely size, accessibility and simplicity.

1.2.1. Development of the neuromuscular junction

During development starting at about embryonic day (E) 11 in mice multinucleated skeletal muscle fibers form by fusion of precursor myoblasts. Shortly after myotubes begin to form (at E12-13 in mice), motoneurons begin to contact muscle cells (Fig.1). Motoneurons can innervate from one to over hundred muscle fibers, but each muscle fiber receives input from only one motoneuron. In the terminal branches of the motor nerve, at dense patches called active zones synaptic vesicles filled with the neurotransmitter acetylcholine (ACh) start to accumulate (Hall and Sanes, 1993).

At E14 first signs of postsynaptic specialization indicated by the aggregation of acetylcholine receptor (AChR) clusters appear on the surface of muscle fibers. Nerve terminal and muscle fiber continue development in the later embryonic stages. At birth, both nerve terminal and opposite areas of muscle fiber are greatly transformed and have nearly accomplished their pre- and postsynaptic specialization. All inputs of motor axon to the muscle fibers except one are withdrawn during early postnatal life. Embryonic AChRs containing a γ subunits ($\alpha 2\beta\gamma\delta$) are replaced by AChRs containing ϵ subunits ($\alpha 2\beta\epsilon\delta$) during the first postnatal weeks (Mishina et al., 1986; Witzemann et al., 1989).

AChRs appear first as a patch-like pattern but further differentiates by time into a characteristically shaped "pretzel-like" pattern.

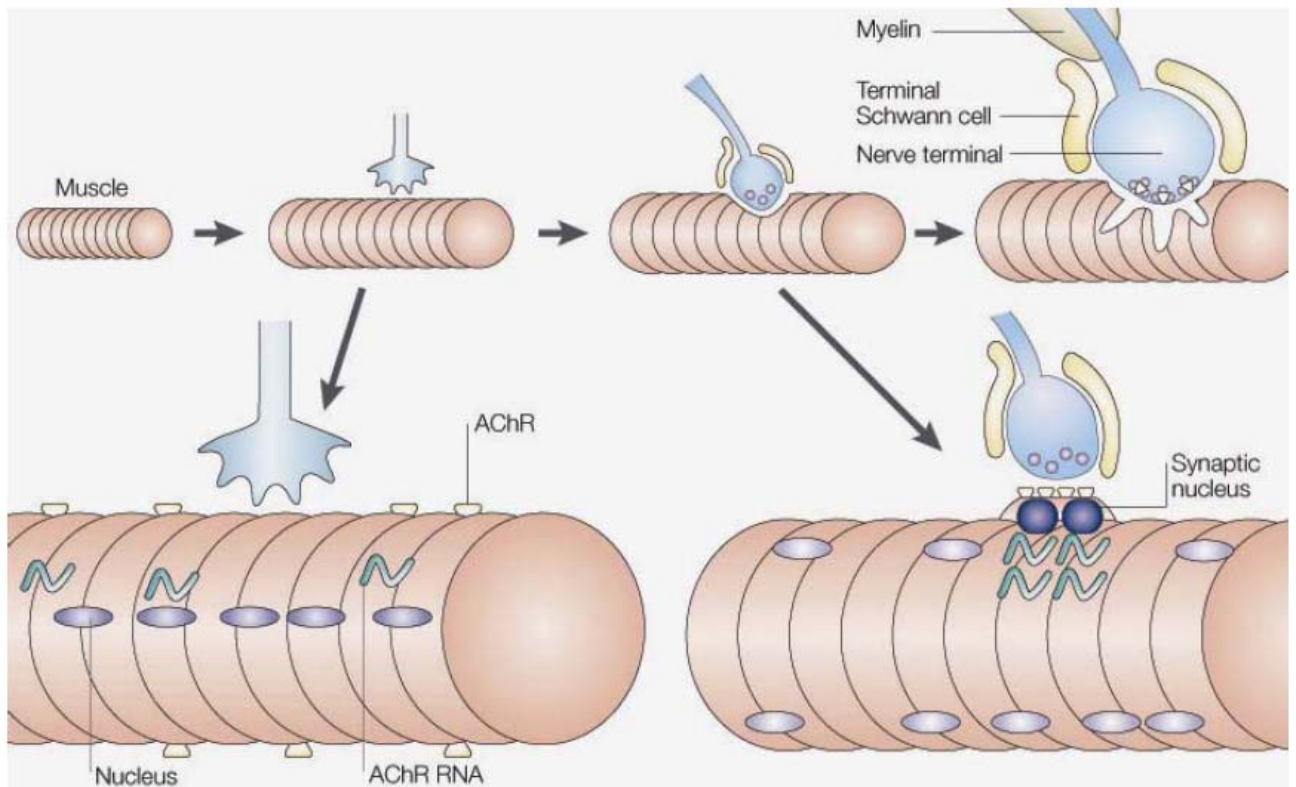


Fig.1: Development of the neuromuscular junction.

The motor axon approaches a newly formed myotube. At the area of contact, the axon differentiates into a motor nerve terminal that is specialized for transmitter release, Schwann cell processes cap the terminal, and the muscle forms a complex postsynaptic apparatus. Acetylcholine receptors (AChRs) are initially present at a moderate level throughout the myotube surface. In adult muscle, by contrast, AChRs are highly concentrated in the postsynaptic membrane and virtually absent extrasynaptically. This clustering involves both redistribution of AChR proteins, and localized synaptic synthesis of AChRs. Modified from (Sanes and Lichtman,2001).

The postsynaptic membrane is invaginated into deep and regular folds, termed postjunctional folds (Fig.1). AChRs and additional proteins are localized to the crests of these postjunctional folds, whereas other proteins, including sodium channels, are enriched in the troughs of the postjunctional folds (Hall and Sanes, 1993).

As the postsynaptic membrane matures, the presynaptic terminal also differentiates dramatically. Synaptic vesicles become clustered at the active zones and the nerve terminal becomes polarized (Hall and Sanes, 1993). Active zones aligned precisely with the postjunctional folds. This precise alignment of active zones and postjunctional folds ensures that acetylcholine encounters a high concentration of AChRs within microseconds after release, thereby ensuring fast synaptic transmission (Hall and Sanes, 1993).

1.3. Clustering of AChRs

Clustering of AChRs in the postsynaptic membrane is critical for synaptic function, as a high density of synaptic AChRs is required to generate a synaptic potential of sufficient magnitude to initiate an action potential in the myofiber. Early in development AChRs are evenly distributed in the plasma membrane of myotubes at a density of $1000/\mu\text{m}^2$. As synapse formation proceeds, the concentration of AChRs reaches $10,000/\mu\text{m}^2$ in the postsynaptic membrane and falls to $10/\mu\text{m}^2$ in extrasynaptic areas of the myotube (Fertuck and Salpeter, 1974; Bevan and Steinbach, 1977). This higher density of AChRs at the subsynaptic membrane is achieved through:

1. clustering of preformed synaptic nuclei (Couteaux, 1963);
2. specialization of subsynaptic nuclei for AChR subunit genes transcription (Merlie and Sanes, 1985; Burden, 1993; Moscoso et al., 1995);
3. suppression of AChR subunit genes transcription in the extrasynaptic area by electric activity (Lomo and Westgaard, 1975; Fambrough, 1979; Schaeffer et al., 2001);
4. formation of new AChR clusters (Frank and Fischbach, 1979);
5. redistribution of AChRs from the extrasynaptic to synaptic sites (Ziskind-Conhaim et al., 1984);
6. lateral diffusion trap of receptors in the membrane (Edwards and Frisch, 1976; Phillips et al., 1993) involving cholesterol-rich lipid microdomains for enhancement of their stabilization through increased phosphorylation (Willmann et al., 2006);
7. increased stability of synaptic proteins within the cluster (Fambrough, 1979).

AChR clustering is thought to be controlled by nerve derived signals that act through different mechanisms (Burden, 2002). The proteoglycan agrin induces the aggregation of AChRs distributed diffusely in the plane of the membrane (McMahan, 1990). Agrin has also been proposed as the signal activating selective AChR transcription in myonuclei at the synaptic site (Meier et al., 1998; Lacazette et al., 2003). For a long time it was believed that neuregulin activate local transcription of AChR subunit genes (Fischbach and Rosen, 1997). However recent evidences have changed this belief (Yang et al., 2001; Escher et al., 2005) awarding agrin the main role in both transcription and clustering of AChR. Neurotransmitter ACh suppresses AChR transcription extrasynaptically (Lin et al., 2005).

1.3.1. Agrin

Agrin was purified from Basal lamina (BL) fractions from the electric organ of the *Torpedo californica* as a factor which aggregates AChR in cultured myotubes (Godfrey et al., 1984; Wallace et al., 1985). Further studies revealed that agrin is synthesized by motor neurons, transported down their axons, released into the synaptic cleft and stably integrated into the synaptic BL (Magill-Solc and McMahan, 1988,1990). Based on these findings, McMahan proposed the 'agrin hypothesis', which states that agrin is a nerve-derived postsynaptic organizing molecule (McMahan, 1990).

In order to verify the validity of the agrin hypothesis in vivo, mice with targeted deletion of agrin were generated (Gautam et al., 1996). Mice lacking agrin die at birth and display dramatically fewer AChR clusters at the NMJ (Gautam et al., 1996). The near absence

of AChR clusters in agrin deficient mice lends credibility to the idea that agrin is a key inducer of postsynaptic differentiation. This hypothesis is further strengthened by ectopic expression of agrin in skeletal muscle leading to new clusters of synaptic proteins (Cohen et al., 1997; Jones et al., 1997; Rimer et al., 1997).

The agrin gene encodes a protein of more than 2,000 amino acids with a predicted molecular mass of 225 kd (Fig.2). The extensive N- and O-linked glycosylation of the amino-terminal half increases the apparent molecular mass of agrin to ~600 kDa (Fig.2). Agrin has several isoforms generated by alternative RNA splicing with distinct biological activity and tissue distribution (see Table. 1.1). The isoforms that contain inserts in Y and Z sites in rodents have higher biological clustering activity (Ferns et al., 1992; Ruegg et al., 1992; Ferns et al., 1993; Gesemann et al., 1995). Agrin molecules with an eight amino acid insertion at Z position are at least 10,000 fold more active than agrins lacking this insertion (Ruegg et al., 1992; Ferns et al., 1993). A four amino acid insertion at the Y position caused a modest additional increase in the activity of agrin having an insertion at the Z position, and the Y insertion also seems to be involved in the binding of agrin to heparin and proteoglycans (Ferns et al., 1993; Hoch et al., 1994a).

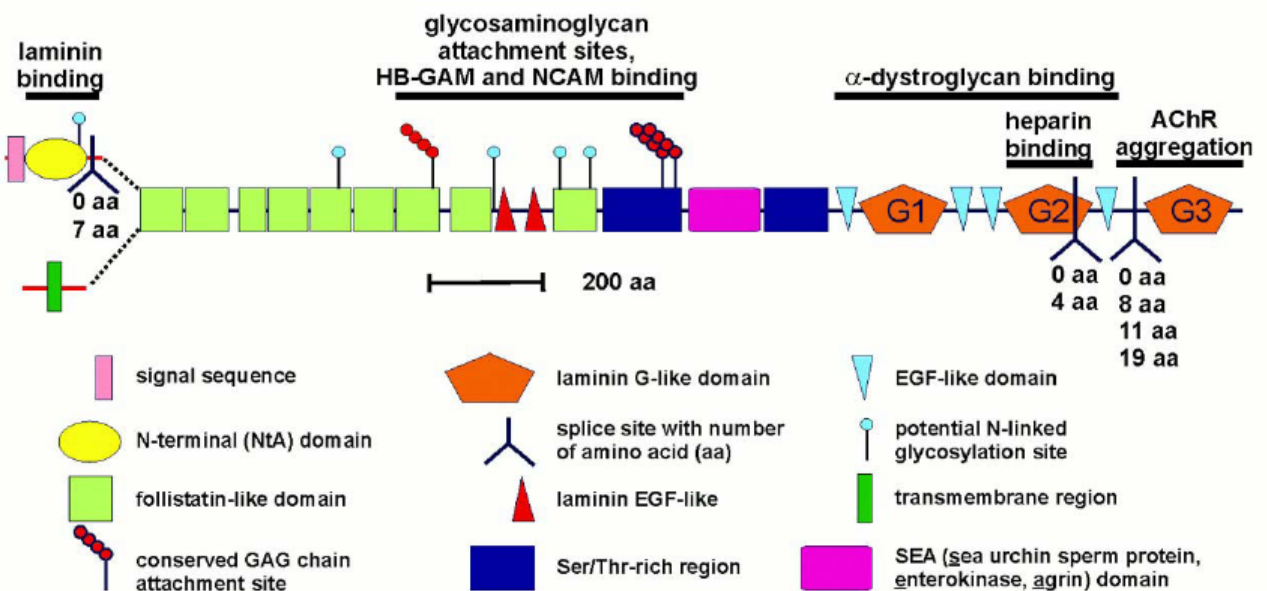


Fig. 2: Schematic representation of the structural domains predicted by the agrin cDNA. The protein modules are represented by the boxes indicated. The sites for alternative mRNA splicing with the possible number of amino acids are shown below the domain structure. Modified from (Kroger and Schroder, 2002).

Agrin synthesized by the nerve is spliced differently from muscle derived agrin isoforms and is of much greater importance for the induction of synapses than its muscle derived counterpart (Ruegg et al., 1992);

1. AChR clustering activity of nerve derived agrin is approximately 1000 fold higher than that of the muscle derived isoforms (Cohen and Godfrey, 1992; Ruegg et al., 1992; Ferns et al., 1993; Hoch et al., 1993);
2. NMJs in mice lacking nerve derived agrin, but not muscle derived agrin, resemble NMJs in mice lacking all forms of agrin (Burgess et al., 1999).

Agrin induced clustering of AChR involves the co-clustering of multiple associated proteins, several of which have been identified to date (Sanes and Lichtman, 1999,2001). These include the muscle specific receptor tyrosine kinase (MuSK) (Glass et al., 1996b), the linker protein rapsyn (Apel et al., 1997) and the scaffolding proteins dystroglycan and utrophin (Jacobson et al., 2001).

Tissue	Agrin N-Terminus C-Terminus	y site	z site
Neuromuscular junction			
Motor neurons	mainly SS-NtA	y+	z- and z+
Skeletal muscle	SS-NtA	mainly y-	z-
Central nervous system			
Overall	SS-NtA and TM	mainly y+	z- and z+
Glia	not determined	mainly y+	z-
Neurons	mainly TM	y+	z- and z+
Retina			
Retinal ganglia cells	TM	y+	z- and z+
Inner limiting membrane	?	?	z-
Inner / outer plexiform layer	?	y- and y+	z- and z+
Inner / outer nuclear layer	?	y- and y+	z- and z+

Table. 1.1: Tissue distribution of different agrin isoforms. Modified from (Bezakova and Ruegg, 2003).

More recently, the agrin hypothesis was challenged when two groups noted that some AChRs cluster in the absence of nerves (Anderson and Cohen, 1977; Frank and Fischbach, 1979; Lin et al., 2001; Yang et al., 2001). They found out that in embryonic day (E) 14.5 diaphragm muscles of wild type mice many of the AChR clusters confined to the center of the muscle are aneural. However, all clusters found at E16.5 in wild-type muscles are innervated (Lin et al., 2001). In addition, in the absence of both motornerves and agrin AChR clusters still formed (Lin et al., 2001). Remarkably, these AChR clusters localize to the central region of the diaphragm where the end-plate band would have formed (Lin et al., 2001). A close examination of agrin deficient mice revealed that prior to motor axon invasion of the myotome, AChR clusters initially form, but in the absence of agrin are not maintained (Lin et al., 2001).

These studies suggested two different possibilities:

1. some AChR clusters form aneurally in the absence of nerve derived agrin;
2. agrin may be required to stabilize the aneural clusters after axon myotube contact.

Secondly, a pair of studies revealed that acetylcholine (ACh) acts as a destabilizing factor on AChR clusters, and that agrin counterbalances this by stabilizing clustered AChRs (Lin et al., 2005; Misgeld et al., 2005). These studies revealed that AChR clusters initially form in agrin mutants, but as ACh is released, these clusters largely diffuse.

Genetic removal of ACh from agrin deficient mutants by deleting the enzyme responsible for generating ACh partially rescues the postsynaptic phenotype in these mice (Lin et al., 2005; Misgeld et al., 2005).

The dispersal mechanism of AChR remains to be clarified, but involves activation of the cytoplasmic kinase Cdk5 (Fu et al., 2005; Lin et al., 2005).

1.3.2. Muscle specific kinase (MuSK)

MuSK is a receptor tyrosine kinase supposed to be expressed specifically by skeletal muscle during synapse formation (Valenzuela et al., 1995; Glass et al., 1996b). A link between MuSK and in vitro by agrin induced postsynaptic differentiation is believed because of the following observations:

1. MuSK deficient myotubes failed to form AChR clusters in the presence of agrin,
2. a soluble, extracellular fragment of MuSK neutralized the ability of agrin to induce AChR clustering (Glass et al., 1996b; Glass et al., 1997),
3. AChR clusters can induce independently of agrin in cultured myotubes by the addition of anti-MuSK antibodies (Xie et al., 1997; Hopf and Hoch, 1998).

Supporting an in vivo role of MuSK in agrin signaling, genetic removal of MuSK results in mice that phenotypically resemble agrin deficient mice (DeChiara et al., 1996). MuSK $-/-$ mice die at birth and show no AChR clustering at all stages of embryonic development (DeChiara et al., 1996; Gautam et al., 1999). Generation of MuSK conditional mice demonstrated that MuSK is required not only for the initial formation of AChR clusters in embryogenesis but also throughout postnatal development to maintain postsynaptic apparatus and to control axonal growth (Hesser et al., 2006). Although it is obvious to assume that MuSK is the agrin receptor, agrin does not bind MuSK directly. Because agrin induces activation of MuSK in muscle cells but not in fibroblasts, and

because binding assays have generally failed to demonstrate direct interactions between the two proteins, a muscle cell surface component known as myotube associated specificity component (MASC) has been hypothesized. This hypothetical component is believed to be co-expressed on muscle surfaces with MuSK and to form together with MuSK the agrin receptor (Glass et al., 1996; Glass et al., 1997). Recombinant agrin added to myotubes can be cross-linked to MuSK on muscle surfaces, demonstrating the existence of a MuSK/agrin complex (Glass et al., 1996a; Glass et al., 1997).

The additional myotube specific component(s) are not known but could include:

1. a membrane protein that binds agrin and acts as a true agrin receptor (Jing et al., 1996);
2. a co-ligand that acts with agrin to bind and activate MuSK (Klagsbrun and Baird, 1991; Lopez-Casillas et al., 1991; Rapraeger et al., 1991; Ferns et al., 1993; Aviezer et al., 1994);
3. posttranslational modifications of MuSK that allow agrin to bind directly to MuSK (Binari et al., 1997).

Consistent with the latter possibility, certain glycosyltransferases are expressed selectively at synaptic sites in skeletal muscle (Scott et al., 1990), resulting in the concentration of certain carbohydrate epitopes, attached to proteins, at neuromuscular synapses (Scott et al., 1988). One such epitope is the cytotoxic T cell (CT) antigen, which is selectively expressed at both the pre- and postsynaptic sides of the NMJ. The CT antigen is an unusual modification in which a terminally sialylated galactosamine residue is further modified with an N-acetylgalactosamine by the CT GalNAc transferase (Martin, 2002). Neural agrin can induce autophosphorylation of immunopurified MuSK in the presence of carbohydrate precursors of the CT epitope, and expression of the CT transferase in HEK cells can increase MuSK phosphorylation in the presence of agrin (Parkhomovskiy et al., 2000). These results suggest that the CT antigen could comprise the MASC hypothesized to be necessary for agrin/MuSK binding. In support of this, it has recently been reported that agrin itself can bear the CT epitope (Xia and Martin, 2002).

The extracellular region of mammalian MuSK contain four immunoglobulin like domains and a cysteine-rich domain (Fig.3); in avian, fish and amphibians, the extracellular region also contains a kringle domain (Jennings et al., 1993; Valenzuela et al., 1995; Fu et al., 1999; Ip et al., 2000). The first Ig-like domain is required for agrin responsiveness (Zhou et al., 1999). MuSK mutants without the fourth Ig-like domain don't co-cluster with rapsyn, suggesting that this domain may be involved in interacting with rapsyn (indirectly via a hypothetic protein RATL, for rapsyn associated transmembrane linker) (Apel et al., 1995). Other noticeable domains include a conserved cysteine rich domain (CRD) known as C6-box, which shows homology to frizzled, a wnt receptor (Masiakowski and Yancopoulos, 1998; Saldanha et al., 1998) and a kringle domain of unknown function that is present in MuSK of *torpedo*, chick and *Xenopus* but absent from mammalian homologues (Jennings et al., 1993; Fu et al., 1999; Ip et al., 2000).

The intracellular region of MuSK contains a 50 amino acid juxtamembrane domain, a kinase domain and a short, eight amino acid carboxyterminal tail (Fig.3). The C-terminus of MuSK contains the consensus sequence for binding to PDZ domains (Fig.3).

However, MuSK mutants with a deletion of the PDZ binding motif are still able to cluster AChRs (Zhou et al., 1999; Herbst and Burden, 2000; Herbst et al., 2002).

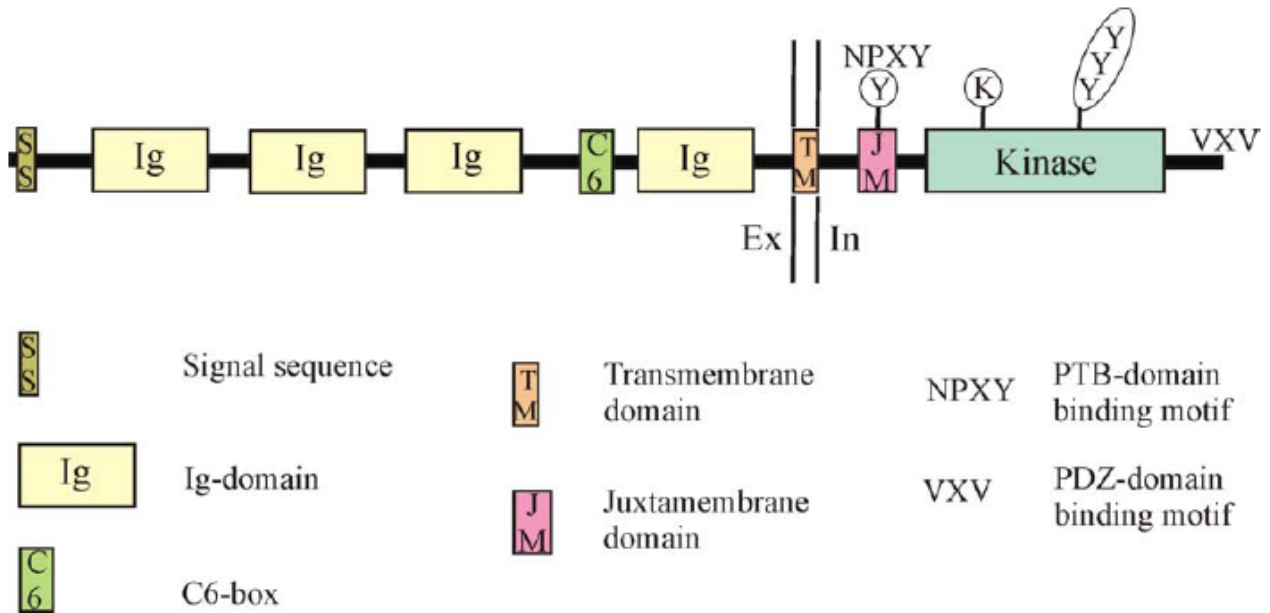


Fig.3: Schematic structure of MuSK. Modified from (Willmann and Fuhrer, 2002)

Stimulation of MuSK by agrin leads to: (1) the clustering of muscle derived proteins, like MuSK, AChRs and ErbBs, (2) activation of synapse-specific gene expression, (3) induction of a retrograde signal for presynaptic and postsynaptic differentiation (DeChiara et al., 1996; Gautam et al., 1996) and (4) stimulation of rapid phosphorylation of MuSK. The kinase activity of MuSK is essential to stimulate clustering and tyrosine phosphorylation of AChR β - and δ -subunits. MAP kinase, PI3-kinase and PLC gamma signaling pathways are neither activated nor required by agrin/MuSK signaling to stimulate AChR clustering (Wallace, 1988; Herbst and Burden, 2000).

MuSK contains nineteen intracellular tyrosine residues. Six of the nineteen are phosphorylated in activated MuSK: the juxtamembrane tyrosine (Y553), the tyrosines within the activation loop (A loop) (Y750, Y754, and Y755), a tyrosine near the beginning of the kinase domain (Y576), and a tyrosine (Y812) within the C-terminal lobe of the kinase domain (Watty et al., 2000). These phosphorylated tyrosines may act as docking sites for signal transducing molecules (Watty et al., 2000). Mutation of all three tyrosines in A loop destroys AChR clustering (Herbst and Burden, 2000) and each A loop autophosphorylation incrementally increases catalytic efficiency (Wei et al., 1995; Favelyukis et al., 2001). Ty-553, an autophosphorylation site in the Juxtamembrane region of MuSK (Watty et al., 2000), also appear to be important for kinase activation; a Tyr-553 \rightarrow Phe mutant form of MuSK does not undergo A loop autophosphorylation in vivo (Herbst and Burden, 2000). Tyr-553 is part of a consensus sequence (NPXY) for phosphotyrosine-binding (PTB) domain (Hopf and Hoch, 1998b). This segment of the MuSK juxtamembrane region has been shown to be essential for downstream signaling. A chimeric receptor containing only this segment of MuSK in the context of the

cytoplasmic domain from the RTK TrkA is capable of inducing AChR clustering upon agrin stimulation (Herbst and Burden, 2000). Kinase domain of MuSK is important for proper orientation of NPXY motif in the JM domain of MuSK (Till et al., 2002).

Activated MuSK clusters MuSK (Jones et al., 1999; Moore et al., 2001), and this positive feedback mechanism may be important to achieve an adequate level of MuSK expression at the synapse, sufficient to cluster more than 10 million AChR molecules per synapse.

Moreover, MuSK is unusual among receptor tyrosine kinases because its kinase activity is not sufficient to mediate all aspects of agrin responsiveness, primarily as measured by AChR clustering (Glass et al., 1997): a chimera composed of the neurotrophin receptor (trkC kinase) ectodomain fused to the MuSK cytoplasmic domain is activated by neurotrophin, but does not induce AChR clustering (Glass et al., 1997; Jones et al., 1999).

Thus, the MuSK ectodomain appears to play roles in addition to that of ligand binding. MuSK ectodomain may help to activate parallel signaling pathway or recruit other critical organizing components of the NMJ to a developing scaffold.

1.4. Signaling downstream of MuSK

1.4.1. Src kinases

Agrin induces tyrosine phosphorylation of the AChR β - and δ -subunits (Wallace et al., 1991; Qu and Haganir, 1994; Ferns et al., 1996). However tyrosine phosphorylation of AChR is not sufficient to cluster AChRs (Glass et al., 1997). Moreover, mutant AChRs lacking cytoplasmic tyrosine residues in β -subunits can still be recruited into clusters in muscle cells (Meyer and Wallace, 1998). It is thought that tyrosine phosphorylation facilitates the interaction of AChRs with cytoskeletal proteins such as F-actin (Dai et al., 2000), leading to focal accumulation of AChR through lateral diffusion. Inhibition of tyrosine phosphorylation of the β -subunit attenuates AChR clustering and increases AChR detergent extractability (Fuhrer and Hall, 1996; Borges and Ferns, 2001; Mohamed et al., 2001). A down stream kinase appears to be essential for agrin mediated signaling, since staurosporine blocks agrin induced AChR clustering and phosphorylation without inhibiting MuSK phosphorylation (Wallace, 1994; Fuhrer et al., 1997). This kinase may be a member of the Src family kinases (SFKs) (Fuhrer and Hall, 1996). Indeed, agrin causes rapid activation of Src-related kinases (Mittaud et al., 2001). Agrin activation of Src or Src-like kinases requires rapsyn (Mohamed and Swope, 1999; Borges and Ferns, 2001; Mittaud et al., 2001; Mohamed et al., 2001). SFKs bind to and phosphorylate the nicotinic acetylcholine receptor of skeletal muscle (Fig.5 (Mohamed et al., 2001)). The association of the receptor with the SFKs is mediated by high affinity binding of AChR subunit to the Src homology 2 (SH2) domains of the kinases (Swope and Haganir, 1994). Studies of mutant mice indicate that Src, Fyn, and Yes are not required for the formation of AChR clusters but are necessary for stabilization of agrin induced clusters (Smith et al., 2001). They act by holding postsynaptic proteins together in clusters through stabilization of rapsyn-AChR interaction and AChR phosphorylation. In addition they control rapsyn protein levels and AChR cytoskeletal linkage (Sadasivam et al., 2005).

1.4.2. Rho-family GTPases

Rho GTPases function in regulating the cytoskeleton in various cells. AChR clusters are tightly associated with selective cell cytoskeletal proteins, either directly or indirectly, including actin (Lubit, 1984; Walker et al., 1985; Bloch, 1986; Hoch et al., 1994; Phillips, 1995; Bloch et al., 1997). Actin polymerization may be directly involved in AChR clustering in cultured *Xenopus* muscle cells (Dai et al., 2000). It was found that Cdc42 and Rac1 are activated by agrin, and inhibition of Cdc42 or Rac blocks agrin induced AChR clustering (Weston et al., 2000). Rac1 may be necessary for the initial phase of agrin induced AChR cluster formation and Rho activation crucial for the subsequent condensation of microclusters into full size AChR clusters (Weston et al., 2003). Studies suggest that downstream of the small GTPases may be p21-activated kinase (PAK), a cytoplasmic kinase involved in cytoskeleton regulation (Luo et al., 2002). PAK in muscle cells is activated by agrin in a manner dependent on Cdc42 or Rac1 and inhibition of PAK attenuates agrin/MuSK mediated AChR clusterin (Luo et al., 2002).

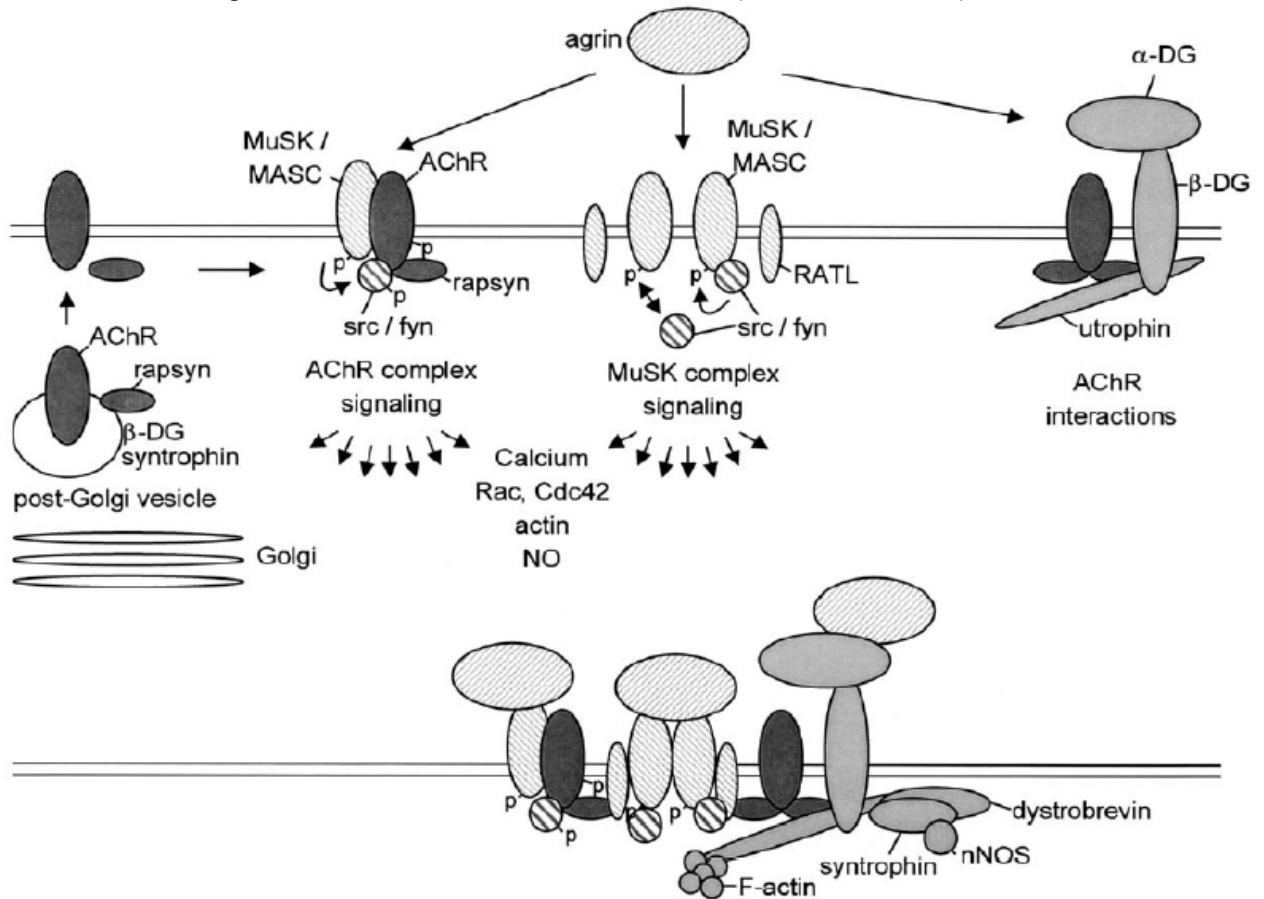


Fig. 5: Agrin induced signaling cascades leading to assembly of the postsynaptic membrane at the NMJ. In the absence of nerve-derived agrin, at least two pre-assembled signaling complexes (AChR complex and a MuSK complex) exist in the muscle membrane. Agrin causes rapid activation of MuSK, which triggers downstream

signaling cascades with the involvement of calcium, Rac, Cdc42, NO, and actin. Upon agrin stimulation Src/Fyn kinases phosphorylate MuSK and AChRs. Preassembled AChR complexes bind to the MuSK complex through rapsyn. Dystrophin/utrophin glycoprotein complex (D/UGC) is additionally recruited, stabilizing the entire postsynaptic apparatus. α -DG, α -dystroglycan; p, tyrosine phosphorylation. Modified from (Huh and Fuhrer, 2002).

1.5. MuSK interacting proteins

1.5.1. MAGI-1c

Analysis of proteins associated with MuSK in *Torpedo* electric organ by cross-linking identified MAGI-1c (Strochlic et al., 2001). MAGI-1c is a membrane associated guanylate kinase (MAGUK) with inverted domain organization. By analogy with CNS synapses where MAGUKs play a primary role as scaffolding proteins that organize cytoskeletal signaling complexes at excitatory synapses (Fanning and Anderson, 1999), likewise, MAGI-1c might be involved in the formation of a specialized protein complex at the NMJ participating to the terminal differentiation of the NMJ (Strochlic et al., 2001).

1.5.2. Synaptic nuclear envelope-1 (Syne-1)

Synaptic nuclear envelope-1 (Syne-1) was identified in yeast-two-hybrid screens using cytoplasmic domain of MuSK (Apel et al., 2000; Grady et al., 2005). Syne-1 is selectively associated with synaptic nuclei. Its location and structure raise the possibility that Syne-1 may be involved in the formation or maintenance of nuclear aggregates at the neuromuscular junction (Apel et al., 2000; Grady et al., 2005).

1.5.3. Dishevelled

Dishevelled was discovered through yeast-two-hybrid screen using the entire cytoplasmic region of MuSK as bait (Luo et al., 2002). Dishevelled is a cytoplasmic protein which contains three conserved domains: DIX (Dishevelled Axin), PDZ and DEP (Dishevelled- Egl-10 Pleckstrin) (Cadigan and Nusse, 1997; Dale, 1998). MuSK interacts directly via the JM and kinase domain with the DEP domain of Dishevelled. Dishevelled mutant that did not interact with MuSK inhibited the ability of agrin to induce AChR clustering indicating that agrin induced AChR clustering involves the Dvl-MuSK interaction (Luo et al., 2002). Dishevelled also interacts with the serine/threonine kinase PAK1 (p21-Activated Kinase) and involve in agrin induced activation of PAK1 in muscle cells (Luo et al., 2002). PAK1 is an effector of Rac and Cdc42 in actin reorganization. Dishevelled, by forming a scaffold with MuSK and PAK1, would thus regulate AChR clustering mediated by agrin (Luo et al., 2002).

1.5.4. CollagenQ (ColQ)/Acetylcholinesterase (AChE)

At the NMJ, AChE is present as asymmetric three tetramers of catalytic subunits which are associated with a structural collagenic tail named ColQ (Legay, 2000). ColQ is responsible for the accumulation of AChE in the synaptic basal lamina (Arikawa-Hirasawa et al., 2002). MuSK is also responsible for the accumulation of AChE at the synapse. In MuSK^{-/-} mouse AChE doesn't cluster (DeChiara et al., 1996) and MuSK injected ectopically in soleus muscle induces the formation of AChE clusters (Sander et

al., 2001). MuSK and ColQ can be cross-linked in situ in *Torpedo* AChR-rich membranes. Both proteins colocalize and coimmunoprecipitate in COS-7 cells after ectopic expression. Moreover, MuSK is required to form cell surface AChE clusters in cultured myotubes (Cartaud et al., 2004).

1.5.5. Src homology 2-domain-containing tyrosine phosphatase 2 (Shp2)

Tyrosine phosphatases interact with MuSK and regulate its tyrosine phosphorylation. It helps to define the AChR boundaries and dispersal of hot spot (Madhavan et al., 2005). For functional MuSK activation in muscle cells tyrosine phosphatase inhibition is sufficient (Meier et al., 1995). Shp2 is a tyrosine phosphatase which expresses in skeletal muscle and localizes at NMJs (Tanowitz et al., 1999). MuSK interacts specifically with Shp2; however the depletion of Shp2 cannot activate MuSK maximally. Which suggest other tyrosine phosphatases might be involved in regulating MuSK activity (Madhavan et al., 2005).

1.5.6. 14-3-3 γ

14-3-3 γ was identified through chemical cross-linking experiments in purified postsynaptic membrane from *Torpedo* electrocytes. The 14-3-3 γ protein co-localizes with+ AChRs at the NMJ in rat muscles and coimmunoprecipitates with MuSK (Strochlic et al., 2004). 14-3-3 proteins constitute an emerging family of signaling molecules present in eukaryotic organisms involved in intracellular signaling (van Hemert et al., 2001). Over expression of 14-3-3 γ in muscle cells specifically represses transcription of several synaptic genes including α -, δ - and ϵ -AChR subunits, utrophin, rapsyn and MuSK. The 14-3-3 proteins are known to interact and modulate the activity of Raf-1 (Fu et al., 1994). 14-3-3 γ represses synaptic gene transcription by interfering with the MAPK/PI3 signaling pathways activated through NRG/ErbB (Tansey et al., 1996; Altioek et al., 1997). 14-3-3 γ does not play a significant role in the clustering of AChR (Strochlic et al., 2004). In vivo 14-3-3 γ expression in muscle fiber display severe morphological perturbations of the NMJ (Strochlic et al., 2004). Interaction of MuSK with 14-3-3 γ suggests the involvement of MuSK in the regulation of synaptic gene expression at the NMJ. Consequently, inhibition of the ϵ -AChR subunit expression is more effective when 14-3-3 γ and MuSK were co-expressed then when the 14-3-3 γ was expressed alone (Strochlic et al., 2004).

1.5.7. Abelson tyrosine kinases (Abl)

Abl1 and Abl2 (also known as Abelson and Arg respectively) are non-receptor tyrosine kinases. They have SH2 and SH3, a tyrosine kinase and a unique C-terminal actin binding domain (Van Etten et al., 1994; Wang et al., 2001; Pendergast, 2002). They are involved in reorganization of cytoskeleton (Lanier and Gertler, 2000; Pendergast, 2002). In *Drosophila* Abl kinases are involved in axon guidance (Wills et al., 1999a; Wills et al., 1999; Lanier and Gertler, 2000; Pendergast, 2002). Abl kinases are localized to the postsynaptic membrane of neuromuscular junction (Finn et al., 2003). Expression of Abl kinases increases during development as has been shown for MuSK and Rapsyn (Finn et al., 2003). Abl kinases interact with MuSK and phosphorylate it which can either increase the kinase activity of MuSK or create new docking sites for signaling molecules

downstream of MuSK. In turn MuSK also phosphorylates Abl kinases. Blocking of Abl kinases in C2C12 myotubes affects agrin-induced acetylcholine receptor clustering (Finn et al., 2003).

1.5.8. Geranylgeranyltransferase 1 (GGT-1)

GGT is involved in prenylation (Zhang and Casey, 1996). Prenylation is the addition of prenyl molecules to a protein to enable its attachment to the cell membrane. MuSK interacts with α G/F subunit of GGT through its kinase domain (Luo et al., 2003) which results in an increase in tyrosine phosphorylation of α G/F subunit. Increase in tyrosine phosphorylation of GGT correlates with its increase in activity (Luo et al., 2003). Activation of Rac1 and the subsequent activation of PAK1 require prenylation by GGT (Luo et al., 2003). Inhibition of GGT leads to attenuation in agrin-induced activation of Rho-GTPases, AChR clustering and NMJ formation (Luo et al., 2003).

1.5.9. Protein interacting with C kinase (PICK1)

PICK1 was originally isolated due to its interaction with protein kinase C α (PKC α) (Staudinger et al., 1995; Staudinger et al., 1997). PICK1, a PDZ domain-containing protein, interacts with the C-termini of α -amino-3-hydroxy-5-methyl-isoxazole-4-propionic acid (AMPA) receptors at excitatory synapses (Xia et al., 1999). PICK1 may play an important role in the modulation of synaptic transmission by regulating the synaptic targeting of AMPA receptors (Xia et al., 1999).

1.5.10. Docking Protein -7 (Dok-7)

Dok-7 is a cytoplasmic protein composed of a pleckstrin-homology (PH) and PTB domains in the N-terminal portion and Src homology 2 (SH2) domain target motifs in the C-terminal region (Carpino et al., 1997; Yamanashi and Baltimore, 1997; Crowder et al., 2004). Dok-7 binds to MuSK through the PTB domain in a manner dependent on the tyrosine phosphorylation of its target motif in MuSK (Okada et al., 2006). However, PH domain, PTB domain and C-terminal all are required for the activation of MuSK in fully differentiated myotubes by Dok-7 (Okada et al., 2006). Dok-7 is essential for the formation of nerve- and agrin-independent and dependent clusters (Okada et al., 2006).

1.5.11. Protein kinase CK2

CK2 is a highly conserved, ubiquitously expressed serine/threonine kinase present in all eukaryotes (Meggio and Pinna, 2003; Olsten and Litchfield, 2004). It is involved in many biological processes, such as proliferation, apoptosis, differentiation and tumorigenesis. The CK2 holoenzyme consists of a tetramer of two catalytic (α/α') and two regulatory (β) subunits (Meggio and Pinna, 2003). CK2 interacts and colocalizes with MuSK at postsynaptic specializations. CK2 mediates phosphorylation of serine residues within the kinase insert (KI) of MuSK which is important for the maintenance of AChR clusters. Inhibition or knockdown of CK2, or exchange of phosphorylatable serines by alanines within the KI of MuSK, impairs acetylcholine receptor (AChR) clustering, whereas their substitution by residues that imitate constitutive phosphorylation led to aggregation of AChRs even in the presence of CK2 inhibitors. Moreover, muscle-specific CK2 β

knockout mice develop a myasthenic phenotype most likely due to impaired muscle endplate stability (Cheusova et al., 2006).

1.5.12. Src-class kinases (SFKs)

Src family of protein tyrosine kinases are non-receptor tyrosine kinase. Src family kinases are composed of six distinct functional regions (i) the Src homology (SH) 4 domain, (ii) the unique region, (iii) the SH3 domain, (iv) the SH2 domain, (v) the catalytic domain, and (vi) a short negative regulatory tail (Brown and Cooper, 1996). Srcclass kinases (Src and Fyn) interact with MuSK through its phosphotyrosine-SH2 domain and mediate the effects of agrin-activated MuSK to regulate clustering and anchoring of AChRs in skeletal muscle (for detail see. 1.4.1. (Mohamed et al., 2001).

1.5.13. Putative ariadne-like E3 ubiquitin ligase (PAUL)

E3 ubiquitin ligase together with ubiquitin activating enzyme E1 and ubiquitin conjugating enzyme E2 covalently attaches ubiquitin to a lysine residue on a target protein. The E3 ubiquitin ligase is typically involved in polyubiquitination which marks proteins for degradation by the proteasome (Sun, 2006). Putative ariadne-like E3 ubiquitin ligase (PAUL) was isolated by yeast-two-hybrid screens by virtue of its interaction with the cytoplasmic domain of MuSK. Paul is expressed at NMJs in muscle fibers but is not concentrated in AChR rich areas (Bromann et al., 2004). It has been recently shown that E3-dependent ubiquitination also serve as a regulatory mechanism for signaling and trafficking of several receptors (de Melker et al., 2001; Shenoy et al., 2001).

2.Aim of the study

Studies published so far have put MuSK in the centre of the signalling process leading to neuromuscular development. However many aspect of this signalling process leading to and from MuSK are not fully worked out yet. To elucidate the signalling mechanism at NMJ we have undertaken a yeast-two-hybrid approach for the identification of proteins involved in signalling down-stream from MuSK. After the yeast-two-hybrid screen MuSK binding partners were further characterized and their biological role for NMJ development was assessed. One of the identified proteins interacting with the intracellular domain of MuSK was the carboxy-terminal part of ErbB2 interacting protein (Erbin). Epitope-mapping studies define the area of Erbin comprising amino acid residues between 1175 and 1229 in the carboxy terminus of the protein is necessary for its interaction with MuSK. This interaction was further characterized and its biological role for NMJ development and function, was assessed.

3. Material and methods

3.1. Materials

3.1.1. Reagents

Basic solutions and reagents used have been purchased from Roche MolecularBiochemicals (Mannheim), Carl Roth (Karlsruhe), Promega (Mannheim), Sigma(Deisenhofen) or R&D Systems (Minneapolis, USA). Specific reagents used are listed below.

Yeast-two-hybrid:	
5-bromo-4-chloro-3-indoxyl-beta-D galactopyranoside (X-Gal)	Sigma
β -Mercaptoethanol	Sigma
3-amino-1,2,4-triazole (3-AT)	Sigma
DMSO	Roth
Minimal SD Base media	Clontech
Amino acids for drop out (DO) supplement	Sigma
Yeast cells AH109, HF7c	Clontech
Carrier DNA	Clontech
YPD Medium	Clontech
Agar	Bacto
<i>E. coli:</i>	
BL21(Rosetta) Competent cells	Novagen
<i>Escherichia coli</i> XL1-Blue Competent cells	Novagen
Isopropyl-beta-D-thiogalactoside (IPTG)	Sigma
LB Broth	Sigma
Molecular Biology and Biochemistry Standard Techniques:	
Agarose electrophoresis grade	Gibco/BRL
Ethidiumbromid	Gibco/BRL
DEPC-treated water	Roth
Oligo-dT	Invitrogen
dNTPs	Fermentas
DNA polymerase 10xBuffer, Mg free	Fermentas
MgCl ₂	Fermentas
MgCl ₂	Fermentas
Ampicillin	Sigma
Luciferin	Promega
TRIzol	Invitrogen
Rotiphorese gel 40 (40% w/v acrylamide solution with 0.8% bisacrylamide in ratio 29:1)	Roth
TEMED	Roth
Dithiothreitol (DTT)	Roth
Protease inhibitor cocktail tablets-Complete and EDTA free	Applichem

Phenylmethanesulfonylfluorid (PMSF)	Roche
Lysozyme	Roth
Coomassie Brilliant Blue	Roche
Protein A Sepharose CL4-B	Amersham
Ni-NTA agarose	Qiagen
Glutathione Sepharose™ 48	Amersham
Ammonium Persulphate (APS)	Roth
Nitrocellulose membrane PROTRAN BA85	Schleicher & Schuell Bioscience
P81 phosphocellulose paper	Whatman
NRG1 -β1/HRG1-β1 Extracellular Domain	R&D Systems
Immunocytochemistry:	
Sodium azide	Sigma
Bovine Serum Albumin (BSA)	Sigma
Fetal Calf Serum (FCS)	Serva
Mowiol	Invitrogen
Proteinase K	Roth
Radiochemicals:	
γ-32P ATP	Amersham

3.1.2. Devices

Horizontal gel electrophoresis apparatus (33 cm x 42 cm)	Gibco/BRL
Horizontal gel electrophoresis apparatus	OWI
Electrophoresis Power Supply PS 304	Life Technologies
Vertical mini-gel system	Sigma
Video documentation system for DNA Gels	Biometra
Gel-Blotting apparatus Multiphor II	Pharmacia
Film developer X-Omat 1000 Prozessor	Kodak
Gel dryer SE1160	Hoefel Scientific Instruments
Phosphoimager	Molecular Dynamics
Water Bath	GFL
Centrifuge 5415D	Eppendorf
Centrifuge 5417R	Eppendorf
Centrifuge 5810R	Eppendorf
Centrifuge RC 5B Plus	Sorvall
Spectro Photometer Ultrospec 3000	Pharmacia
Vortexer REAX2000	Heidolph
Thermo mixer compact	Eppendorf
Luminescence reader Lumat LB9501	Berthold
PCR-Thermocycler PTC-2000 Peletier Thermal Cycler	MJ Research

Lightcycler	Roche
Glass Teflon homogenizer	Wheaton
Homogenizer	Kinematica AG (Dispersing and Mixing Technology)
Ultrasonic Desintegrator Sonifier	Branson
Confocal laser-scanning microscope (LSM 5 Pascal)	Leica
Microscope MZ75	Leica
Microscope DMIL	Leica
Inverted microscope (DMIRB) equipped with a cooled MicroMax CCD camera	Leica/ Princeton Instruments
Cryotom CM3050S	Leica Microsystems, Nussloch
Liquid Scintillation machine	Wallac 1410 Pharmacia

3.1.3. Oligonucleotides

Oligonucleotides were synthesized by MWG-Biotech AG or Invitrogen. Their positions on the relative transcripts are indicated and correspond to the beginning of the coding sequence for forward (-bp) and the end of complementary sequence for reverse (bp-) primer.

Name of the primer	Sequence (5'-3')	Restriction site	Acc.No.	Position (bp)
Agrin-1	GTGGCGGCCGCAGCTGGAGATGCAGAGGCCA	Not I	M94271.1	-5275
Agrin-2	CGAAGATCTCTATTTGGCTGAGCAGTG	Bgl II	M94271.1	5869-
MUSK-10	CGGAATTCAGCGGGACTGAGAACTTC	EcoR I	NM_010944.2	-52
MUSK-19	CGCGGATCCTTAGCAGCAGTAGATGCCATC	BamH I	NM_010944.2	297-
MUSK-20	CGCGGATCCTTACGGCAGAACTGCCCTTCAA	BamH I	NM_010944.2	424-
MUSK-21	ACGCGTCTGACTTAGGAGTACGCAGGCGAGAC	Sal I	NM_010944.2	1476-
MuSK-22	CCGGAATTCGAGTCGACCGCGGTGACC	EcoR I	NM_010944.2	- 1585

MuSK-23	CGCGGATCCTTACAGGCTGAGCAACTT AGG	BamH I	NM_010944 .2	1701-
MuSK-38	GGAATTCTATTGCTGCCGAAGGAGGA AA	EcoR I	NM_010944.2	1552-
MuSK-61	ACGCGTCTGACTTACTTGGGATTCAGAA GGA	Sal I	RNU34985	-1809
MuSK-62	ACGCGTCTGACTTAGCGCTGCAGGATCC GGT	Sal I	RNU34985	-2164
MuSK-63	ACGCGTCTGACTTACAGGTCCTGTGGC TGA	Sal I	RNU34985	-2688
MuSK-64	ACGCGTCTGACTTAGACGCCTACCGTTC CCA	Sal I	RNU34985	-2724

Table 3.1: Oligonucleotides, which were used for the generation of MuSK bait plasmids for a yeast-two-hybrid screening and mapping experiments.

Name of the primer	Sequence (5'-3')	Restriction site	Acc.No.	Position (bp)
Erbin-11	CGGAATTCCGTGTCCTCCACAGCCT CT	EcoR I	NM_018695.2	-3238
Erbin-12	CGGAATTCCGTACTTCGACATATTG AA	EcoR I	NM_018695.2	-3598
Erbin-13	CGGAATTCCCCTCCATATACACAG CCC	EcoR I	NM_018695.2	-3781
Erbin-14	CCGCTCGAGTTATGAGGAACTTC TCG	Xho I	NM_018695.2	4116-
Erbin-16	CCGCTCGAGTTACGAGCACTCTGA GGTCTTG	Xho I	NM_018695.2	3437-
Erbin-17	CCGCTCGAGTTATTCAATATGTCGA AGTAC	Xho I	NM_018695.2	3613-

Table 3.2: Oligonucleotides used for subcloning of Erbin epitopes into yeast-two-hybrid prey vectors.

Primer	Sequence (5'-3')	Restr. site	Acc.No.	Position (bp)
Erbin-2	ATAGGTACCGTGTCTCCACAGCCTCT	Kpn I	NM_018695.2	-3238
Erbin-3	ATAGGTACCGTACTTCGACATATTGAA	Kpn I	NM_018695.2	-3598
Erbin-4	ATAGGTACCCCTCCATATACACAGCCC	Kpn I	NM_018695.2	-3781
Erbin-5	ATAAAGCTTTTATGAGGAACTTCTCG	Hind III	NM_018695.2	4116-
Erbin-6	ATAGGTACCCCTCAGCTCCTTCCTAGA	Kpn I	NM_018695.2	-3019
Erbin-10	CCCAAGCTTTTAAGAGGCTGTGGAGGACAC	Hind III	NM_018695.2	3255-
Erbin-15	AACTGCAGGCTTCACCATGACTACAAAAC	Pst I	NM_018695.2	-1
Erbin-26	CCCAAGCTTGCCATGTCGCTGTCTACGAGG	Hind III	NM_021563.2	-37
Erbin-27	CCGCTCGAGTTAAAAGTCCTGGAGGTTTTCACA	Xho I	NM_021563.2	773-
Erbin-28	CCCAAGCTTAGTGCATTTAAAAATGACTACAAAACG	Hind III	NM_021563.2	-314
Erbin-29	ACGCGTCGACTGGCTCAATTAAGAAACATCAGG	Sal I	NM_021563.2	-275
Erbin-30	CGCGGATCCTTTGGGCTGATTAATCGAGG	BamH I	NM_021563.2	2193-
Erbin-31	AGCAGCATGAAGATCAGCAAG		NM_021563.2	-1882
Erbin-32	ATAGCGGCCGCCCCTCTAACCACAAGGTCCA	Not I	NM_021563.2	4615-
Erbin-45	CCGCTCGAGCATGACTACAAAACGAAGTTTG	Xho I	NM_018695.2	-1
Erbin-46	CCTAGGATTTGGTCTTTTTGAAGGAC	Avr II	NM_018695.2	3522-
Erbin-47	CCTAGGCCTTTGAGTAATGGAC	Avr II	NM_018695.2	-3636
Erbin-48	CTAGCTAGCTTATGAGGAACTTCTCGTAC	Nhe I	NM_018695.2	4118-
Erbin-62	CTAGGGCCCTTATGAGGAACTTCTCGTAC	Apa I	NM_018695.2	4117-
GPI-3	CGGAATTCCGCTTTGACTCCAG	EcoRI	NM_005898.4	-1028
GPI-4	CCGCTCGAGTGGATTGGAATGG	Xho	NM_005898.4	1546-
NEDD-6	CCGCTCGAGTCAGAACGTTGCCATCTC	Xho I	NM_006403.2	2503-
NEDD	GGGAATTCGTCAAACCAGCCATGAC	EcoR I	NM_006403.2	- 1499
Phosphatase -3	CGGAATTCCG TGTTCACCAAGG	EcoR I	BC002657.2	-13
CK1 α -1	ATAGGATCCCATGGCGAGCAGCAGCGGCTC	BamH I	NM_146087.1	-1

Table.3.3: Oligonucleotides used for subcloning of CMV-driven plasmids.

Name of the primer	Sequence (5'-3')	Restriction site	Acc.No.	Position (bp)
MuSK-39	GGAATTCGTATTGCTGCCGAAGGAGG AAA	EcoR I	NM_010944	1552-
MuSK-40	CCGCTCGAGTTACTTAGGATTCAGAAG GAG	Xho I	NM_010944	-1698
MuSK-41	CCGCTCGAGTTAGCGCTGCAGGATCCT GTG	Xho I	NM_010944	-2580
MuSK-42	CCGCTCGAGTTACAGGTCAGTGTGGCT GAG	Xho I	NM_010944	-2055
MuSK-44	CCGCTCGAGTTAGACACCCACCGTTCC CTC	Xho I	MMU37709	-2755

Table.3.4: Oligonucleotides used for the PCR amplification of different MuSK intracellular domains for the generation of CMV - expression plasmids.

Erbin-9	CGGAATTCTACCTCCATATACACAGCC C	EcoRI	NM_018695.2	-3781
Erbin-10	CCCAAGCTTTTAAGAGGCTGTGGAGGA CAC	Hind III	NM_018695.2	3255-
Erbin-16	CCGCTCGAGTTACGAGCACTCTGAGGT CTTG	Xho I	NM_018695.2	3437-
Erbin-17	CCGCTCGAGTTATTCAATATGTGAAG TAC	Xho I	NM_018695.2	3613-
Erbin-18	CCGCTCGAGTTAGGGCTGTGTATATGG AGG	Xho I	NM_018695.2	3798-
Erbin-19	CGGAATTCGGCACGAGCTCGTGCCGC	EcoR I	NM_018695.2	-3017
Erbin-33	CCGCTCGAGTTATGTGCTGGATTGTA CTTCG	Xho I	NM_018695.2	3230-

Erbin-34	CGGAATTCCAGCAAGACATGGGGAAAT GT	EcoR I	NM_018695.2	-3148
Erbin-35	CCGCTCGAGTTAATTTCATTAATAGAG GGTCGAGCA	Xho I	NM_018695.2	3455-
Erbin-36	CGGAATTCTGATGCCAGGATCACAGAG A	EcoR I	NM_018695.2	-3356
Erbin-37	CCGCTCGAGTTATGCATTTGGTCTTTTT GAAGG	Xho I	NM_018695.2	3525-
Erbin-38	CGGAATTCGTGCTCGACCCTCTATTAAT GAAAT	EcoR I	NM_018695.2	-3431
Erbin-39	CCGCTCGAGTTAATAATTTGCCTGAGG CCTGA	Xho I	NM_018695.2	3687-
Erbin-40	CGGAATTCTTCGACATATTGAAGCCAA AAA	EcoR I	NM_018695.2	-3601
Erbin-41	CCGCTCGAGTTACTTGTTTTGCCAGTTC ATGG	Xho I	NM_018695.2	3838-
Erbin-42	CGGAATTCTGAAAGTGGCCCACCAG	EcoR I	NM_018695.2	-3763
Y2H-1	CCCCGGGCTGCAGGAATTCTGGCACG AG	Eco R I	pGAD.GH	- 839
Y2H-2	AATGGGTACCGGGCCCCCCTCGAGGT G	Xho I	pGAD.GH	908-

Table 3.5: Oligonucleotides used for the generation of pGEXKG constructs, expressing the GSTfusions of Erbin epitopes.

Name of the primer	Sequence (5'-3')	Acc.No.	Position (bp)
Erbin-22	CCAGGCTCTACAAGGCGGGCTCAGATTGCTGAAGG AGATTATTTATCATACAGAG	NM_018695.2	-3271
Erbin-23	CTCTGTATGATAAATAATCTCCTTCAGCAATCTGAG CCCGCCTTG TAGAGCCTGG	NM_018695.2	3325-

Erbin-24	CCACTCAGCGGGAAGAACTCCTGCAATGATGGCAG GATCACAGAGACCCCTTTCTGC	NM_018695.2	-3330
Erbin-25	GCAGAAAGGGGTCTCTGTGATCCTGCCATCATTGC AGGAGTTCTTCCCGCTGAGTGG	NM_018695.2	3386-
Erbin-43	CCAGAGAGAACTATGTCAGTTAGTGATTTCAATGC TTCACGGACTAGTCCTTCAAAAAGACCAAATGC	NM_018695.2	-3457
Erbin-44	GCATTTGGTCTTTTTGAAGGACTAGTCCGTGAAGCA TTGAAATCACTAACTGACATAGTTCTCTCTGG	NM_018695.2	3524-

Table.3.6: Oligonucleotides used for the generation of Erbin point mutants. Sites of mutation are underlined.

Name of the primer	Sequence (5'-3')	Restriction site	Acc.No.	Position (bp)
MuSK-83	CGGAATTCTACTATGGAATGGCCC ACGA	EcoR I	NM_010944.2	- 2403
MuSK-84	CCGCTCGAGTGGATACTGCAGAAG CTGGGTCT	Xho I	NM_01094.2	2555-
MuSK-86	CGCGGATCCTGCTGCCGAAGGAGG AAAGA	BamH I	NM_010944.2	- 1546
MuSK-87	CGGAATTCATACTCCAGGCTGAGC AACT	EcoR I	NM_010944.2	1707-

Table 3.7: Oligonucleotides used for the generation of pET28a constructs, expressing the Hisfusions of MuSK epitopes.

Name of the primer	Sequence (5'-3')	Acc.No.	Position (bp)	Product size (bp)
AChR α -1	ACGCTGAGCATCTCTGTCTT	NM_007389	810-	448
AChR α -2	TTGGACTCCTGGTCTGACTT	NM_007389	-1258	
MuSK-24	GCCTTGGTTGAAGAAGTAGC	NM_010944	115-	353
MuSK-25	CTTGATCCAGGACACAGATG	NM_010944	-488	
Erbin	CAGGAGAGTGTTGCCAAGAT	NM_021563.2	-3629	210
Erbin	CATGGCCTTGTCTAG GAG AA	NM_021563.2	3838-	
mbact-111	TGGAATCCTGTGGCATCCATGA AA	NM_007393	885-	350

mbact-112	TAAAACGCAGCTCAGTAACAGT CCG	NM_007393	-1235	
MuSK	GCT CTT CTC ACC ATC GCT AC	NM_010944	1519	
MuSK	GGA CAT ACT TCG GAG GAA CT	NM_010944	2010	
β -actin	TGG AAT CCT GTG GCA TCC ATG AAA	NM_007393	Pos. 806	
β -actin	TAA AAC GCA GCT CAG TAA CAG TCC G	NM_007393	Pos. 1154	
MuSK in rats	AGA GGA TGC CAC TCC TTC TG	NM_031061.1	Pos. 1661	
MuSK in rats	CGG AGG AAC TCA TTG AGG TC	NM_031061.1	Pos. 2000	
β -actin rats	TCT ACA ATG AGC TGC GTG TG	NM_031144.2	Pos. 269	
β -actin rats	CCA TCT CTT GCT CGA AGT CT	NM_031144.2	Pos. 682	

Table 3.8: Oligonucleotides pairs used for quantitative PCR reactions. Size of resulting PCR product is given in bp.

Name of the primer	Sequence (5'-3')	Restriction site	Acc.No.	Position (bp)
MuSK-52	ATAGGATCCACCGTGGTGCTTCC TAAGCTCAGAG	BamH I	Mouse Genomic locus	12865-
MuSK-53	ATAGAATTCGTTCTAAGTCTGCA GGCACAAGACCC	EcoR I	Mouse Genomic locus	-12865
MuSK-54	ATACGGACCGGTAGAACCGCTCC AATGACCTTTGTG	Rsr II	Mouse Genomic locus	14675-
MuSK-60	ATAGAGCTCGGATTTAGTAGTCA AATGAAGCAG	Sac I	Mouse Genomic locus	- 10246
MuSK-100	CTGGTTCCGTGTGTATGTGTG		Mouse Genomic locus	-9509

Table 3.9: Oligonucleotides used for the generation of MuSK conditional Knockout mice.

3.1.4. siRNAs

For silencing of Erbin, pSUPERneoGFP (Oligoengine) based shRNAs were used. Targeting sequences were designed using Sfold program (Ding et al., 2004). Targeting oligonucleotides were synthesized by Invitrogen.

Name	Target	Inhibition efficiency	Primers	Sequence of primers	Acc.No.	Pos.
pSuper Neo (E979)- Erbin-siR 36	Erbin	53%	Erbin-siRNA-1	GATCCCCACCATG TCGCTGTCTACGAT TCAAGAGATCGTA GACAGCGACATGG TTTTTTGGAAA	NM_021563.2	-36
			AGCTTTTCCAAAA siRNA-2	AACCATGTCGCTG TCTACGATCTCTTG AATCGTAGACAGC GACATGGTGGG		
pSuper Neo (E979)- Erbin-siR NA-175	Erbin	76%	Erbin-siRNA-3	GATCCCCGAAGAGCT TCCAAAGCAACTCA AGAGAGTTGCTTTGG AAGCTCTCTTTTTG GAAA	NM_021563.2	-175
			AGCTTTTCCAAAAAG siRNA-4	AAGAGCTTCCAAAG CAACTCTCTTGAAGT TGCTTTGGAAGCTCT TCGGG		

Table.3.10: Erbin siRNA

3.1.5. Enzymes

Restriction enzymes	New England BioLabs, Gibco/BRL, Roche, Fermentas
RNase A	Roth
M MuLV Reverse Transcriptase	New England Biolabs
APex TM Heat-Labile alkaline phosphatase	Epicenter
Taq DNA polymerase	Fermentas
T4 DNA ligase	Roche

3.1.6. Kits and Columns

Plasmid DNA Purification Kit (Nucleobond AX)	Macherey-Nagel
DNA Purification Kit (Nucleospin Extract)	Macherey-Nagel
High Pure Plasmid Isolation Kit	Roche
Quikchange XL Site-directed Mutagenesis Kit	Stratagene
Lightcycler-FastStart DNA Master SYBR Green Kit	Roche
Centricon Plus-20 Centrifugal Filter Device	Amicon bioseparations

3.1.7. Antibodies

Antigen (species)	Use and Dilution	Company/Suppliers
T7 (mouse monoclonal)	WB 1:10000 IP 1:1000	Novagen
Myc (mouse monoclonal)	WB 1:10000 IP 1:1000	Cell Signaling
α -HA (mouse monoclonal)	WB 1:10000 IP 1:1000	Cell Signaling
α -MuSK Rb194T (rabbit polyclonal)	WB 1:1000 IHC 1:1000 IP 1:10	Dr. Markus Ruegg, Biocenter, Basel, Switzerland
α -GFAP	IHC 1:500	Chemicon, Temecula, CA
α -glutamine synthetase mouse	IHC 1:500	BD Transduction Laboratories
α -choline acetyltransferase	IHC 1:1,000	Chemicon
α -Thy1 mouse	IHC 1:500	BD Transduction Laboratories
α -Agrin (AGR-540) mouse	IHC 1:500	Stressgen
α -MuSK 20kD (rabbit polyclonal)	WB 1:3000	self-generated

B. Secondary antibodies

Antigen (species)	Use and Dilution	Company/Suppliers
-------------------	------------------	-------------------

Goat anti-mouse IgG HRP-conjugated	WB 1:10,000	Amersham Pharmacia Biotech
Protein A HRP-conjugated	WB 1:3,000	Amersham Pharmacia Biotech
Cy2-cojugated goat anti-mouse IgG	IHC 1:100	Dianova
Cy2-cojugated goat anti-rabbit IgG	IHC 1:100	Dianova
Cy3-cojugated goat anti-mouse IgG	IHC 1:200	Dianova
Cy2-cojugated goat anti-mouse IgG	IHC 1:200	Dianova
Alexa (fluorescence) anti-rabbit IgG 488 (green) conjugated goat	IHC 1:500	Molecular Probes

3.1.8. Frequently used solutions

Solution name	Composition
10xDNA loading buffer	50% Glycerin, 0.1% Xylene cyanol FF, 0.1% Bromophenol blue
1xTBE buffer	88 mM Tris, 88 mM Boracid, 2 mM EDTA pH 8.3
3x Lamml buffer	187 mM Tris, 6% SDS, 30% Glycerin, 0.02% Bromophenol blue, 15% β -Mercaptoethanol
1xPBS	140 mM NaCl, 2.7 mM KCl, 8.1 mM Na ₂ HPO ₄ x 2 H ₂ O, 1.5 mM KH ₂ PO ₄
PBST	PBS, 0.1% Tween-20
Mowiol	6 ml water was added to 6.0 g Glycerol and 2.4 g Mowiol and left for 2 h at RT. Afterwards, 12 ml 0.2 M Tris pH 8.5 was added and the solution was rotated for 24 h at 53°C, followed by centrifugation at 3220 rcf and aliquoting. Mowiol solution was stored at -20°C for up to 12 months.

4% PFA	20 g Paraformaldehyde (PFA) was dissolved in 300 ml water (65°C). After pH was adjusted to 7.4 water was added up to 500 ml, and the solution was sterile filtered, aliquoted and stored at -20°C.
Tail lysis buffer	50 mM Tris-HCl pH 8.0, 100 mM EDTA, 0.1 M NaCl, 1% SDS

3.1.9. Cell culture

Human embryonic kidney 293 cells (HEK293)	American Type Culture Collection
Cos7	American Type Culture Collection
C2C12	Gift from Dr. Hans-Rudolf Brenner
MuSK-deficient myoblasts (MuSK ^{-/-}) C3.16	Gift from Drs. Ruth Herbst and Steven Burden
HEK293 cells expressing continuously secretable active (4.8.) or inactive (0.0) agrin	Gift from Dr. Stefan Kröger
Dulbecco's MEM (DMEM) with Glutamax TM -1 with Sodium Pyruvate and 4500 mg/L Glucose	Gibco/BRL
Fetal Calf Serum (FCS)	Invitrogen
Heat-inactivated Horse Serum (HS)	Invitrogen
Chick Embryo Extract (CEE)	SLI
Mouse recombinant interferon- γ	Sigma
Matrigel	Becton Dickinson
Apigenin	Sigma, HCLP grade
2-Dimethylamino-4,5,6,7-tetrabromo-1H-benzimidazole (DMAT)	Gift from Drs. Flavio Meggio and Lorenzo A. Pinna
Rhodamine- α -bungarotoxin (Rh- α -BTX) or Alexa- α -bungarotoxin (Alexa- α -BTX)	Molecular Probes, Eugene
SuperFect	Qiagen
Lipofectamine TM 2000	Invitrogen
DEAE-Dextran	Pharmacia, Sigma

3.2. Methods

Standard methods were performed according to: Sambrook, J., Russell D.W., Molecular Cloning: A Laboratory Manual, 3rd edition (Volume 1-2-3), Cold Spring Harbor Laboratory Press, 2001.

3.2.1. Molecular Biology Methods

3.2.1.1. Isolation of plasmid DNA

Up to 10 µg of plasmid DNA was isolated using the following protocol. Bacterial cells were pelleted by centrifugation. Cell pellet was resuspended in 100 µl of buffer S1 (50 mM Tris, 10 mM EDTA, 100 µg/ml RNase A pH 8.0). Then 200 µl of S2 buffer (200 mM NaOH, 1% SDS) was added and mixed gently by inverting to avoid shearing of the genomic DNA. After 5 min of incubation 150 µl of S3 buffer (2.8 M KAc pH 5.1) was added and mixed gently. The mixture was put on ice for 5 min. After 5 min of incubation mixture was centrifuged at 4°C (20000 rcf for 10min). To precipitate the plasmid DNA, 1 ml of absolute Ethanol was added to the supernatant, mixed and centrifuged at 4°C (20000 rcf for 10 min). The pellet was centrifuged once more with 300 µl of 70% Ethanol at 4°C (20000 rcf for 5 min), air dried, and resuspended in 50 µl water.

Larger amounts of plasmid DNA (20-2500 µg) was isolated with the use of Macherey-Nagel Plasmid DNA Purification Kit (Nucleobond AX) according the manufactures protocol, which is based on a modified alkaline lyses procedure followed by binding of plasmid DNA to an anion-exchange resin under appropriate low-salt and pH conditions. RNA, proteins and low molecular weight impurities were removed by a medium-salt wash; DNA is eluted in a high salt buffer and then concentrated and desalted by isopropanol precipitation.

3.2.1.2. Determination of DNA/RNA concentration

The concentration of DNA/RNA in solution was determined in a spectrophotometer, measuring the absorption of the solution at 260 nm and using the following formulas:

1A₂₆₀ = 50 µg double stranded DNA

1A₂₆₀ = 33 µg single stranded DNA

1A₂₆₀ = 40 µg RNA

3.2.1.3. Electrophoretic separation of DNA fragments in agarose gel

DNA was loaded on 0.7-2 % agarose gels prepared in 1xTBE buffer with 0.5 µg/ml ethidium bromide. The electrophoresis was performed for ~1 h at 120 V (Horizontal gel electrophoresis apparatus -Gibco/BRL). The DNA fragments were visualized under UV light.

3.2.1.4. PCR amplification of DNA

The Polymerase-Chain-Reaction (PCR) was performed according to the method of Saiki (Saiki et al., 1986). A standard PCR reaction to amplify DNA from plasmid template contained about 50 ng plasmid DNA, forward and reverse primers (10 pmol each), 200 µM dNTPs, 1xTaq-polymerase buffer + (NH₄)₂SO₄, 2 mM MgCl₂ and 1U Taq DNA polymerase (Fermentas), in a total volume of 50 µl.

The amplification was carried out in a PCR-Thermocycler PTC-2000 Peletier Thermal Cycler (MJ Research). The amplification conditions were as follows:

(1) Initial denaturation for 2 min at 94°C.

(2) 25-30 cycles of 10-30 sec at 94°C, 10-30 sec at the annealing temperature of the primer pair and extension of 1 min/kbp at 72°C.

(3) Incubation for 5 min at the extension temperature to allow for the complete amplification of all products.

The annealing temperature, the time of denaturation, annealing and the extension were optimized for each experiment. The PCR products were then analyzed in an agarose gel by separation according to their size.

3.2.1.5. Cloning techniques

The DNA fragment to be subcloned was amplified by PCR (see 3.2.1.4.) using specific primers containing unique restriction sites, analyzed on an agarose gel (see 3.2.1.3.) and purified either by using DNA Purification Kit - Nucleospin Extract (Macherey Machinery) or by the Tombstone procedure. To carry out the Tombstone procedure the gel area directly above (towards the cathode) and under (towards to anode) the band of the PCR product was cut and pieces of DE81 cellulose paper were inserted into the nicks.

During further migration of the DNA the desired PCR product was transferred and bound to the lower DE81 paper, while the upper DE81 paper prevented contamination of the PCR product with other DNA fragments. The DE81 paper with the PCR product was removed from the gel and placed into a 0.5 ml PCR tube with a hole at the bottom and inserted into the 1.5 ml Eppendorf tube. Residual TBE buffer was removed from the DE81 paper by centrifugation (16000 rcf for 30 sec.). DNA of the PCR fragment was eluted three times from the DE81 paper with high salt Tombstone buffer (1 M LiCl, 20% Ethanol, 10 mM Tris pH 7.5, 1 mM EDTA) and precipitated with three volumes of absolute Ethanol, washed with 80% Ethanol, air dried and dissolved in 20 µl of water. The purified PCR product and the subcloning vector were digested in a total volume of 20 µl comprising of about 1 U of restriction enzyme per 1 µg of DNA, 2 µl of 10x corresponding restriction buffer and sterile water. Digestion mixture was incubated at 37 °C for 1 hour. When the vector ends were blunt or compatible with each other, the vector was dephosphorylated prior to ligation to prevent self-ligation. To remove 5' phosphates from the vector, 1 U of APex™ Heat-Labile alkaline phosphatase (Epicenter) was added

directly to the digestion reaction. The reaction was incubated for 20 min at 37°C. Phosphatase was heat inactivated at 70°C for 5 min. After enzymatic digestion or dephosphorylation the vector or PCR product were purified by agarose gel electrophoresis. Before ligation the concentrations of PCR-fragment and vector were roughly estimated on an agarose gel. A typical ligation reaction contained vector and insert at a molar ratio of about 1:2 (600 ng total DNA), 1x ligase buffer (New England BioLabs), and 1 U of T4 DNA Ligase (New England BioLabs) in a volume of 10 µl. The incubation was carried out at RT for 5 h or at 16°C for 12-16 h. After that, 1 µl of the ligation reaction was transformed in *Escherichia coli* competent cells.

3.2.1.6. Plasmid constructs

Plasmid constructs generated according to the basic cloning techniques (3.2.1.5.) are listed in the Table 3.11. For primers sequences and Acc.No. position: see 3.1.3.

Plasmid name	Primers used for subcloning	Restriction digestion sites used for subcloning	Template used for PCR/subcloning
pCMX.PL1-T7-CK2 β	CK2 β -3/CK2 β -4	Hind III/Xho I	pGADGH-CK2 β -full length (fished by Y2H)
pCDNA3-6HA-CK1 α 1	CK1 α 1-1/CK1 α 1-2	BamH I/EcoR I	Brain 1st strand cDNA
pCDNA3-6HA-CK1 δ	CK1 δ -1/CK1 δ -1	BamH I/EcoR I	Brain 1st strand cDNA
pCDNA3-6HA-CK1 ϵ	CK1 ϵ -3/CK1 ϵ -4	EcoR I/Xho I	Brain 1st strand cDNA
pCDNA3-6HA-CK1 γ 1	CK1 γ 1-1/CK1 γ 1-2	BamH I/EcoR I	Brain 1st strand cDNA
pCDNA3-6HA-CK1 γ 3	CK1 γ 3-1/CK1 γ 3-2	BamH I/EcoR I	Brain 1st strand cDNA
pCDNA3-6HA-Fzd3	Fzd3-1/Fzd3-2	BamH I/EcoR I	Brain 1st strand cDNA
pCMX.PL1-T7-Fzd4	Fzd4-1/Fzd4-2	EcoR I/Pst I	Brain 1st strand cDNA
pCDNA3-6HA-LRP6	LRP6-1/LRP6-2	BamH I/Xho I	Brain 1st strand cDNA
pBSK+MuSK Long Left Arm	MuSK-60/MuSK-52	BamH I/Sac I	ES mouse Genomic DNA
pBSK+ MuSK Long Left Arm-LoxP	LoxP-BgIII-SacI-I/ LoxP-BgIII-SacI-II	Avr II	
pBSK+ MuSK Long Left Arm-LoxP-Neo		Hpa I/Sma I	pJNI-Neo vector
pBSK+ MuSK Long Left Arm-LoxP-Neo-Right Arm.	MuSK-53/MuSK-54	EcoR I/Rsr II	ES mouse Genomic DNA
pBSK+ MuSK Long Left Arm-LoxP-Neo-Right Arm-DT		Rsr II	pKO-DT
pCDNA3-6HA-ErbinY2H		BamH I/Xho I	pGAD-GH-Erbin-Y2H(fished by Y2H)
pCMV5-T7b-		Hind III/Not 1	pCDNA3-

MuSk2xwt			MuSK2xwt
pCMV5-c-myc-tag-Erbin-deletion mutants	Erbin -2, Erbin -3, Erbin -4, Erbin -5/Erbin -6	Kpn I/Hind III	pGAD-GH-Erbin-Y2H(fished by Y2H)
pCMV5-T7a-Erbin38		BamH I/Hind III	pGEX.KG-Erbin38
pCMV5-T7a-Erbin	Erbin-29/Erbin 30 Erbin-31/Erbin-32	Sal I/BamH I Hpa I/Not I	C2C12 1st strand cDNA
pCMV5-T7a-MuSk2xKD-myc		Hind III/Not I	pCDNA3-MuSK2xKD
pCMX.PL1-CKII	CK2 β -3/CK2 β -4	Hind III/Xho I	pGADGH-CK2 β -full length (fished by Y2H)
pCMX.PL1-Luc-Erbin-human	Erbin-10/Erbin-15	Pst I	pRK5-myc-Erbin
pCMX.PL1-Luc-Erbin-mouse	Erbin-26/Erbin-27	Hind III/Xho I	C2C12 1st strand cDNA
pCMX.PL1-T7-ERBIN-Y2H		EcoR I	pGAD-GH-Erbin-Y2H (fished by Y2H)
pCMX.PL1-T7-GPI-4	GPI-3/GPI-4	EcoR I /Xho I	pGAD.GH-GPI (fished by Y2H)
pCMX.PL1-T7-	Phosphatase-3/Y2H-3	EcoR I/Hind III	pGAD.GH-

Table 3.11. Plasmid constructs.

pcDNA-MuSK2xwt-myc and pcDNA-MuSK2xkd-myc constructs have been generated and kindly provided by the group of Prof. Hans-Rudolf Brenner. For their generation two intracellular domains of MuSK or its kinase defective mutant (aa 467-868; Acc.No. U34985) were linked together by five E/G (E-Glutamic Acid, G-Glycine) modules. The first intracellular MuSK domain was subcloned into Hind III/Nhe I of myc-tagged pcDNA3 (Invitrogen). The second intracellular MuSK domain was joined by ligation into the Nhe I and EcoR I sites of the plasmid.

For the generation of pSUPERneoGFP based siRNAs (3.1.4.) used for silencing of mouse Erbin a pair of oligonucleotides according to the following design was synthesized:

compatible with BgIII

5' – GATCCCCC (sense) **TTCAAGAGA** (anti sense) TTTTTGGAAA – 3'

3' – GGG (anti sense) **AAGTTCTCT** (sense) AAAAACCTTTTCGA – 5'

hairpin loop compatible with HindIII

Sense and anti sense specific sequences targeting the mRNA of corresponding genes were designed with the software Sfold (Ding et al., 2004). The oligos were hybridized

and subcloned into restriction digestion sites Hind III/Bgl II of pSUPERneoGFP(E979) (Oligoengine) destroying at the same time the Bgl II site.

CMV expression plasmids pCMX.PL1, carrying the luciferase gene and Erbin' cDNA as bicistronic message were constructed as follows. Luciferase gene was amplified by PCR from the plasmid pGL2-basic (using primers Luc-1: 5'-CGGGATCCATGGAAGACGCCAAAAAC-3' and Luc-2: 5'-CGGGATCCTTACAATTTGGACTTTCC-3' and subcloned into BamH I site of pCMX.PL1 (then named pCMX.PL1-Luc). Erbin cDNA was amplified from 1st strand cDNA from C2C12 myotubes and ligated into the Hind III/Xho I of pCMX.PL1-Luc.

3.2.1.7. Transformation of *E. coli* competent cells

While XL1-blue cells were used for subcloning of plasmid vectors, BL21 cells were used for protein expression. 1-10 ng of plasmid DNA or an aliquot from a ligation reaction (1 µl) were added to 50 µl of *E. coli* XL1-Blue or BL21 (Rosetta) electrocompetent cells (Novagen). The cell-DNA mixture was transferred into a prechilled electroporation cuvette (EquiBio). DNA was transformed into the bacteria cells by means of an electric impulse (1800 V, 7.5 ms). After electroporation the bacteria were shaken for 30 min at 37°C in 200 µl of LB medium, then plated on LB plates containing antibiotic (100 µg/ml ampicillin or kanamycin) and incubated at 37°C for about 16 h, until colonies appeared.

3.2.1.8. Site directed mutagenesis

Substitutions of P (Proline) residues by A (Alanine) within the pRK5-myc-Erbin and pGEXKG-Erbin-Y2H and Y (Tyrosine) by A (Alanine) within the pGEXKG-Erbin-38 were introduced, using the Quikchange XL Site-directed Mutagenesis Kit (Stratagene).

Primers for the site directed mutagenesis should fulfill the following criteria: have a length 25-50 bp, $T_m > 78^\circ\text{C}$ and carry a mutation of nucleotide(s), which would lead to the exchange of the desired amino acid without a shift in the open reading frame of the targeted gene. A plasmid carrying the target gene serves as a template for the mutagenesis PCR. Usage of PfuTurbo DNA-Polymerase ensures high fidelity of the PCR reaction. Dpn I digestion results in the elimination of the methylated form of the template plasmid. Remaining unmethylated plasmid produced by PCR and carrying the mutated gene is subsequently transformed into *E. coli* competent cells.

A 20 µl PCR reaction contains: 2 µl of 10x reaction buffer, 1.2 µl Quicksolution, 0.4 µl dNTP Mix, 125 ng of two primers and 10 ng of template plasmid. Combinations of the primers and templates used as well as the resulting mutations are indicated in the Table 3.12.

Primer combination	Template	Mutation	Resulted plasmid
Erbin22 and Erbin23	pGEX-KG-ERBIN 1118 PA + 1121 PA	P-1121 →A P-1118 →A P-1100 →A	pGEX-KG-ERBIN 1110 PA + 1118 PA + 1121 PA (3PA)
Erbin 22 and Erbin 23.	pGEX-KG-ERBIN-Y2H	P-1100 →A	pGEX-KG-ERBIN 1100 PA (1PA)
Erbin24 and Erbin25	pGEX-KG-ERBIN-Y2H	P-1121 →A P-1118 →A	pGEX-KG-ERBIN 1118 PA + 1121 PA (2PA)
Erbin43 and Erbin44	pGEX-KG-ERBIN38	Y-1164 →A	pGEX-KG-ERBIN38-YA
Erbin22 and Erbin23	pRK5-myc-ERBIN	P-1100 →A	pRK5-myc-ERBIN 1100 PA (1PA)
Erbin24 and Erbin25	pRK5-myc-ERBIN	P-1118 →A P-? →A	pRK5-myc-ERBIN 1118 PA + 1121 PA (2PA)
Erbin22 and Erbin23	pRK5-myc-ERBIN 1118 PA + 1121 PA	P-1110 →A P-1118 →A P-1121 →A	pRK5-myc-ERBIN 1110 PA + 1118 PA + 1121 PA (3PA)

Table 3.12: Combination of primers (see Table.3.6) and templates used for site directed mutagenesis of MuSK.

Mutagenesis PCR for pRK5-myc-Erbin was carried out according to the program indicated in the Table 3.13.

Step	Number of cycles	Temperature	Time
Denaturation	1	95°C	1 min
Amplification	18	95°C	50 sec
		60°C	50 sec
		68°C	10 min
Elongation	1	68°C	14 min

Table 3.13: The program of the site directed mutagenesis PCR for pRK5-myc-Erbin.

Mutagenesis PCR for pGEX-KG-ERBIN-Y2H was carried out according to the program indicated in the Table 3.14.

Step	Number of cycles	Temperature	Time
Denaturation	1	95°C	1 min
Amplification	18	95°C	50 sec
		60°C	50 sec
		68°C	7 min
Elongation	1	68°C	10 min

Table 3.14: The program of the site directed mutagenesis PCR for pGEX-KG-ERBIN-Y2H.

Mutagenesis PCR for pGEX-KG-ERBIN38 was carried out according to the program indicated in the Table 3.15.

Step	Number of cycles	Temperature	Time
Denaturation	1	95°C	1 min
Amplification	18	95°C	50 sec
		60°C	50 sec
		68°C	6 min
Elongation	1	68°C	8 min

Table 3.15: The program of the site directed mutagenesis PCR for pGEX-KG-ERBIN38.

The PCR product was digested with 1 µl Dpn I at 37°C for 1 h. XL1-Blue electrocompetent bacteria were transformed with 1 µl of digested PCR product. Plasmid DNA was isolated from bacterial clones and verified by sequencing.

3.2.1.9. Total RNA isolation

Total RNA was extracted from rat or mouse tissues, C2C12 myoblasts, C2C12 myotubes treated with inactive 0.0 or active 4.8 isoforms of agrin using the TRIzol Reagent (Invitrogen). 1 ml of TRIzol reagent was used per 50-100 mg of tissue or per 10 cm cell plate area. To follow developmentally regulated MuSK expression, rat eye tissue because of its larger size was used due to easier dissection compared with mice. Total RNA was extracted from eyes of rats at different stages (the term adult reflects rats aged from 2 to 4 month).

Tissues were homogenized using an automatic homogenizer (Kinematica); insoluble material was removed by centrifugation (12000 g for 10 min at 2-8°C). After 5 min at RT 0.2 ml chloroform was added per 1 ml TRIzol Reagent, vortexed for 15 sec, incubated additional 3 min at RT and centrifuged (12000 g for 15 min at 2-8°C). The aqueous phase was transferred to a fresh tube and RNA was precipitated with 0.5 ml isopropanol per 1 ml TRIzol reagent for 10 min at RT. After centrifugation (12000 g for 15 min at 2-8°C) the RNA pellet was washed with 75% Ethanol, briefly dried and dissolved in RNase free water. RNA was aliquoted and stored at -80°C.

3.2.1.10. Complementary DNA-synthesis (Reverse Transcription)

The reverse transcription (RT) allows the transcription of RNA into complementary DNA (cDNA) that can be subsequently used as template for PCR. For cDNA-synthesis, 2 µg of total RNA was incubated in a total volume of 15.5 µl, including 1 µl of oligo-dT (0.5 µg/µl) (Invitrogen) and DEPC water at 70°C for 10 min and then quickly chilled on ice to open secondary structures. The following mix: 2.5 µl of 10x First-Strand Buffer (New England BioLabs), 4 µl dNTP mix (10 mM) and 2 µl of DEPC water, was then added to each tube and was incubated for 1 min at 37°C. After that 200 U of M MuLV Reverse Transcriptase (New England BioLabs) was added and the reaction was incubated for 50 min at 37°C. Finally the enzyme was inactivated at 70°C for 15 min and the cDNA was aliquoted and stored at -80°C.

3.2.1.11. Lightcycler PCR

Lightcycler PCR allows to quantitatively estimate the amounts of gene transcripts and to compare them for different tissues, cells or developmental stages. The Lightcycler-FastStart DNA Master SYBR Green Kit allows quantifying the amount of PCR products by means of incorporated SYBR Green fluorescence, which is proportional to the amount of double stranded DNA. cDNA was used as a template for Lightcycler PCR reaction. A 10 µl reaction contained 1 µl of cDNA (in dilution 1:10), 1.2 µl MgCl₂ (25 mM), 1 µl of two primers (10 pmol each) and 1 µl Master SG mix (*Taq* DNA-Polymerase, SYBR Green, dNTPs and 10 mM MgCl₂). Lightcycler PCR was performed, using the Lightcycler Thermal Cycle System (Roche). The PCR program for mouse brain, spinal cord, C2C12 myoblasts, and C2C12 myotubes treated with inactive 0.0 or active 4.8 isoforms of agrin given in the Table 3.16.

Step	Number of cycles	Temperature	Time
Denaturation	1	95 °C	8min
Amplification	40	95 °C	0 sec
		62 °C	7 sec
		72 °C	1min
Elongation	1	95 °C	30sec
	1	67 °C	30sec
	1	95 °C	0 sec

Table 3.16: Lightcycler PCR program.

The amount of gene transcripts was defined for MuSK, AChR α subunit and Erbin and normalized to the amount of transcripts of a housekeeping gene (β -actin). Respective primers used for PCR reactions and sizes of resulting PCR products are listed in the Table (see 3.8.).

3.2.1.12. Yeast-two-hybrid techniques

The MATCHMAKER yeast-two-hybrid System 3 (Clontech) was used to identify protein-protein interactions in yeast cells. It comprises a bait sequence expressed as a fusion to the GAL4 DNA-binding domain (DNA-BD) from the pGBKT7 plasmid (Table 3.11.), while prey sequences are expressed as a fusion to the GAL4-activation domain (AD) from pGADT7 or from pGAD424 (Table 3.11.). When bait and prey fusion proteins interact, the DNA-BD and AD of GAL4 are brought into proximity, thus activating transcription of reporter genes. Yeast strains HF7c and AH109 have been used for the yeast-two-hybrid screens. The elimination of false positives have been performed by using the reporter genes - HIS3, lacZ (for HF7c) and ADE2, HIS3, lacZ (for AH109), which are under the control of distinct GAL4 upstream activating sequences (UASs) and TATA boxes.

For generation of bait constructs for the yeast-two-hybrid screens, different domains of MuSK were amplified by PCR using pMT-MuSK-full-length as a template and subcloned in frame into the EcoR I/Sal I restriction sites of pGBKT7 (Table 3.1). MuSK2xwt and MuSK2xkd baits were generated and kindly provided by the group of Prof. Hans-Rudolf Brenner. In brief, two intracellular domains of rat MuSK or its kinase defective mutant (Acc.No. U34985) were linked together by five E/G modules. As restriction sites for the first intracellular MuSK domain NcoI and EcoRI and for the second intracellular MuSK domain EcoRI and SalI of pGBKT7 were used.

Cloning vectors	Epitope	Yeast selection	Bacterial selection
pGBKT7 (bait)	myc	TRP1	kanamycin
pGADT7 (prey)		LEU2	ampicillin
pGAD.GH (prey)		LEU2	ampicillin
Control vectors	Epitope	Yeast selection	Bacterial selection
pGADT7-T	HA	LEU	ampicillin
pGBKT7-53	myc	TRP1	kanamycin

Table 3.18: Yeast vectors used.

Bait	MuSK domains	Aa position	Primers used for subcloning (see Table 3.3.)
pBridge-agrin-MuSK-1	Part between and signal sequences and IgI + Ig- I		MuSK-10 + MuSK-19

pBridge-agrin-MuSK-2	Part between Ig1 and Ig2 + Ig2		MuSK-10 + MuSK-20
pGBKT7-MuSK-5	whole extracellular domain		MuSK-10 + MuSK-21
pGBKT7-JM	Juxtamembrane (JM)	481-520	MuSK-22 + MuSK-23
pGBKT7-MuSK2xwt	Two times whole intracellular domain	2x (467-868)	Gift from Prof. Hans-Rudolf Brenner

Table 3.19. Bait plasmids generated for yeast-two-hybrid screens.

Before starting the screens, transformation efficiency of competent yeast cells were analyzed in order to ensure high efficiencies while performing screens. Bait constructs were also tested for autonomous transactivation of yeast reporter genes. Furthermore, the growth kinetic of transformed yeast was not disturbed indicating the absence of toxicity for the bait (data not shown). Some screens were done with 3-AT (3-amino-1, 2, 4- triazole, Sigma; 0/5/10/20 mM) in the medium. 3-AT is a competitive inhibitor of the histidine biosynthetic enzyme His3p protein (His3p), is used to inhibit low levels of His3p expressed in a leaky manner in some reporter strains (Feilotter et al., 1994). To screen for MuSK interacting proteins, yeast HF7c and AH109 cells were sequentially transformed with each bait vector and 1 µg of a human HeLa cDNA MATCHMAKER library (Clontech), using the lithium acetate method (Schiestl and Gietz, 1989) (see Table 3.18.).

1x Tris EDTA (TE) pH 7.5	From 10x TE: 100 mM Tris-Cl, 10 mM EDTA
1x TE/LiAc pH 7.5	From: 10x TE, 10x LiAc
PEG/LiAc/TE pH 7.5	40% PEG 3350 1x TE buffer 1x LiAc
DNA carrier	Yeastmaker carrier DNA
DMSO	10% final concentration

Table 3.20. Solutions for yeast transformation.

The yeasts were plated on selection media (SD -Leu, -Trp) to estimate the efficiency of transformation and on selection media (SD -Leu, -Trp, -His or SD -Leu, -Trp, -His, -Ade) containing 5, 10 or 20mM 3-AT for the reporter gene activations. Yeast colonies growth was evaluated after 5 days of incubation at 30°C. Selected positive clones were further confirmed by colony-lift filter assays for β-galactosidase activity according to the Clontech Manual. Transformation efficiency was calculated for every screen after

counting colonies (c.f.u. - colony forming unit) growing on SD -Leu, -Trp dilution plates (1:10; 1:10²; 1:10³; 1:10⁴) according to the formula:

$$\frac{(\text{Counted c.f.u.}) * \text{Total suspension volume } (\mu\text{l})}{\text{Volume plated } (\mu\text{l}) * \text{Dilution factor} * \text{Amount of DNA used } (\mu\text{g})}$$

Prey plasmids were isolated from positive yeast colonies for all screens according to the Clontech Manual protocol for preparation of plasmids from yeasts and then shuttled into *E. coli* XL1-Blue electrocompetent cells to get higher quality and concentration of prey plasmid. Plasmids were digested with EcoR I/Xho I or Alu I restriction enzyme in order to get rid of identical clones based on the restriction pattern. Independent clones from the screen were retransformed into the yeast together with respective bait or empty plasmid in order to confirm the specificity of the interaction and to remove the unspecific interaction with Gal4-DBD. Library inserts of positive, re-tested interactors were sequenced and analyzed with protein and nucleotide databases of the National Center for Biotechnology Information (NCBI, Bethesda, MD) using the Basic Local Alignment Search Tool (BLAST). Only candidates, whose coding sequences were in frame with the GAL4 AD, have been selected for further investigation.

For binary epitope-mapping yeast-two-hybrid studies PCR-amplified intracellular epitopes of mouse MuSK (Acc.No. MMU37709) were subcloned into pGBKT7 using restriction digestion sites EcoR I and Sal I (see Table 3.21).

Bait	MuSK epitope	aa position	Primers used for subcloning (see Table 3.1.)
pGBKT7-MuSK-563	JM	467-563	MuSK-38 + MuSK-61
pGBKT7-MuSK-682	JM + half of kinase domain	467-682	MuSK-38 + MuSK-62
pGBKT7-MuSK-857	JM + kinase domain	467-857	MuSK-38 + MuSK-63
pGBKT7-MuSK-868	Whole intracellular domain	467-868	MuSK-38 + MuSK-64

Table 3.21: MuSK bait constructs used in epitope-mapping experiments.

Different epitopes of human Erbin (Acc.No. NM-018695.2) were PCR amplified and subcloned into the restriction sites EcoR I and Xho I of the prey vector pGAD.GH as GAL4 AD fusions (see Table 3.22).

Bait	Amino acid position	Primers used for subcloning (see Table 3.4.)
pGAD-GH-Erbin-11	aa 1079-1371	Erbin-11/Erbin-14
pGAD-GH-Erbin-12	aa 1200-1371	Erbin-12/Erbin-14
pGAD-GH-Erbin-13	aa 1261-1371	Erbin-13/Erbin-14

pGAD-GH-Erbin-16	aa 1007-1146	Erbin-19/Erbin-16
pGAD-GH-Erbin-17	aa 1007-1205	Erbin-19/Erbin-17
pGAD-GH-Erbin-18	aa 1007-1266	Erbin-19/Erbin-18
pGAD-GH-Erbin-20	aa 1007-1085	Erbin-19/Erbin-20

Table 3.22: Erbin prey constructs used in epitope-mapping experiments

For binary yeast-two-hybrid interaction assays transactivation of reporter genes were analyzed in AH109 stain on selective plates (SD -Leu, -Trp, -His). Functionality of yeast-two- hybrid assays was always tested using the positive control plasmids pGBKT7-53 or pGADT7-T of the MATCHMAKER GAL4 Two-Hybrid System 3 (Clontech), encoding for the murine tumor suppressor protein p53 and the SV40 large T-antigen, respectively.

3.2.2. Protein Biochemistry Methods

3.2.2.1. Preparation of protein extract from cells and tissues

For preparation of protein extract HEK293 cells were transfected with Superfect (Qiagen) and Ca-Phosphate methods in 10 cm plates. Cos7 cells were transfected in 10 cm plates using DEAE-dextran technique followed by chloroquine treatment. Whole cell protein extracts were prepared from transfected HEK293 or Cos7 cells or nontransfected C2C12 cells. For the preparation of protein extract for MuSK, cells were lysed in the presence of Buffer A (10 mMm HEPES (pH 7.9), 10 mM KCl, 0.8 mM EDTA, 0.417 M NaCl, 1% Nonidet P-40, 2 mM DTT, 10 µg/ml aprotinin and 10 µg/ml leupeptin). Immediately after the lyses, NaCl was added to a final concentration of 400 mM. After incubation for

15 min (for HEK293 cells) or 30 min (for C2C12 cells) under constant rotation, cell debris was removed from the extract by centrifugation (20817 rcf for 10 min).

In order to get Erbin lysate; we used the method describe by (Borg et al., 2000). For that cells were washed twice with cold PBS and lysed in lyses buffer (50 mM HEPES pH 7.5, 10 % glycerol, 150 mM NaCl, 1 % Triton X-100, 1.5 mM MgCl₂, 1 mM EGTA) supplemented with 1 mM phenylmethylsulphonylfluoride (PMSF), 10 µg/ml aprotinin and 10 µg/ml leupeptin. After incubation for 30 min under constant rotation, cell debris was removed from the extract by centrifugation (13000 rcf for 20 min).

For preparation of muscle tissue extract, tissues were frozen in liquid nitrogen, mashed and further homogenized in ice cold lyses buffer (50 mM HEPES pH 7.5, 10 % glycerol, 150 mM NaCl, 1 % Triton X-100, 1.5 mM MgCl₂, 1 mM EGTA) supplemented with 1 mM phenylmethylsulphonylfluoride (PMSF), 10 µg/ml aprotinin and 10 µg/ml leupeptin for 20 min. Cell debris was removed from the extract by centrifugation (13000 rcf for 20 min).

3.2.2.2. Immunoprecipitation

For immunoprecipitation experiments HEK293 or Cos7 cells were transiently transfected with one of the following CMV-expression plasmids encoding for: T7- or myc-tagged MuSK2xwt and MuSK2xkd constructs, HA tagged full length MuSK, T7-tagged MuSK C-terminal truncations, myc-tagged full length Erbin, T7- and myc- tagged CK2 β, HAMaterial and methods tagged CK2 α, HA-CK1 and HA-tagged Wnt receptors. Protein

extract was prepared as described above (3.2.2.1). For each extract the expression level of protein was analyzed by Western blot (3.2.2.7) and adjusted. Lysates containing expressed proteins were mixed and the final volume set to 500 μ l with the buffer containing 50 mM HEPES pH 7.5, 10 % glycerol, 150 mM NaCl, 1 % Triton X-100, 1.5 mM MgCl₂, 1 mM EGTA. 1 μ l of a monoclonal antibody against the T7- (Novagen), myc- or HA- (Cell Signaling) was added and the reaction was incubated under constant rotation at 4°C for overnight. Next, 20 μ l of PBS equilibrated Protein A Sepharose CL-4B beads (Amersham) were added and incubation continued two hours. After washing the beads three times with buffer containing 50mM Hepes, pH7.5, 150mM NaCl, 1mM EDTA, 10% glycerol, 1mM PMSF, 10 μ g/ml leupeptin, 10 μ g/ml aprotinin the precipitated proteins were analyzed by SDS-PAGE and Western blot.

For immunoprecipitation of endogenous Erbin and MuSK proteins from C2C12 cells or tissue extract, a polyclonal rabbit serum against MuSK (abcam or MuSK-Rabbit, 20 kd) or Erbin was pre-conjugated with Protein A Sepharose. 20 μ l of antibody was incubated with 40 μ l of Protein A Sepharose in 1 ml of PBS overnight at 4°C under constant rotation. Then Sepharose beads containing MuSK or Erbin antibody on their surface were washed two times with 500 μ l of PBS and equilibrated with PBS in a 1:1 ratio. A 10 μ l aliquot of MuSK-antibody-Sepharose conjugate was added to the extracts. Samples were incubated under the constant rotation overnight. After washing three times with 50 mM Hepes, pH7.5, 150 mM NaCl, 1 mM EDTA, 10% glycerol, 1m M PMSF, 10 μ g/ml leupeptin and 10 μ g/ml aprotinin, proteins bound to the Sepharose beads were resolved by SDS gel and analyzed by Western blot.

3.2.2.3. Protein expression and extraction from bacteria

Full length, N-terminal or C-terminal truncations of pGAD.GH-Erbin-Y2H clone were ligated in-frame to the coding sequence of glutathione-S-transferase (GST) in pGEXKG (3.2.1.6). cDNA encoding for the Juxtamembrane epitope and Kinase epitope of mouse MuSK were fused in frame to the His-tag of pET28b (3.2.1.6). Plasmids were transformed in *E. coli* BL21 (Rosetta). Bacteria expressing GST-fusions of Erbin were grown in 50 ml cultures until OD₆₀₀ 0.4. Protein expression was induced by 1 mM isopropyl-beta-D-thiogalactoside (IPTG; Sigma) for 4 h. Afterwards bacteria were collected by centrifugation, incubated in sonification buffer (50 mM NaH₂PO₄, 300 mM NaCl, 25 U/ml Benzonase, 10 μ g/ml leupeptin, 10 μ g/ml aprotinin, 1 μ l/ml Triton X-100, 10 μ g/ml DNaseI, 15 U/ μ l Lysozym) at 4°C for 30 min, lysed by sonification and centrifuged (14000 rpm for 10 min). The supernatants containing the GST-fusion proteins were collected and used freshly for the further GST-pulldown experiments (3.2.2.4).

Bacteria expressing His-tag fusions of Juxtamembrane epitope and Kinase epitope of mouse MuSK were grown in 4 l culture until OD₆₀₀ 1.0 and protein expression was induced by 1 mM IPTG for 4 h. Bacteria were pelleted by centrifugation. The pellet was dissolved in 270 ml buffer A, pH 8.0 (6 M guanidine hydrochloride, 0.1 M NaH₂PO₄, 0.01 M Tris pH 8.5) and shook overnight at 250 rpm. The lysate was centrifuged to remove cell debris, the supernatant was collected and incubated with 6 ml Ni-NTA agarose (Qiagen) under constant rotation during 3 h at RT. Ni-NTA beads were washed five times in buffer B pH 8.0 (8 M Urea, 0.1 M NaH₂PO₄, 0.01 M Tris), three times with

buffer B pH 6.6 and the protein was eluted by washing the beads five times with 7.5 ml buffer B pH 4.5.

3.2.2.4. GST-pulldown

The supernatants containing the GST-fusion proteins were supplemented by 30 μ l equilibrated Glutathione-Sepharose beads and incubated under constant rotation at 4°C for 2 h. After washing three times with washing buffer containing 4.3 mM Na₂HPO₄, 1.47 mM KH₂PO₄, 1.37 mM NaCl, 2.7 mM KCl an aliquot of the beads was loaded on a SDS gel for estimation of the concentration by a Coomassie Brilliant Blue (Roche) staining. Then the beads carrying the GST-fusion protein were incubated together with 25 μ l of extract from cells expressing the desired protein after transient transfection. After washing three times with the washing buffer, proteins bound to the beads were analyzed by SDS-PAGE and Western blot.

3.2.2.5. Electrophoresis of proteins

Proteins were resolved on denaturing SDS polyacrylamide gels, using the Vertical Minigel system (Sigma). The separating gel contained 8, 10, 12.5 or 15% polyacrylamide depending on the molecular weight of the protein and the stacking gel was always 5% (see Table 3.24). The proteins were mixed with sample loading Lamlli buffer, denatured at 100°C for 5 min and loaded on the gel. Electrophoresis was carried out constantly at 80 or 100V for 1-2 h in SDS gel running buffer depending on the protein dimensions.

Separating gel buffer	1.5 M Tris-Base pH 8.8, 0.4% (w/v) SDS
Stacking gel buffer	500 mM Tris-HCl pH 6.8, 0.4% (w/v) SDS
10 x Running buffer	250 mM Tris-Base pH 8.3, 1.92 M Glycin 1% (w/v) SDS

Table 3.23: Solutions for SDS-PAGE.

Separating gel	8%	10%	12.5%	15%	Stacking gel	5%
H ₂ O	2.9 ml	2.5 ml	2 ml	1.5 ml	H ₂ O	1.5 ml
Separating buffer	1.5 ml	1.5 ml	1.5 ml	1.5 ml	Stacking gel buffer	625 μ l

Acrylamide/Bisacrylamide (30%)	1.625 ml	2 ml	2.5 ml	3 ml	Acrylamide/Bisacrylamide (30%)	425 μ l
APS (20% w/v)	22.5 μ l	22.5 μ l	22.5 μ l	22.5 μ l	APS (20% w/v)	5 μ l
TEMED	5 μ l	5 μ l	5 μ l	5 μ l	TEMED	2 μ l

Table 3.24: Separating gels and stacking gel for SDS-PAGE (calculated for one gel of 11 cm x 8 cm x 0.7 mm size).

3.2.2.6. Staining of protein gels

Coomassie staining was used to detect proteins in SDS polyacrylamide gels. After electrophoresis, the gel was placed in the staining solution (30% Methanol, 10% acetic acid, 0.05% Coomassie Brilliant Blue) for 15 min at RT and then destained overnight in a solution containing 25% Methanol and 15% acetic acid. The gel was dried on Whatman paper covered with a cellophane sheet on a Gel dryer SE1160 (Hoefer Scientific Instruments).

3.2.2.7. Western blot

Proteins resolved on SDS polyacrylamide gels were transferred to nitrocellulose membrane in blotting buffer (see Table 3.25) for ~1.5 h at 150 mA. The membrane was then blocked in blocking buffer (see Table 3.25) for 1 h at RT and further incubated for a minimum of 1 h up to overnight with the first antibody diluted in washing buffer (see Table 3.25). A monoclonal antibody directed against the T7-tag (Novagen), myc-tag, HA-tag (Cell Signaling) and or polyclonal sera against either Erbin (Gift from Borg et al., 2000) or MuSK (ABR, abcam, 194T or 20kD) served as primary antibodies. 1:10000 dilution was used for anti-T7, HA-tag and anti-myc-tag antibodies; 1:100 for all polyclonal antibodies (except 1:3000 for α -MuSK 20kD). The membrane was washed three times for 5 min with the washing buffer, incubated for 1 h with secondary antibody (Horseradish-peroxidase-coupled-Protein A or anti-mouse-Ig-coupled-horseradishperoxidase in 1:3000 dilution), and subsequently washed three times for 5 min with the washing buffer. The bound antibodies were detected by the ECL system (Amersham) according to the manufacturer's protocol, and the membrane was exposed to X-ray film super RX (FUJI Medical) that was developed in a film developer X-Omat 1000 Processor (Kodak).

Blotting buffer	480 mM Tris, 380 mM Glycin, 0.1% SDS, 20% Methanol
Blocking buffer	PBS, 0.1% Tween-20, 5% dry milk powder
Washing buffer	PBS, 0.1% Tween-20

Table 3.25: Western blot buffers

3.2.3. Cell culture methods

3.2.3.1. Cultivation of HEK293, Cos7, C2C12 and MuSK-deficient myoblasts

HEK293 or Cos7 cells were maintained in Dulbecco's modified Eagle's medium (DMEM; Gibco/BRL) containing 10% (v/v) fetal calf serum (FCS; Invitrogen) at 37°C and 5% CO₂. C2C12 cells were maintained for proliferation in DMEM containing 20% (v/v) FCS, for differentiation the medium was replaced by DMEM with 5% (v/v) heatinactivated horse serum (HS, Invitrogen) at the same growth conditions. Myotubes were formed after 4-6 days.

3.2.3.2. Transient transfection of cells

24 h before transfection exponentially growing cells were replated in growth medium and transfected at 50-60% (HEK293, Cos7) or 80-90% (C2C12, MuSK-deficient myoblasts) confluence.

A. Superfect transfection

For preparation of protein extracts HEK293 cells were transiently transfected with CMV expression plasmids (see 3.2.1.6) in 10 cm dishes with 10 µg of expression vectors using Superfect (Qiagen). In order to test the efficiency of siRNAs against Erbin RNA HEK293 cells were transfected in 6 cm plates with 0.2 µg of CMV-expression vectors encoding for Erbin cDNA together with 1.8 µg of the respective pSUPERneoGFP(E797)-siRNA constructs. For 10 cm plate transfection DNA was dissolved in 300 µl of DMEM medium lacking FCS. Then 30 µl of Superset reagent was added to the DNA solution and mixed by vortexing for 10 sec. The samples were incubated for 5-10 min at RT to allow transfection complex formation. In the meantime the growth medium was aspirated from the dishes and the cells were washed once with 4 ml of PBS. Then 4 ml of cell growth medium (containing FCS) were added to the reaction tube containing the transfection complex, mixed by pipetting and immediately transferred to the cells. Cells were incubated with the transfection complexes for 3-12 h under their normal growth conditions. After that the medium containing the remaining complexes was removed from the cells, cells were washed once with 4 ml of PBS and fresh growth medium was added. Transfection efficiency was controlled by transfection of one cell plate with the plasmid expressing Green Fluorescence Protein (GFP) with nuclear localization signal pnlsgfp (Hashemolhosseini et al., 2000). At 48 h post-transfection, cells were harvested for extract preparation as described (see 3.2.2.1.).

B. Calcium Phosphate transfection

In some cases HEK-293 cells were transfected using the Calcium Phosphate technique. Transfection reaction for 10 cm plates was made as follows: 10 µg of expression plasmid DNA was mixed with 800 µl water and 100 µl 10x HEBS (1.4 M NaCl, 50 mM KCl, 50 mM Glucose 7.25 mM Na₂HPO₄ and 210 mM HEPES, pH 7.2). 100 µl 1M CaCl₂ was added to the transfection mixture. Mixture was vortexed immediately for 30 seconds. The transfection mixture was incubated at room temperature for 45 minutes. The mixture was mixed again and added to the growth medium of the cells. After incubation for three hours under standard growth conditions, the medium was

replaced by 8 ml of fresh medium. At 48 h post-transfection, cells were harvested for extract preparation as described (see 3.2.2.1.).

C. DEAE-Dextran transfection

In some cases Cos7 cells were transfected using the DEAE-Dextran technique. The transfection reaction for 10 cm dish was made as follows: 10 µg of expression plasmid DNA were mixed with 187.5 µl of PBS and 375 µl of DEAE-Dextran. The mix was added to the growth medium of the cells. After incubation for 30 min under standard growth conditions, the medium was replaced by 8 ml of fresh medium and 80 µl of Chloroquin was added. Cells were incubated for 3 h, and then the growth medium was changed once again. At 48 h post-transfection, cells were harvested for extract preparation as described (see 3.2.2.1.).

D. LipofectamineTM 2000 transfection

For immunocytochemistry C2C12 cells were transiently transfected in 3.5 cm plates with either 0.4 µg of plasmid expressing nuclear localized GFP - pnlsGFP together with 3.6 µg pSUPERneoGFP (E797)-siRNA constructs or 1 µg of plasmid expressing nuclear localized GFP - pnlsGFP together with 3 µg pRK5-myc-Erbin constructs. 24 h before transfection cells were replated in growth medium without antibiotic. 4 µg of DNA was dissolved in 250 µl of DMEM medium lacking FCS. 10 µl of Lipofectamine was diluted separately in 250 µl DMEM medium lacking FCS. After incubation for 5 min at RT the mixtures were combined and incubated for 20 min at RT. Then 500 µl of DNALipofectamine complex was added to each plate. The medium was replaced by differentiation medium after one day.

3.2.3.3. Luciferase reporter test

The ATP dependent oxidation of luciferin by luciferase is accompanied by the light emission, which can be measured. The luciferase activity test was performed to check the ability of different siRNAs to knockdown the mRNAs of Erbin. The cDNAs of the respective genes were subcloned together with the luciferase gene to be transcribed as a bicistronic message (see 3.2.1.6.). An effective siRNA would target the chimeric luciferase-Erbin mRNA which would result in its degradation and lead to a decrease of luciferase activity. HEK293 cells transfected with the constructs described above were lysed 48 h posttransfection. The lyses of the cells was performed in 300 µl per well of Luciferase Harvest/Assay Buffer, which contained 88 mM Tris/MES pH 7.8, 12.5 mM MgAc, 2.5 mM ATP, 1 mM DTT and 0.1% Triton X-100. Measuring of the chemiluminescence reaction was performed for 200 µl of the cell lysate in a luminometer (Berthold–Lumat LB9501), after injection of 100 µl of 0.5 mM luciferin dissolved in 5 mM KHPO₄. The luciferase activity was calculated in Relative Light Units (RLU).

3.2.3.4. Agrin treatment

The production of agrin-conditioned media was performed as described before (Kröger, 1997). In brief, stably transfected HEK293 cells (gift from Dr. Stephan Kröger) expressing continuously secreted active agrin 4.8 or inactive agrin 0.0 were grown in DMEM containing 10% FCS until 80-90% confluence. After another 4 days of proliferation in serum-free DMEM, agrin-conditioned medium was collected, aliquoted and frozen. Agrin-conditioned medium was added at 1:8 dilution (125 µl per 3.5 cm dish)

to C2C12 myotubes. AChR aggregates were detected or quantified 16 h later as described below (see 3.2.3.5.).

3.2.3.5. Immunocytochemistry

AChR clusters on the surface of C2C12 were visualized by α -Bungarotoxin staining. 0.5 μ l Rhodamine-conjugated- α -Bungarotoxin (Rh- α -BTX) was added in the medium and cells were kept for 1 h in the growth chamber. Cultivation medium was aspirated from the dishes and cells were washed three times with PBS. Then cells were fixed with 2% PFA solution in PBS for 20 min at RT. After washing three times with PBS the bottoms of the dishes with cells on their surface were cut out and mounted on cover slides with Mowiol. Slides were analyzed and documented using the Cy3 filter of a Leica inverted microscope (DMIRB) equipped with a cooled MicroMax CCD camera (Princeton Instruments, Stanford, CA).

3.2.3.6. Quantification analysis of AChR clusters

The numbers of AChR aggregates were quantified as follows: using the Cy3 filter pictures were taken from myotubes randomly expressing nuclear localized GFP – pnlS GFP. AChR clusters were counted for each myotube. Quantification analysis of AChR clusters was performed for three independent experiments.

3.2.3.7. Immunohistochemistry

For immunohistochemical analysis, all muscles were quick-frozen in prechilled isopentane and embedded in Tissue-Tec (Leica Instruments). Muscles from adult mice were cryotome-sectioned to 12 μ m slices and placed on glass slides (HistoBond, Adhesion Micro Slides, Jung HistoService). Sections were air-dried for 1 h at RT and stored at -80°C or directly subjected to the immunohistochemical staining. Unfixed sections were rinsed with PBS and permeabilized for 5-10 min in PBS supplemented with 0.1% Triton-X100, blocked in 10% fetal calf serum and 1% bovine serum albumin for 1- 2 h. Cryotome sections were stained for AChR with Alexa- α -Bungarotoxin or Rhodamin- α -Bungarotoxin at 1:2,500 dilution (BTX; Molecular Probes, Eugene, OR) or incubated with anti-Erbin (1:100) (gift from Dr. Jean Paul). As MuSK specific antibodies either a self-made antibody (anti-MuSK20kd; 1:100) was used or anti-MuSK (1:100) which was kindly provided by Markus Ruegg. Incubation was done in the blocking solution at 4°C in a humid environment overnight. After washing the sections six times for 5 min in PBS, secondary antibodies conjugated to Cy2, Cy3 or Alexa 488 immunofluorescent dyes (Dianova, Molecular probes) were applied in 1:100, 1:200 or 1:500 dilutions respectively for 1 h at RT. Subsequently, sections were washed six times for 5 min in PBS and covered with Mowiol.

For immunohistochemical analysis, rat retinae were fixed with 2% PFA for 30 min, washed several times with PBS and embedded in Tissue-Tec (Leica Microsystems, Wetzlar, Germany). Frozen tissue was sectioned to 10 μ m slices. Sections were rinsed with PBS and permeabilized for 5-10 min in PBS supplemented with 0.5 % Triton-X100, blocked in 10% fetal calf serum (FSC) and 1% bovine serum albumin (BSA) for 1-2 h.

Sections were stained with anti-MuSK antibodies from rabbit (Rb194T, recognizing an extracellular epitope, 1:1,000, gift from Markus Ruegg; for simplicity this antibody is named α MuSK throughout the manuscript) or from guinea pig (gpMuSK-20kd, recognizing an intracellular epitope, 1:1,000), mouse anti-GFAP (1:500, Chemicon, Temecula, CA), mouse anti-glutamine synthetase (1:500, BD Transduction Laboratories, San Diego, CA), mouse anti-choline acetyltransferase (1:1,000, Chemicon), mouse anti-Thy1 (1:500, BD Transduction Laboratories) and mouse anti-agrin (AGR-540, 1:500, Stressgen). Secondary antibodies conjugated to Cy2 or Cy3 immunofluorescent dye (1:200, Dianova, Hamburg, Germany) were used. Staining with Rb194T antibody preincubated for 2 h with lysate of HEK293 cells containing MuSK protein or preimmune serum of gpMuSK-20kd served as negative control. Co-immunostainings with primary antibodies from the same species were performed in a sequential manner. Cross-reaction of secondary antibodies was excluded by running in parallel negative controls without the second primary antibodies. Additionally, retina sections were co-stained with DAPI (1:1,000, Sigma-Aldrich, Deisenhofen, Germany). Results were documented using a Leica inverted microscope (DMIRB) equipped with a cooled MicroMax CCD camera (Princeton Instruments, Trenton, NJ) or Leica confocal microscope TCS SL equipped by Leica confocal software TCS SL version 2.5.1347a.

4. Results

4.1. Yeast-two-hybrid screens

4.1.1. Generation of MuSK baits

For the bait consisting of the juxtamembrane domain of MuSK aminoacids 481 to 520 was subcloned in frame with GAL4-DNA-BD in pGBKT7 (Fig. 7). For the generation of MuSK2xwt bait two complete intracellular domains of MuSK were fused by a flexible G/E linker) thereby creating a dimer most likely resembling the *in vivo* active MuSK dimer (Fig. 7). A second fusion was generated the same way for a kinase defective MuSK variant, bearing substitution of lysine in the ATP binding site (Zhou et al., 1999) of the kinase domain (named MuSK2xkd) to explore if binding depends on the phosphorylation of the intracellular domain of MuSK (Fig. 7). These two baits were kindly provided by the group of Dr. Hans-Rudolf Brenner (Biocenter, Basel, Switzerland).

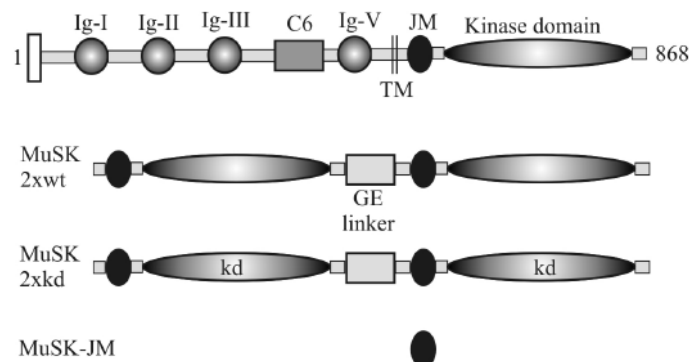


Fig.7: JM representing juxtamembrane domain and MuSK2xwt mimicking kinase-active dimeric MuSK were used for identification of MuSK intracellular downstream effectors.

Candidates from yeast-two-hybrid screen with MuSK2xwt were checked for interaction with kinase defective MuSK2xkd bait.

4.1.2. Outcome of the yeast-two-hybrid screens

Outcome of the yeast-two-hybrid screens is summaries in the Table 4.1. In all screens, the number of examined colonies was higher than the number of independent clones of the library to ensure that statistically every clone of the library was tested at least one time.

Bait	Conditions	No of independent clones screened	Candidates	Confirmed	Potential MuSK binding partners	No of identification	Amino acid Sequence
MuSK2xwt	T-L-H - 5mM 3AT	1,3 x 10 ⁶	210	26	CK2 β BC003775	89	1-215
	T-L-H-A- 20 mM 3AT	3,2 x 10 ⁶	99	11	Erbin NM_018695.2	2	1007- 1371
					Phosphatase2A BC002657.2	1	5-309
					Stat5B NM_012448.3	1	565-787
MuSK-JM	T-L-H- 5mM 3AT	1,1 x 10 ⁶	34	3	-	-	-

Table.4.1: Results of the yeast-two-hybrid screens with the MuSK domains.

Only relevant candidates, e.g. with the corresponding tissue expression, signaling pathways and sub-cellular localization to that of MuSK, are shown in the column “potential MuSK binding partners”. The number of independent sequences and amino acid region of candidate obtained from the yeast-two-hybrid screen are indicated.

One of the candidates, which have been identified many times in the yeast-two-hybrid screen with the MuSK intracellular domain, is the regulatory β subunit of protein kinase CK2 (the holoenzyme was formerly called casein kinase 2). CK2 is a highly conserved and ubiquitously expressed serine/threonine kinase, which is involved in many biological processes such as gene expression, protein synthesis and signal transduction (Meggio and Pinna, 2003; Olsten and Litchfield, 2004).

Among the other clones identified, two clones consisted of the carboxyterminal part beginning at amino acid residue 1007 until the stop codon of the LAP protein family member Erbin (Erbin-N Δ -1007).

4.3. Detailed investigation of MuSK - Erbin interaction

To evaluate the significance of the interaction between MuSK and Erbin following experiments have been performed:

- Investigation of the temporal and spatial expression profile of Erbin at the NMJ
- Co-localization of MuSK and Erbin proteins at the NMJ
- Biochemical verification of the interaction between MuSK and Erbin
- Mapping of the binding epitopes for both proteins
- Investigation of the biological significance of the interaction between MuSK and Erbin
WB:α-HA (CK1)

4.3.1. Quantitative determination of Erbin transcript level in different tissues

Given that Erbin and MuSK interact physically, we sought to determine the spatial expression profile of Erbin in synaptic and extrasynaptic regions of skeletal muscle. Considering the fact that transcripts of MuSK as well as other proteins of postsynaptic specialization, for example AChR subunits, are upregulated at the synapse (Witzemann et al., 1991; Moore et al., 2001), we intended to investigate whether the same is true for Erbin. By quantitative real-time PCR we measured the quantity of transcripts of Erbin and compared them with transcript amounts of molecules known to accumulate at the NMJ, such as MuSK and AChRα.

For 1st strand cDNA preparation, we used RNA from mouse synaptic and extrasynaptic region of the diaphragm, C2C12 myoblasts and C2C12 myotubes. The C2C12 myotubes were treated with conditioned media containing either nerve-derived or muscle-derived agrin. As control, we used 1st strand cDNA from mouse brain which should contain only marginal amounts of MuSK transcript. As expected, the amount of MuSK and AChRα mRNA accumulated both in the synaptic region of the diaphragm and in C2C12 myotubes especially after treatment with the nerve-derived agrin isoform (Fig. 11a, 11b).

The quantity of transcripts of Erbin was significantly higher in muscle tissue compared to brain, with Erbin transcript levels higher in the synaptic vs. extrasynaptic part of the diaphragm (Fig. 11c). C2C12 myotubes contained a slightly higher amount of Erbin transcript than myoblasts. Erbin transcript levels were even higher in response to nervederived agrin (Fig. 11c). Finally, we confirmed the formation of PCR-derived Erbin DNA fragments by agarosegel electrophoresis (Fig. 11d).

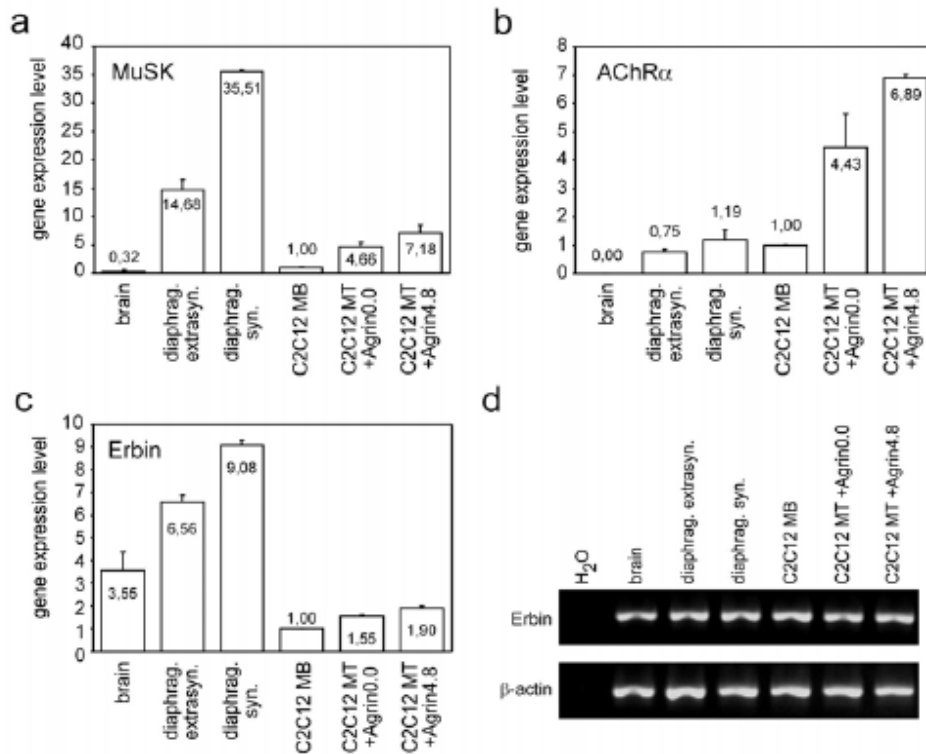


Fig.11: Distribution of transcripts of AChR α , MuSK and Erbin at the postsynapse. Realtime quantitative PCR data show the distribution of different transcripts in brain (used as control), extrasynaptic or synaptic diaphragm, C2C12 myoblast, C2C12 myotubes treated either with muscle-derived agrin or a nerve-derived agrin isoform (for 16h) which is very potent in its ability to aggregate AChRs. The setup was verified by measuring the transcript quantities of known players at the NMJ, such as MuSK (a) or AChR α (b). Similarly, the distribution of transcripts for Erbin was studied (c). The PCR-amplified Erbin fragments were verified by agarose gel electrophoresis (d). Since relative quantification data normalized to β -actin are shown, C2C12 myoblast levels are always set to 1. Interestingly, even bath-applied nerve-derived agrin which was not anchored to the surface of the petridish by precoating the dish with laminin or Matrigel (Becton Dickinson) led to an increase of AChR transcript levels in C2C12 myotubes.

4.3.2. Localization of Erbin at the NMJ

Previously, Erbin was detected at postsynaptic specializations of the hindlimb muscle of mice (Huang et al., 2001). We also observed by immunohistochemical co-staining of cross-sections of gastrocnemius and soleus mouse (hindlimb) muscle a significant accumulation of Erbin at the NMJ where it perfectly co-localized with synaptic AChRs (Fig. 12a). Preterminal localisation of Erbin was excluded by the observation that colocalization of both Erbin and AChR markers remained five days after nerve resection,

i.e. when presynaptic terminals had degenerated (Fig. 12b). Additionally, we confirmed using the same muscle cross-sections like before direct co-localisation between Erbin and MuSK (Fig. 12c). But these observations still does not rule out a possible co-localization of AChRs with Schwann cell derived Erbin. For that, we investigated co-localization of Erbin and AChRs in wildtype electrically active muscles by recombinant neural agrin, which induced ectopic postsynaptic membranes known to be free of Schwann cells (Fig. 13a, b). We confirmed by confocal microscopy a perfect co-localization of both Erbin and ectopic AChR aggregations (Fig. 13b).

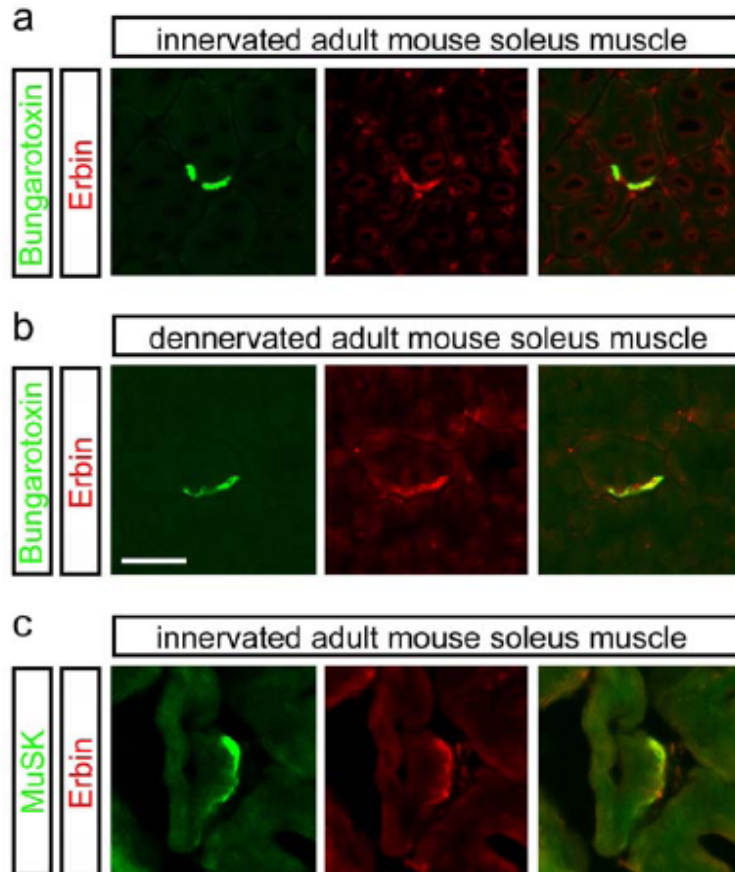


Fig.12: Erbin co-localizes with postsynaptic specializations *in vivo*. Frozen 12 μ m thick cryotome cross-sections of surgically denervated (5d post-operation) or innervated (contralateral) mouse hindlimb muscle immunostained with BTX (shown in red) and an Erbin reactive antibody (shown in green) (a, b). Note, the colocalization between Erbin and postsynaptic specializations is present in the absence of the nerve in the denervated state. To verify co-localization between MuSK and Erbin, muscle cross-sections were also stained with MuSK and Erbin recognizing antibodies (c). Scale bar, 20 μ m (the figure is kindly provided by Tatiana Cheusova).

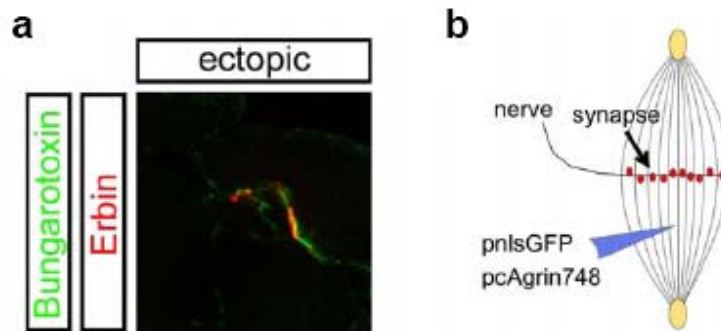


Fig.13: Erbin co-localizes with postsynaptic specializations *in vivo*.

To exclude a possible Erbin staining of terminal Schwann cells, ectopic postsynaptic membranes were generated according to a previously described methodology, as illustrated in (b), by intracellular injection of nerve-derived agrin and a nuclear localized GFP into single myotubes (Escher et al., 2005). Subcellular colocalization of BTX and Erbin at ectopic postsynaptic membranes (a). Note, in panel (a) a single projected image of a set of Z-images obtained by confocal microscopy is shown. Scale bar, 80.

4.3.3. Verification of the interaction between Erbin and MuSK in HEK293 cells, myotubes and muscle extracts

To biochemically confirm the interaction between Erbin and MuSK outside of yeasts, we transiently transfected HEK293 cells with Erbin alone or together with MuSK2xwt or MuSK2xkd. We immunoprecipitated proteins from these cell extracts with an antibody reactive against the T7 tag of the MuSK mutants and observed co-precipitation of full length Erbin (Fig. 14a). Even if we transfected full length MuSK in HEK293 cells we detected co-precipitation of Erbin by MuSK (Fig. 14b). To analyze whether the interaction between Erbin and MuSK also occurred in a physiological context, we used either C2C12 extract or tissue extract from muscle, where Erbin and MuSK are endogenously coexpressed (Fig. 14c, d). When we precipitated Erbin or MuSK from these extracts, we were also able to coprecipitate the endogenous complementary protein (Fig. 14c, d). These data demonstrate that Erbin and MuSK interact with each other *in vivo*.

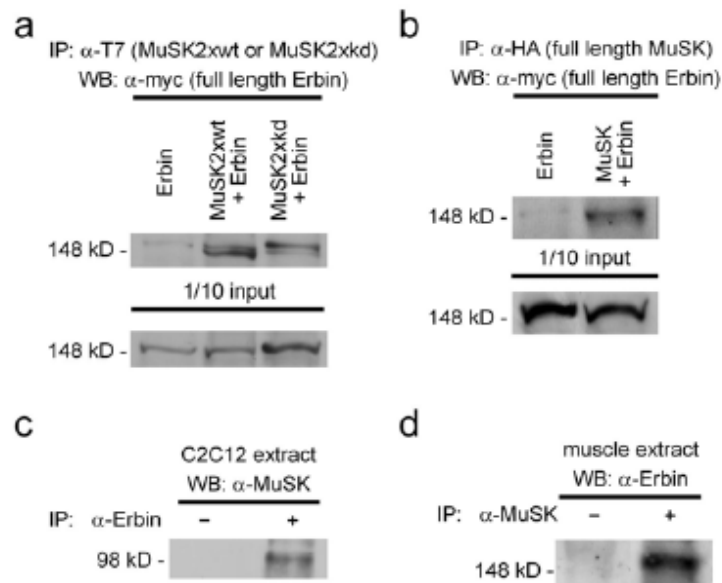


Fig.14: Verification of the interaction between Erbin and MuSK by co-immunoprecipitation studies.

Images of Western blots decorated with an anti-T7, anti-hemagglutinin, anti-Erbin or anti-MuSK antibody as indicated are shown. (a) Extracts of transiently transfected HEK293 cells were used to precipitate either MuSK2xwt or MuSK2xkd and detect for co-precipitation of transfected Erbin. (b) The precipitation of full-length MuSK in extracts from transiently transfected HEK293 cells led to co-precipitation of Erbin. Co-precipitability of both proteins from endogenous origin could be demonstrated in C2C12 and muscle cell extracts (c, d).

4.3.4. Mapping of epitopes of MuSK interacting with Erbin

To map the epitopes of MuSK and Erbin interacting with each other, we used the MuSK protein and a series of carboxyterminal truncations thereof (Fig. 15a). We used Erbin- Δ -1007 as bait in yeast-two-hybrid assays and found growth of the yeast which proved interaction between bait and prey constructs only if the MuSK kinase domain was not cut away (Fig. 15b). We re-used the same truncations of MuSK to perform GST pulldown experiments with a GST tagged Erbin- Δ -1007 protein (Fig. 15c). The same carboxyterminally truncated MuSK variants as used for yeast-two-hybrid assays were pulled down in these experiments. Finally, we transiently transfected again the MuSK constructs trimmed at their carboxytermini together with myc tagged full length Erbin protein in HEK293 cells (Fig. 15d). Using these cell extracts, co-immunoprecipitation was also observed with the intracellular part of MuSK containing the MuSK kinase domain (Fig. 15d). Altogether, we demonstrated by (i) yeast two-hybrid assays, (ii) GST pulldown experiments, and (iii) co-immunoprecipitation studies that the kinase domain of MuSK is required for binding to Erbin.

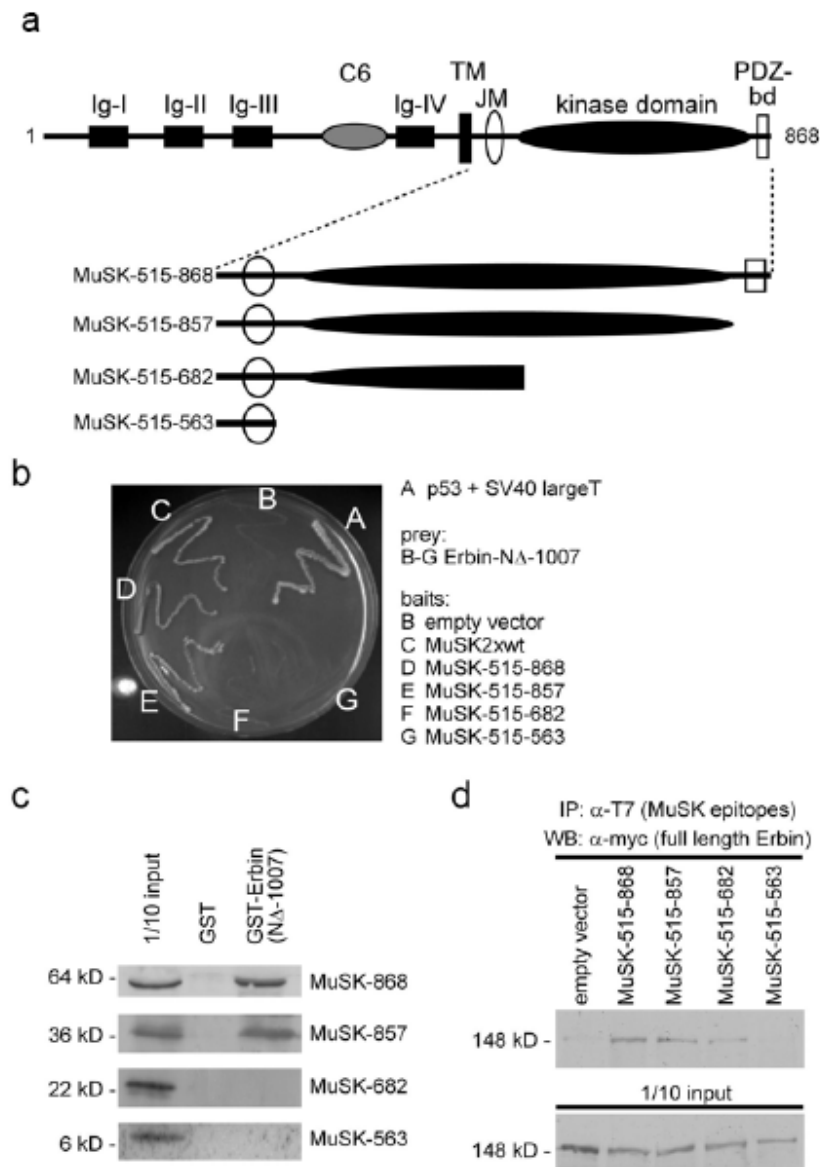


Fig.15: The interaction between MuSK and Erbin requires the juxtamembrane together with the kinase domain of MuSK.

(a) Schematic presentation of generated MuSK mutants containing carboxyterminal truncations of the intracellular domain for the use in yeast-two-hybrid experiments, GST pull-down assays, and co-immunoprecipitation studies. (b) Growth of yeast clones containing different combinations of bait and prey plasmids as indicated on agar lacking histidine and adenine. Apart from the positive control, only yeasts containing baits composed of MuSK mutants bearing at least the whole kinase domain are able to interact with Erbin as prey. (c, d) Western blots demonstrating that by GST pull-down and co-immunoprecipitations MuSK mutants lacking any part of their kinase domain are unable to interact with Erbin.

4.3.5. Mapping of epitopes of Erbin interacting with MuSK

Our next purpose was to identify the area of Erbin-N Δ -1007 which interacts with MuSK. To this end, we generated a large number of Erbin constructs, truncated at either the aminoterminal or carboxyterminal parts or even at both end (Fig. 16a). The latter constructs were generated such that they, as depicted, represent slightly overlapping fragments spanning from the amino- to the carboxyterminus of Erbin-N Δ -1007 (Fig. 16a). First, we transformed the Erbin-N Δ -1007 prey constructs trimmed at their amino- or carboxytermini together with a bait plasmid bearing MuSK2xwt into yeast. Only yeast cells which contained in addition to MuSK2xwt an Erbin fragment starting at amino acid residue 1200 were able to grow on selective agar medium (Fig. 16b). Considering the Erbin fragments which were trimmed at their carboxyterminus, only the one beginning with amino acid residue 1007 and ending at 1204 mediated interaction with MuSK2xwt (Fig. 16c). Further, we confirmed these epitopes of Erbin which interact with MuSK by GST pulldowns (Fig. 16d, e). Since our yeast-two-hybrid studies and GST pulldowns indicated a two partite area around amino acid residue 1200 of Erbin involved in binding to MuSK, we created a series of GST tagged fragments representing areas of the Erbin protein between amino acid residue 1007 and the end of the protein (Fig. 16a). We purified these GST-Erbin constructs from bacteria and used them to investigate which of these Erbin fragments enabled to pull down transiently transfected MuSK2xwt from HEK293 cell extracts (Fig. 16f). The GST pulldown assay showed that the area of Erbin comprising amino acid residues between 1175 and 1229 is necessary for the interaction between Erbin and MuSK (Fig. 16f).

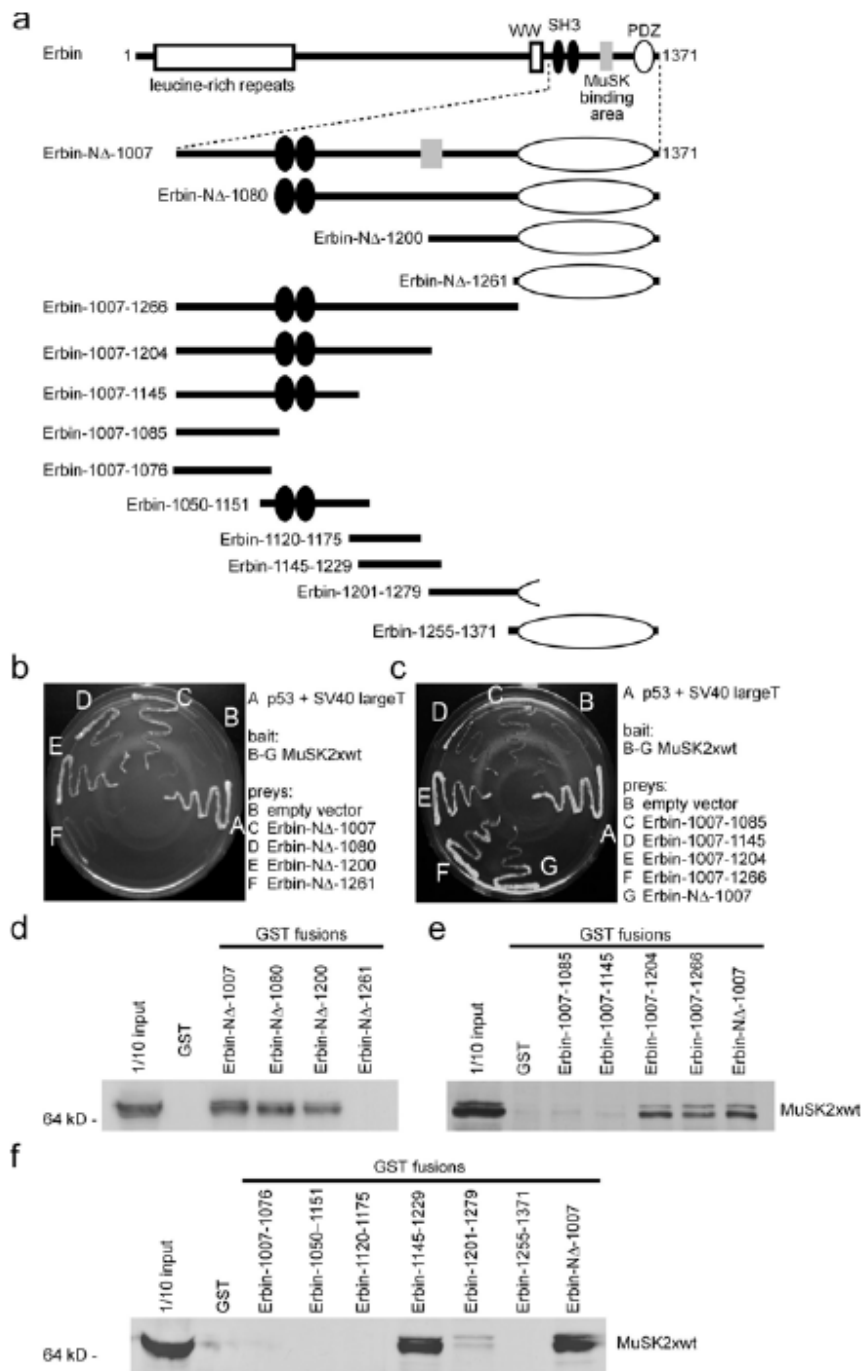


Fig.16: Identification of the epitope of Erbin which interacts with MuSK.

(a) Illustration of the creation of different amino- and carboxyterminal truncations of Erbin used for yeast-two-hybrid studies and GST pull-downs. (b, c) Growth of yeast clones containing different combinations of bait and prey plasmids as indicated on agar lacking histidine. Apart from the positive controls, only yeasts containing bait plasmids composed of Erbin mutants bearing the region between amino acids 1201 and 1279 show the ability to interact with MuSK.

4.3.6 The Smad-interacting domain of Erbin mediates the interaction with the kinase domain of MuSK

To map the epitopes of MuSK and Erbin interacting with each other, we used a series of carboxy-terminal truncations of MuSK. First, in yeast two-hybrid assays we observed growth of the yeast only when hErbin- Δ -1007 was used as bait together with the prey constructs MuSK-515-868 and MuSK-515-857 which comprise the full length MuSK intracellular or the MuSK kinase domain, respectively. Next, we transfected HEK293 cells with expression plasmids for the same truncations of MuSK. GST pull down experiments with a GST tagged hErbin- Δ -1007 protein from the cell extracts showed that the same carboxy-terminally truncated MuSK variants, MuSK-515-868 and MuSK-515-857, able to promote the growth of yeast were pulled down. Next we sought to identify the part of hErbin- Δ -1007 interacting with MuSK. To this end, we generated several hErbin- Δ -1007 deletion mutants, truncated at either their amino-terminal or carboxy-terminal ends. First, we transfected each of the hErbin- Δ -1007 mutants as preys together with a bait plasmid bearing MuSK2xwt into yeasts. Only yeast cells which contained, in addition to MuSK2xwt, the Erbin fragment deleted up to amino acid residue 1200 (hErbin- Δ -1200), like hErbin-PDZ (= hErbin- Δ -1261), grew on selective medium. When the hErbin- Δ -1007 fragments were trimmed at their carboxy-terminus, only yeasts containing Erbin starting from amino acid residue 1007 and ending at amino acid residue 1266 (hErbin- Δ PDZ) or 1204 (hErbin-1007-1204) grew on selective medium. Further, we confirmed the epitopes of Erbin which interact with MuSK by GST pull downs. Since, based on our yeast two-hybrid studies and GST pull downs, aa 1145 to 1261 were required for interaction, but, on the other hand, regions comprising aa 1145 to 1204 or 1200 to 1261 might be sufficient for interaction with MuSK2xwt, we continued to define more precisely the area of Erbin most important for this interaction. To this end we created a series of overlapping GSTtagged fragments representing parts of the hErbin- Δ -1007 protein. After purification these GST-Erbin constructs from bacteria, we incubated them with HEK293 cell extracts containing MuSK2xwt to identify those able to pull down MuSK2xwt. These experiments showed that the area of hErbin- Δ -1007 comprising aa 1175 and 1229 is required for the interaction between Erbin and MuSK. This area is encoded by the 3'-end of exon 21 and 5'-end of exon 23, because hErbin- Δ -1007 is part of splice variant hErbin-v2 which lacks exon 22. We generated more mutants of hErbin- Δ -1007 which were used in GST pull down assays to find out if epitopes encoded by both exons 21 and 23 are necessary for hErbin- Δ -1007 to interact with MuSK2xwt. Our results narrowed down the MuSK binding domain of hErbin- Δ -1007 to amino acid residues 1145 to 1211 which are encoded only by exon 21. Conspicuously, the identified MuSK binding domain nearly overlaps with a recently identified Smad-interacting domain of Erbin (Dai et al., 2007). Therefore, we asked whether muscle cells expressed different isoforms of Erbin at the NMJ, some with and others without exon 21. PCR studies with Erbin splice variant-specific primers and 1st cDNA, reverse transcribed from total RNA of C2C12 cells or diaphragms from mice, revealed three different Erbin transcripts. Next to the hErbin-v2 transcript, C2C12 cells and diaphragm express a full length Erbin transcript and a variant which lacks both exons 22 and 23. Note, the bands for the three different spliced transcripts of Erbin

appear in similar ratios regardless whether RT-PCRs were performed using total RNA from C2C12 myoblasts, muscle- or nervederived agrin treated myotubes, or synaptic or extra-synaptic parts of diaphragms. Next, we examined whether the same area of Erbin will interact with full length MuSK, as it did by GST pull down assays with MuSK2xwt. First, we generated three additional different Erbin variants cloned in expression plasmids: (1) a full length containing the splice variant which lacks exons 22 and 23, (2) a variant which specifically lacks the MuSK binding domain, (3) solely the MuSK binding domain (Fig. 17a). The expression of each variant was verified by immunodetection using cell extracts of transiently transfected HEK293 cells (Fig. 17b). Each Erbin variant was then co-expressed with full length MuSK, and the cell extracts were used for co-immunoprecipitation studies (Fig. 17c-e). Precipitating only the MuSK binding domain of Erbin, full length hErbin-v2, mErbin Δ exon22/23, or full length mouse Erbin caused coprecipitation of full length MuSK, but not hErbin Δ MuSK-bd (Fig. 17c, d). This indicates that the MuSK binding domain of Erbin is sufficient to interact with MuSK and that other epitopes of Erbin do not contribute to this interaction (hErbin Δ MuSK-bd does not coprecipitate MuSK, Fig. 17d). To further assess if all three proteins ErbB2, Erbin, and MuSK concomitantly interact and form a trimeric complex, we purified GST-tagged recombinant Erbin variants, composed of hErbin-N Δ -1007, hErbin-PDZ, or hErbin MuSK-bd, and incubated them with full length MuSK or ErbB2- containing HEK293 cell extracts (Fig. 17d, e). Indeed, pulling down hErbin-N Δ -1007 allowed coprecipitation of full length ErbB2 and MuSK (Fig. 17e). If HEK293 cell extracts additionally contained hErbin-PDZ or hErbin-MuSK-bd the co-precipitation of ErbB2 or MuSK was abolished, respectively (Fig. 17e). As control, human Erbin-PDZ or Erbin- Δ PDZ were able to precipitate only ErbB2 or MuSK, respectively, from an ErbB2- and MuSK-containing HEK293 cell extracts (Fig. 17e). It has been reported that Neuregulin stimulates transcription of the ϵ -subunit of the AChR (Si et al., 1997). Here, we used a AChR ϵ -subunit reporter gene which was previously shown to be inhibited by Erbin (Huang et al., 2003). This inhibition was assigned to the LRR domain of Erbin (Dai et al., 2005). We asked whether Erbin mutants either lacking or solely composed of the MuSK binding domain might influence Neuregulin-mediated AChR ϵ -subunit reporter gene activation. C2C12 cells were transiently transfected with the reporter gene together with hErbinv2 or either of the Erbin mutants, myoblasts were extracted after 48 hours or after myotube formation, and luciferase activities assayed. As shown before, we demonstrate that Erbin inhibits AChR ϵ -subunit reporter gene transcription in C2C12 myotubes (Fig. 17f, lower panel). The inhibition by the Erbin mutant lacking the MuSK binding domain was slightly weaker (Fig. 17f, lower panel). Surprisingly, the MuSK binding domain alone inhibited activation of the AChR ϵ - subunit reporter as observed with hErbin-v2 (Fig. 17f, lower panel). We asked whether the Erbin variants have a different impact on the transcription of the AChR ϵ -subunit reporter gene in C2C12 myoblasts. While hErbin-v2 and Erbin Δ MuSK-bd still inhibited AChR ϵ -subunit reporter gene transcription, Erbin MuSK-bd did not inhibit the reporter at all (Fig. 17f, upper panel).

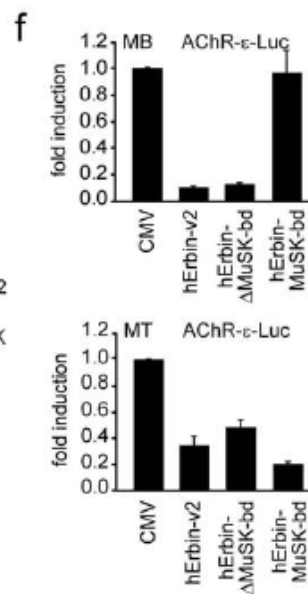
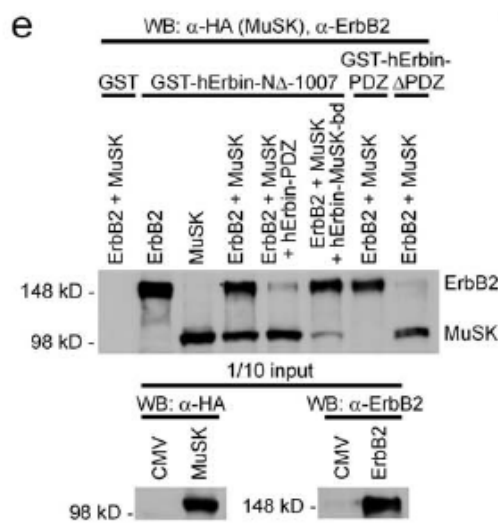
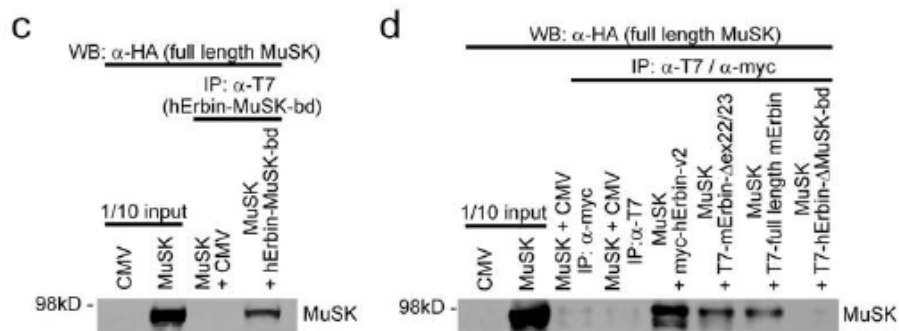
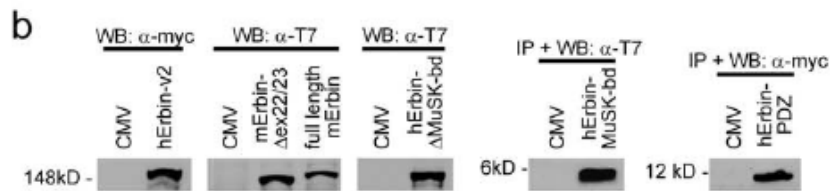
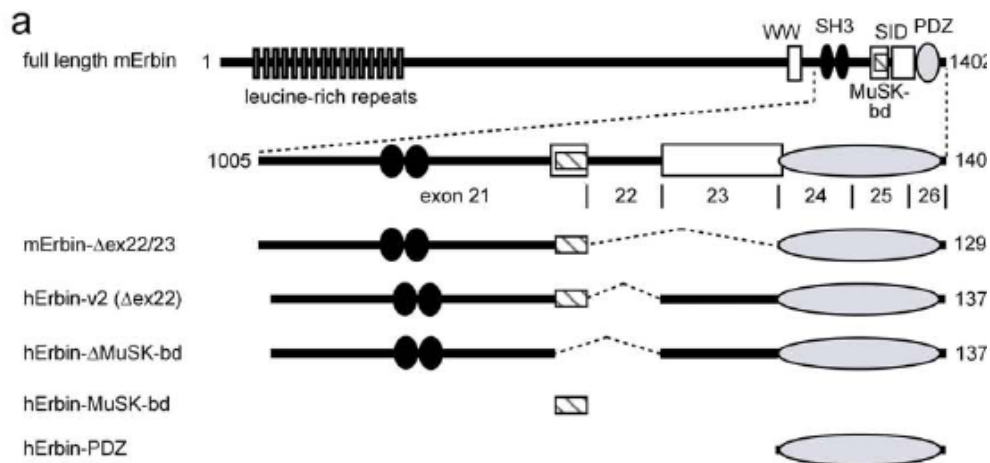


Fig. 7: Erbin interacts concomitantly with MuSK and ErbB2.

(a) Scheme of full length mouse Erbin and mutants thereof. The carboxy-terminal area is encoded by exons 21 to 26. Below this scheme, mouse or human Erbin variants lacking different exons are depicted. Other drawn human Erbin variants only consist of the MuSK binding domain or the PDZ domain. (b) Expression of these different mouse and human Erbin variants, as presented in (a) was ascertained by Western blot. (c) Precipitation of the human Erbin MuSK binding domain using transiently transfected HEK293 cells co-precipitates full length MuSK as shown by Western blot. (d) Extracts from transiently transfected HEK293 cells expressing different Erbin variants were used for co-immunoprecipitation studies. Precipitates were analyzed for the presence of full length MuSK by Western blot. Note, precipitation of a human Erbin mutant which does not contain the MuSK binding domain is unable to co-precipitate MuSK (e) GST fusions of either human Erbin- Δ 1007, Erbin-PDZ, or Erbin- Δ PDZ, immobilized on Glutathione beads, were incubated with HEK293 cell extracts containing full length ErbB2 and MuSK in different combinations, as indicated, and bound proteins were analyzed by Western blot. Note, GST-hErbin-PDZ pulls down ErbB2 but not MuSK, while GSThErbin- Δ PDZ pulls down MuSK but not ErbB2. Further, the specificity of this binding was demonstrated by addition of either human Erbin-PDZ or Erbin-MuSK-bd which inhibits the pull down of either ErbB2 or MuSK, respectively. (f) To investigate if over-expression of Erbin variants in C2C12 cells affects ErbB- and MuSK-dependent gene expression, the cells were transfected in duplicate three independent times by a human type of Erbin-v2, Erbin- Δ MuSK-bd, or Erbin-MuSK-bd together with an AChR ϵ -luciferase reporter. Luciferase activities were

4.3.7. Erbin enhances aggregation of AChRs *in vivo*

Previously, Erbin was shown to interact with ErbB2 and to be enriched at the NMJ (Borg et al., 2000; Huang et al., 2001). Having identified Erbin interacting with MuSK thereby linking MuSK with ErbB2, we aimed to investigate the biological significance for an interaction between Erbin and MuSK. To this end, we set up experiments to investigate if ablation or over-expression of Erbin affects AChR clustering. First, we designed several different plasmid-derived shRNAproducing vectors and demonstrated their efficiency to knock down Erbin transcript levels. As examined by luciferase reporter assays, one of the shRNA species reduced the amount of Erbin transcript by approx. 80% (Fig. 18a). Co-transfection of Erbin expression- and Erbin shRNAsplasmids in HEK293 cells abolished Erbin protein expression almost completely (Fig. 18b). To examine the effect of different Erbin protein levels on AChR aggregation in muscle cells, we transiently transfected an Erbin expression-, or the Erbin shRNA- plasmid, together with pnlsgFP into C2C12 cells (Hashemolhosseini et al., 2000). After myotube formation, addition of nerve-derived agrin to the myotubes and staining with rhodamine-labeled bungarotoxin, the influence of modulated Erbin protein amounts on AChR cluster formation was investigated. Surplus of Erbin did not influence AChR clustering (data not shown). Diminishing Erbin protein significantly reduced the density of aggregated AChR (Fig. 18d). If scrambled shRNA was transfected AChR aggregation was not affected (Fig. 18d). To find out if the size of AChR aggregates differs between muscle cells transfected with Erbin- or scrambled shRNA, the length of the AChR

aggregates were compared to their area (Fig. 18e). No difference could be detected, arguing that the physical dimensions of AChR aggregates have not changed if Erbin was knocked down. On the other hand, comparing the mean fluorescence intensity of AChR aggregates with the length or area of AChR aggregates showed that knockdown of Erbin decreases the density of AChR aggregates (Fig. 18f, g). Altogether, we confirmed that aggregates formed in the absence of Erbin are in general of significantly less fluorescence intensity, as detected by confocal microscopy, reflecting in total a lower density of AChRs in the aggregates. To find out if AChR aggregates are disappearing faster in the absence of nerve-derived agrin and Erbin, we transiently transfected C2C12 cells with either an empty plasmid, scrambled shRNA, or Erbin shRNA, and measured the number of AChRs clusters remaining after removal of nerve-derived agrin (Fig. 18c). The number of remaining AChR clusters decreased with time independently of the presence or absence of agrin (Fig. 18c).

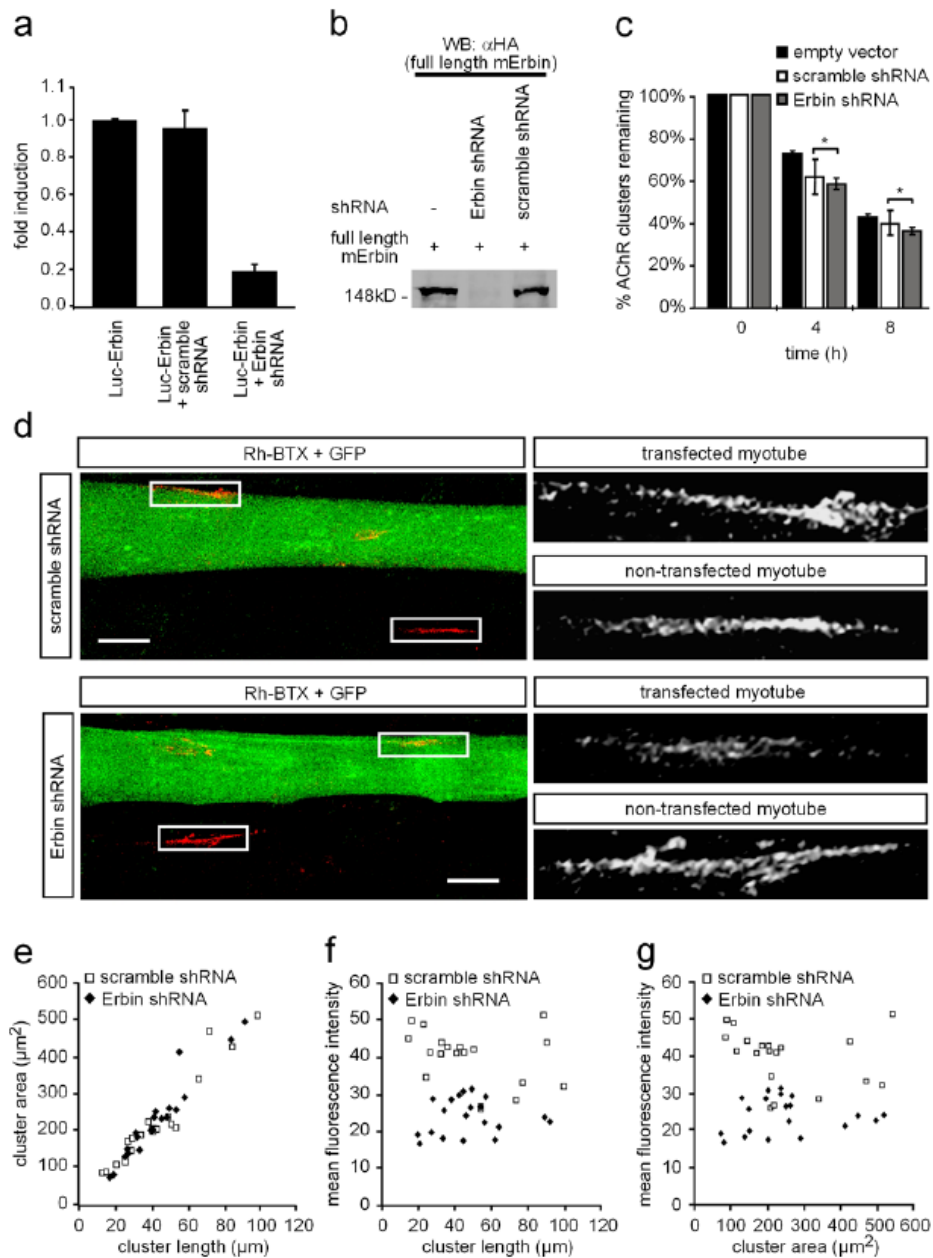


Fig. 8: Knockdown of Erbin reduces the density of AChR aggregates.

(a) Luciferase activity assays using extracts from transiently transfected HEK293 cells demonstrate a reduction of Erbin mRNA upon treatment with an Erbin-specific shRNA, but not scrambled shRNA. Note, the Erbin-specific shRNA reduced the quantity of Erbin transcripts by more than 80%. (b) Diminished amount of Erbin protein by transfection of cells with shRNA was ascertained by Western blot. (c) To find out if AChR cluster stability decreased in the absence of Erbin, nerve-derived agrin was depleted from cell media and remaining AChR aggregates counted at the same time (pSuper, scramble,

Erbin-specific, n=76 / 67 / 70) or after, 4 (n=80 / 67 / 82) and 8 hours (n=71 / 72 / 79) and presented as % of remaining clusters. (d) C2C12 cells were transfected with shRNA (Erbin-specific or scrambled) cloned in pSuperGFPneo, differentiated to myotubes, and incubated with nerve-derived agrin. On the left, typical confocal images (compressed Z-stack) are shown. On the right, high resolution gray scale images of AChR cluster of transfected and non-transfected myotubes are shown. Note that the AChR clusters formed in GFP-positive myotubes are less dense. Scale bar, 25 μ m. (e) Comparison of areas of AChR clusters with their length as determined on C2C12 cells transiently transfected with either scrambled or Erbin-specific shRNA as indicated (n>20). (f, g) Mean fluorescence intensity of AChR clusters as described in (e) were plotted against AChR clusters length or area. Note, fluorescence intensity of AChR clusters was significantly lower if C2C12 cells which were transfected with Erbin-specific shRNA. A cluster was defined as an aggregation of AChRs with more than 10 μ m in length.

4.3.8 Erbin associates ErbB2 with MuSK and TGF- β signalling at the NMJ

Smad proteins are intracellular signaling mediators of TGF- β (ten Dijke and Heldin, 2006). Recently, it was reported that Erbin inhibits TGF- β signaling through a novel Smad-interacting domain (Dai et al., 2007). We asked if C2C12 muscle cells express TGF- β receptors and Smad and if this happens in a nerve-derived agrin-dependent manner. We extracted total RNA from C2C12 myoblasts or from myotubes which were treated with muscle- or nerve-derived agrin. Using quantitative RT-PCR, we detected receptors TGF- β RI and TGF- β RII and Smad3 in C2C12 cells (Fig. 19a). Both TGF- β receptors and Smad3 are transcribed at higher amount in myotubes, and even higher in cells treated with nerve-derived agrin, compared to myotubes incubated with muscle-derived agrin (Fig. 19a). To further assess the role of Erbin and MuSK in TGF- β signalling, we transiently transfected C2C12 cells with an expression plasmid encoding Smad3. As it was reported, Smad3 inhibited myotube formation from C2C12 myoblasts (Fig. 19b) (Liu et al., 2001). Co-transfection of the C2C12 cells with hErbin-v2, or hErbin-v2 and MuSK, released this inhibition and cells differentiated and formed myotubes (Fig. 19b). This finding is in agreement with previous data showing that increased Erbin expression in HEK293 cells physically sequesters, by its Smad-interacting domain, Smad2/Smad3 from their association with Smad4 and, thus, negatively modulates TGF- β -dependent transcriptional responses and inhibition of cell growth (Dai et al., 2007). To verify the physiological consequence of the MuSK-Erbin-Smad interaction, the influence of Erbin alone or combined with MuSK on Smad2/Smad3-mediated transcriptional activation of TGF- β target genes was examined. Direct Smad2/Smad3-dependent transcription was investigated using the SBE4-Luc reporter, which contains four copies of a Smad binding site (Zawel et al., 1998). Transient transfection of C2C12 cells with Smad3 but not hErbin-v2 or MuSK led to a significant increase of luciferase activity (Fig. 19c). If either hErbin-v2, MuSK, or both together were co-transfected with Smad3, less luciferase activity was detectable (Fig. 19c). These data implicate that MuSK, Erbin, or both together have no influence on activation of Smad3-dependent target promoters by themselves but inhibit partially Smad3-mediated transactivation of respective target genes.

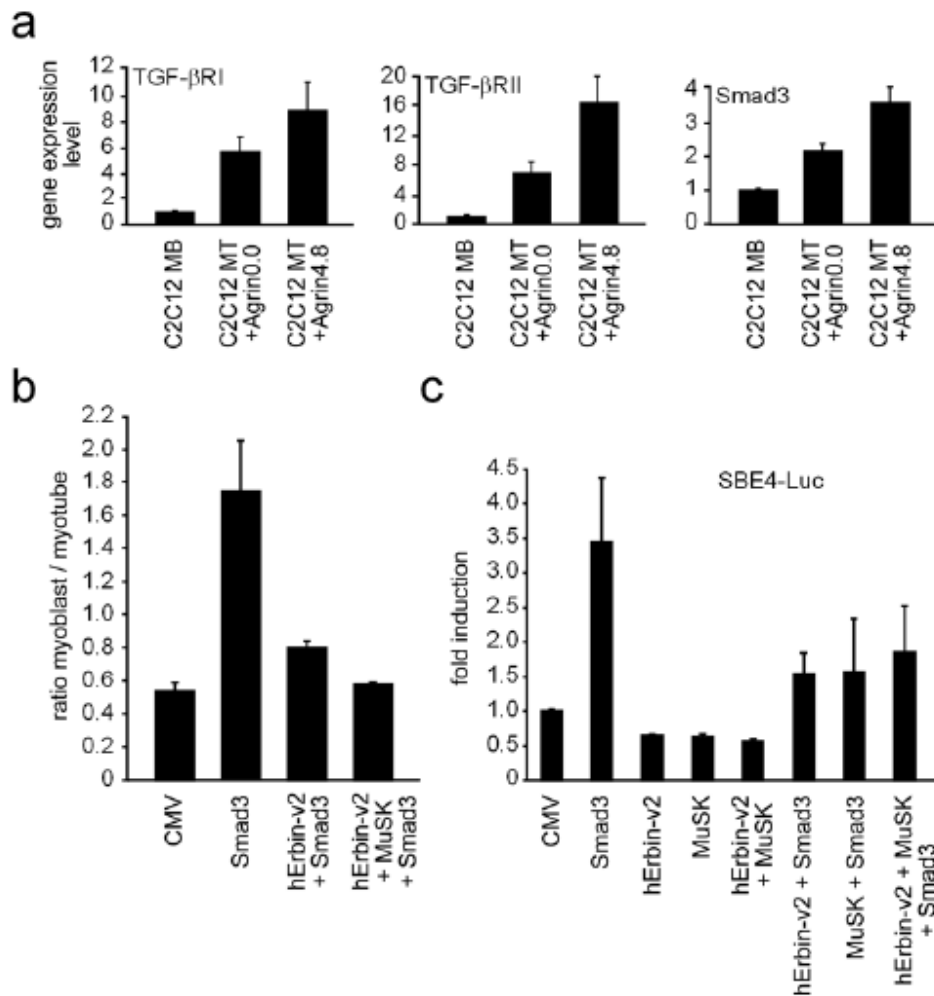


Fig. 9: MuSK impinges on the modulation of TGF-β signalling by Erbin.

(a) Expression profiles of TGF-β receptors I, II and Smad3 in C2C12 cells were examined by quantitative RT-PCRs and the results depicted as graphs. (b) C2C12 cells were transfected with GFPnIs (Hashemolhosseini et al., 2000) together with Smad3, human Erbin-v2 and MuSK in different combinations. GFP-positive cells were counted in myoblasts and myotubes and their ratio presented as graph. Note, Smad3 inhibits C2C12 cell differentiation. Erbin sequesters Smad3 thereby ensuring C2C12 myotube formation. (c) Competition between Erbin binding either Smad3 or MuSK was studied by transfecting Smad3, human Erbin-v2, and MuSK, as indicated, together with a Smad3-responsive reporter into C2C12 cells. Note, Smad3 strongly transactivates SBE4-Luc, while Erbin or MuSK transfected together with Smad3 resulted in less SBE4-Luc derived activity.

4.3.9 LAP family members like Lano and Scribble but not Densin-180 are expressed at the NMJ

To find out if other LAP family members are expressed in muscle cells, we performed RT-PCR experiments with C2C12 myoblasts and myotubes incubated with muscle- or nerve-derived agrin. We detected PCR-amplified fragments from C2C12 cells for Scribble, Lano, but not Densin-180 arguing that Scribble and Lano are expressed in muscle cells (Fig. 20a). Next, we quantified transcript levels of Scribble and Lano in C2C12 cells. It turned out that Scribble is expressed at very high amounts compared to Lano in C2C12 cells and its transcription is even higher if C2C12 myotube were incubated with nerve-derived agrin compared to muscle-derived agrin (Fig. 20b).

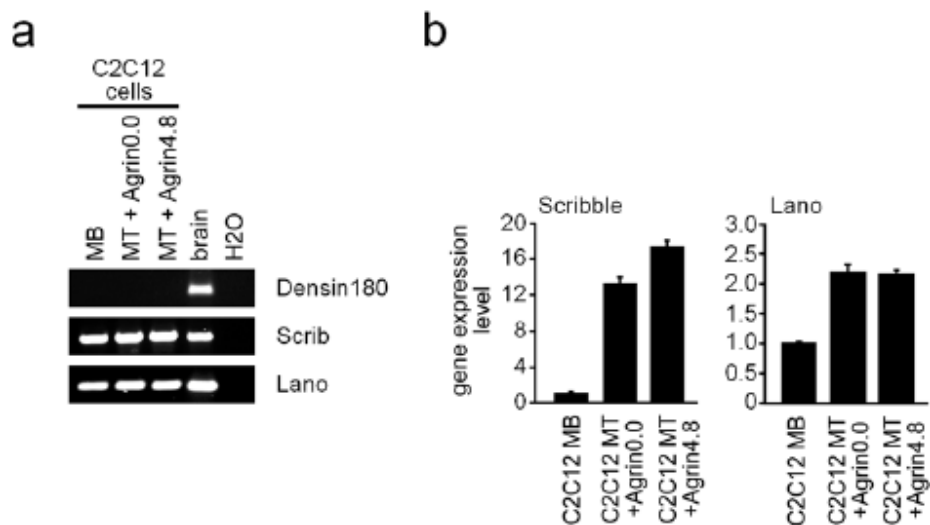


Fig. 10: Expression profile of other LAP protein family members in muscle cells.

(a) RT-PCR data from C2C12 myoblasts and myotubes incubated with agrin as indicated. Note, Scribble and Lano, but not Densin-180, are expressed in C2C12 cells. (b) Expression profiling by quantitative RT-PCR demonstrated Scribble and Lano expression rather in myotubes than in myoblasts. A high expression profile for Scribble in C2C12 cells was detected, especially in myotubes and even more in nerve-derived agrin treated cells.

5. Discussion

Our data demonstrate for the first time an interaction between Erbin and the muscle-specific receptor tyrosine kinase MuSK at the postsynaptic apparatus of the NMJ. Since MuSK bears a PDZ-binding domain at the very carboxy-terminus it was attractive to assume its interaction with the PDZ domain of Erbin thereby linking together both receptor tyrosine kinases ErbB2 and MuSK (Jean-Paul Borg, personal communication). Previous approaches failed to detect such an interaction because, as we present here, it is not the PDZ domain (aa 1280-1368) of human Erbin which interacts with the receptor tyrosine kinase MuSK. The area of Erbin which contacts MuSK is located at the carboxy-terminus of Erbin and is positioned between amino acids 1145 and 1229. In

close proximity to the MuSK binding domain of Erbin previously a WW (aa 973-977), two SH3 (aa1100-1104, 1115-1121) and the PDZ epitopes were identified (Borg et al., 2000). Further, the MuSK binding domain of Erbin is part of a recently reported domain of Erbin involved in Smad3 binding (and is named SID, aa 1172-1282) (Dai et al., 2007). This is surprising as the overlapping binding domains of TGF- β and MuSK might implicate that their signaling cross-talks at the NMJ. Different TGF- β members and their receptors were found at the vertebrate NMJ but not much is known about their role at the postsynaptic apparatus (McLennan and Koishi, 1994; Jiang et al., 2000). Previously, TGF- β members were postulated to control the onset of secondary myotube formation by preventing the fusion of late myoblasts (Sanchez and Robbins, 1994). All three known members of TGF- β (1 to 3) were independently knocked out in mice, but turned out not to be involved in the onset of myotube formation (TGF- β 1), or the skeletal muscles of the knockout mice were not studied in detail (Kaartinen et al., 1995; Proetzel et al., 1995; Sanford et al., 1997; McLennan et al., 2000). TGF- β 2 was reported to be expressed in motoneurons where it is up-regulated after nerve injury (Jiang et al., 2000). All this is in contrast to invertebrate NMJs where p.ex. TGF- β signalling is known to play an essential role for the development of the *Drosophila* NMJ (Packard et al., 2003). It was found that TGF-type I receptor *Saxophone* and the downstream transcription factor *Mothers against dpp* are essential for the normal structural and functional formation of the *Drosophila* NMJ (Rawson et al., 2003). It was postulated that alternative TGF- β like factors might be also involved in vertebrate neuromuscular synapse formation (Packard et al., 2003). We followed up this question and identified TGF- β receptors and Smad3 being expressed in myoblasts, up-regulated in myotubes, significantly stronger if they were incubated with nerve-derived agrin. Further, our studies narrowed down the MuSK binding domain of Erbin to an epitope encoded by exon 21. It seemed unlikely to assume that the MuSK binding domain is encoded by two exons 21 and 23 but not 22, because during evolution functional epitopes of proteins are in many cases known to be encoded and transmitted on single exons (Doolittle, 1995). Consequently, it might be speculated if the SID of Erbin really spans from exon 21 to 23, if it overlaps more precisely with the MuSK binding domain or if it is encoded only on exon 23. The detection of different splice variants of Erbin at the NMJ might help to answer this question since all splice variants detected contain exon 21, which in part encodes the MuSK binding domain, but two of them lack either exon 22, or both 22 and 23. In other words, these two splice variants might of Erbin interact in a Smad3- independent manner. Interestingly, the three different splice variants of Erbin detected in muscle cells are differentially regulated for their expression arguing that they might be required in different ways at the NMJ. To find out about competition of MuSK and Smad3 for the same binding site on Erbin, transient transfections of MuSK, Smad3, Erbin and a Smad3-dependent luciferase reporter (SBE4-luc) into C2C12 myotubes were performed. We expected to observe a higher luciferase activity if MuSK was co-transfected because it might compete for the domain of Erbin which interacts with MuSK and Smad3, thereby increasing the amount of available Smad3 for activation of the SBE4-luc reporter. But we failed to detect any competition between Smad3 and MuSK for the same binding site in Erbin arguing that MuSK did not sequester Erbin thereby releasing Smad3. Further experiments should help to solve the question whether MuSK and TGF- β signalling

cross-talk together. We are aware that data presented here mark the beginning in understanding the biological role of LAP proteins at the NMJ. Knocking down Erbin, we observed a significant decrease of density of AChR aggregates. This change was unrelated to the physical dimensions of AChR aggregates. No difference between AChR aggregates of muscle cells transfected with scrambled or Erbin-specific shRNA was observable if the length of the AChR aggregates were plotted against their area. It was obvious to test if there are other LAP family members expressed at the NMJ. Their presence might permit compensation of each other. Other LAP family members are p.ex. Densin-180 (Apperson et al., 1996), Lano (Saito et al., 2001) and Scribble (Murdoch et al., 2003). Densin-180 is associated with postsynaptic density in rat brain and might be involved in localization of synaptic proteins (Huang et al., 2001). Scribble is a junctional protein involved in establishment and maintenance of epithelial cell polarity (Navarro et al., 2005). In fact, we could detect next to Erbin, Lano and Scribble but not Densin-180 at the NMJ. All three LAP proteins are expressed at significantly higher rates in myotubes compared to myoblasts. It turned out that our quantitative RT-PCR data about the localization of Erbin transcripts in C2C12 myotubes treated with muscle- and nerve-derived agrin did not perfectly reflect the synaptic and extra-synaptic localization of their transcripts in muscle tissue. While the quantitative RT-PCR data only indicate an increase of Erbin transcripts in C2C12 cells incubated with nerve-derived agrin compared to myotubes treated with muscle-derived agrin, in situ hybridization of diaphragm tissue convincingly prove only restricted synaptic expression of Erbin at the NMJ. Accordingly, our presented quantitative RT-PCR data about the expression profile of Scribble and Lano do not exclude restricted synaptic expression of both. Here, we demonstrate that (1) Scribble is expressed in cultured muscle cells approx. 6-fold higher compared to its family members Erbin and Lano, (2) expression of Scribble is most up-regulated if myotubes were incubated with nerve-derived agrin. Additional experiments are necessary to find out, (1) if Scribble and Lano also interact with either MuSK, Erbin or both, (2) if knockdown of all three LAP proteins will end in complete failure of AChR aggregation, and (3) what will be the phenotype of mice if all LAP genes present in muscle cells will be knocked out. Our data support the view that balanced physiological amounts of LAP family members play a crucial role at the NMJ.

6. References

- Altiok N, Bessereau JL, Changeux JP (1995) ErbB3 and ErbB2/neu mediate the effect of heregulin on acetylcholine receptor gene expression in muscle: differential expression at the endplate. *Embo J* 14:4258-4266.
- Apperson ML, Moon IS, Kennedy MB (1996) Characterization of densin-180, a new brain-specific synaptic protein of the O-sialoglycoprotein family. *J Neurosci* 16:6839-6852.
- Borg JP, Marchetto S, Le Bivic A, Ollendorff V, Jaulin-Bastard F, Saito H, Fournier E, Adelaide J, Margolis B, Birnbaum D (2000) ERBIN: a basolateral PDZ protein that interacts with the mammalian ERBB2/HER2 receptor. *Nat Cell Biol* 2:407-414.
- Bryant PJ, Huwe A (2000) LAP proteins: what's up with epithelia? *Nat Cell Biol* 2:E141-143.
- Cheusova T, Khan MA, Schubert SW, Gavin AC, Buchou T, Jacob G, Sticht H, Allende J, Boldyreff B, Brenner HR, Hashemolhosseini S (2006) Casein kinase 2-dependent serine phosphorylation of MuSK regulates acetylcholine receptor aggregation at the neuromuscular junction. *Genes Dev* 20:1800-1816.
- Dai F, Chang C, Lin X, Dai P, Mei L, Feng XH (2007) Erbin inhibits transforming growth factor beta signaling through a novel Smad-interacting domain. *Mol Cell Biol* 27:6183-6194.
- Dai P, Xiong W, Mei L (2005) Erbin inhibits RAF activation by disrupting the SUR-8-RAS-RAF complex. *J Biol Chem*.
- DeChiara TM, Bowen DC, Valenzuela DM, Simmons MV, Poueymirou WT, Thomas S, Kinetz E, Compton DL, Rojas E, Park JS, Smith C, DiStefano PS, Glass DJ, Burden SJ, Yancopoulos GD (1996) The receptor tyrosine kinase MuSK is required for neuromuscular junction formation in vivo. *Cell* 85:501-512.
- Doolittle RF (1995) The multiplicity of domains in proteins. *Annu Rev Biochem* 64:287-314.
- Escher P, Lacazette E, Courtet M, Blindenbacher A, Landmann L, Bezakova G, Lloyd KC, Mueller U, Brenner HR (2005) Synapses form in skeletal muscles lacking neuregulin receptors. *Science* 308:1920-1923.
- Falls DL, Rosen KM, Corfas G, Lane WS, Fischbach GD (1993) ARIA, a protein that stimulates acetylcholine receptor synthesis, is a member of the neu ligand family. *Cell* 72:801-815.
- Favre B, Fontao L, Koster J, Shafaatian R, Jaunin F, Saurat JH, Sonnenberg A, Borradori L (2001) The hemidesmosomal protein bullous pemphigoid antigen 1 and the integrin beta 4 subunit bind to ERBIN. Molecular cloning of multiple alternative splice

variants of ERBIN and analysis of their tissue expression. *J Biol Chem* 276:32427-32436.

Garcia-Osta A, Tsokas P, Pollonini G, Landau EM, Blitzer R, Alberini CM (2006) MuSK expressed in the brain mediates cholinergic responses, synaptic plasticity, and memory formation. *J Neurosci* 26:7919-7932.

Garcia RA, Vasudevan K, Buonanno A (2000) The neuregulin receptor ErbB-4 interacts with PDZ-containing proteins at neuronal synapses. *Proc Natl Acad Sci U S A* 97:3596-3601.

Hashemolhosseini S, Moore C, Landmann L, Sander A, Schwarz H, Witzemann V, Sakmann B, Brenner HR (2000) Electrical activity and postsynapse formation in adult muscle: gamma-AChRs are not required. *Mol Cell Neurosci* 16:697-707.

Henriquez JP, Webb A, Bence M, Bildsoe H, Sahores M, Hughes SM, Salinas PC (2008) Wnt signaling promotes AChR aggregation at the neuromuscular synapse in collaboration with agrin. *Proc Natl Acad Sci U S A* 105:18812-18817.

Huang YZ, Wang Q, Xiong WC, Mei L (2001) Erbin is a protein concentrated at postsynaptic membranes that interacts with PSD-95. *J Biol Chem* 276:19318-19326.

Huang YZ, Zang M, Xiong WC, Luo Z, Mei L (2003) Erbin suppresses the MAP kinase pathway. *J Biol Chem* 278:1108-1114.

Jaworski A, Burden SJ (2006) Neuromuscular synapse formation in mice lacking motor neuron- and skeletal muscle-derived Neuregulin-1. *J Neurosci* 26:655-661.

Jiang Y, McLennan IS, Koishi K, Hendry IA (2000) Transforming growth factor-beta 2 is anterogradely and retrogradely transported in motoneurons and up-regulated after nerve injury. *Neuroscience* 97:735-742.

Jones G, Moore C, Hashemolhosseini S, Brenner HR (1999) Constitutively active MuSK is clustered in the absence of agrin and induces ectopic postsynaptic-like membranes in skeletal muscle fibers. *J Neurosci* 19:3376-3383.

Kaartinen V, Voncken JW, Shuler C, Warburton D, Bu D, Heisterkamp N, Groffen J (1995) Abnormal lung development and cleft palate in mice lacking TGF-beta 3 indicates defects of epithelial-mesenchymal interaction. *Nat Genet* 11:415-421.

Kim N, Stiegler AL, Cameron TO, Hallock PT, Gomez AM, Huang JH, Hubbard SR, Dustin ML, Burden SJ (2008) Lrp4 is a receptor for Agrin and forms a complex with MuSK. *Cell* 135:334-342.

Kolch W (2003) Erbin: sorting out ErbB2 receptors or giving Ras a break? *Sci STKE* 2003:pe37.

Li Q, Esper RM, Loeb JA (2004) Synergistic effects of neuregulin and agrin on muscle acetylcholine receptor expression. *Mol Cell Neurosci* 26:558-569.

Liu D, Black BL, Derynck R (2001) TGF-beta inhibits muscle differentiation through functional repression of myogenic transcription factors by Smad3. *Genes Dev* 15:2950-2966.

Luo ZG, Wang Q, Zhou JZ, Wang J, Luo Z, Liu M, He X, Wynshaw-Boris A, Xiong WC, Lu B, Mei L (2002) Regulation of AChR clustering by Dishevelled interacting with MuSK and PAK1. *Neuron* 35:489-505.

McLennan IS, Koishi K (1994) Transforming growth factor-beta-2 (TGF-beta 2) is associated with mature rat neuromuscular junctions. *Neurosci Lett* 177:151-154.

McLennan IS, Poussart Y, Koishi K (2000) Development of skeletal muscles in transforming growth factor-beta 1 (TGF-beta1) null-mutant mice. *Dev Dyn* 217:250-256.

Merlie JP, Sanes JR (1985) Concentration of acetylcholine receptor mRNA in synaptic regions of adult muscle fibres. *Nature* 317:66-68.

Moscoso LM, Chu GC, Gautam M, Noakes PG, Merlie JP, Sanes JR (1995) Synapse-associated expression of an acetylcholine receptor-inducing protein, ARIA/heregin, and its putative receptors, ErbB2 and ErbB3, in developing mammalian muscle. *Dev Biol* 172:158-169.

Murdoch JN, Henderson DJ, Doudney K, Gaston-Massuet C, Phillips HM, Paternotte C, Arkell R, Stanier P, Copp AJ (2003) Disruption of scribble (Scrb1) causes severe neural tube defects in the circletail mouse. *Hum Mol Genet* 12:87-98.

Navarro C, Nola S, Audebert S, Santoni MJ, Arsanto JP, Ginestier C, Marchetto S, Jacquemier J, Isnardon D, Le Bivic A, Birnbaum D, Borg JP (2005) Junctional recruitment of mammalian Scribble relies on E-cadherin engagement. *Oncogene* 24:4330-4339.

Packard M, Mathew D, Budnik V (2003) Wnts and TGF beta in synaptogenesis: old friends signalling at new places. *Nat Rev Neurosci* 4:113-120.

Ponomareva ON, Ma H, Vock VM, Ellerton EL, Moody SE, Dakour R, Chodosh LA, Rimer M (2006) Defective neuromuscular synaptogenesis in mice expressing constitutively active ErbB2 in skeletal muscle fibers. *Mol Cell Neurosci* 31:334-345.

Proetzel G, Pawlowski SA, Wiles MV, Yin M, Boivin GP, Howles PN, Ding J, Ferguson MW, Doetschman T (1995) Transforming growth factor-beta 3 is required for secondary palate fusion. *Nat Genet* 11:409-414.

Rangwala R, Banine F, Borg JP, Sherman LS (2005) Erbin regulates mitogen-activated protein (MAP) kinase activation and MAP kinase-dependent interactions between Merlin and adherens junction protein complexes in Schwann cells. *J Biol Chem* 280:11790-11797.

Saito H, Santoni MJ, Arsanto JP, Jaulin-Bastard F, Le Bivic A, Marchetto S, Audebert S, Isnardon D, Adelaide J, Birnbaum D, Borg JP (2001) Lano, a novel LAP protein directly connected to MAGUK proteins in epithelial cells. *J Biol Chem* 276:32051-32055.

Sanchez A, Robbins J (1994) Unprocessed myogenin transcripts accumulate during mouse embryogenesis. *J Biol Chem* 269:1587-1590.

Sanes JR, Lichtman JW (1999) Development of the vertebrate neuromuscular junction. *Annu Rev Neurosci* 22:389-442.

Sanford LP, Ormsby I, Gittenberger-de Groot AC, Sariola H, Friedman R, Boivin GP, Cardell EL, Doetschman T (1997) TGFbeta2 knockout mice have multiple developmental defects that are non-overlapping with other TGFbeta knockout phenotypes. *Development* 124:2659-2670.

Si J, Miller DS, Mei L (1997) Identification of an element required for acetylcholine receptor-inducing activity (ARIA)-induced expression of the acetylcholine receptor epsilon subunit gene. *J Biol Chem* 272:10367-10371.

ten Dijke P, Heldin C-H (2006) Smad signal transduction: Smads in proliferation, differentiation and disease. *Springer*, Berlin, Germany.

Trinidad JC, Cohen JB (2004) Neuregulin inhibits acetylcholine receptor aggregation in myotubes. *J Biol Chem* 279:31622-31628.

Trinidad JC, Fischbach GD, Cohen JB (2000) The Agrin/MuSK signaling pathway is spatially segregated from the neuregulin/ErbB receptor signaling pathway at the neuromuscular junction. *J Neurosci* 20:8762-8770.

Valenzuela DM, Stitt TN, DiStefano PS, Rojas E, Mattsson K, Compton DL, Nunez L, Park JS, Stark JL, Gies DR, et al. (1995) Receptor tyrosine kinase specific for the skeletal muscle lineage: expression in embryonic muscle, at the neuromuscular junction, and after injury. *Neuron* 15:573-584.

Weston C, Yee B, Hod E, Prives J (2000) Agrin-induced acetylcholine receptor clustering is mediated by the small guanosine triphosphatases Rac and Cdc42. *J Cell Biol* 150:205-212.

Wilkes MC, Repellin CE, Hong M, Bracamonte M, Penheiter SG, Borg JP, Leof EB (2009) Erbin and the NF2 tumor suppressor Merlin cooperatively regulate cell-type-specific activation of PAK2 by TGF-beta. *Dev Cell* 16:433-444.

Zawel L, Dai JL, Buckhaults P, Zhou S, Kinzler KW, Vogelstein B, Kern SE (1998) Human Smad3 and Smad4 are sequence-specific transcription activators. *Mol Cell* 1:611-617.

Zhu D, Xiong WC, Mei L (2006) Lipid rafts serve as a signaling platform for nicotinic acetylcholine receptor clustering. *J Neurosci* 26:4841-4851.

Zhu X, Lai C, Thomas S, Burden SJ (1995) Neuregulin receptors, erbB3 and erbB4, are localized at neuromuscular synapses. *Embo J* 14:5842-5848.

7. Appendice

7.1.1 Laboratori frequentati

I laboratori presso cui si è svolta la mia attività di ricerca, sono:

1. Dipartimento di Biochimica e Biotecnologie Mediche (DBBM)

Il Policlinico – Università Federico II

Via S.Pansini, 5

80131 Napoli, Italy

Docente - guida: Prof.ssa Gabriella Esposito

2. Institute of Biochemistry “E. Fischer”

Department of Neurobiology

University of Erlangen – Nuernberg

Fahrstrasse, 17

91054 Erlangen, Germany

Periodo di lavoro: Da Gennaio 2008 a Dicembre 2008